KFKI-71-47

E. Pásztor
P. Kostka
E. Klopfer
Gy. Berecz
G. Bürger
P. Gombos
B. Horváth
L. Királyhidi
P. Riedl

THE NEW 5 MeV VAN DE GRAAFF ION ACCELERATOR AT THE CENTRAL RESEARCH INSTITUTE FOR PHYSICS OF THE HUNGARIAN ACADEMY OF SCIENCES, BUDAPEST

Hungarian Academy of Sciences

CENTRAL
RESEARCH
INSTITUTE FOR
PHYSICS

BUDAPEST

KFKI-71-47

THE NEW 5 MeV VAN DE GRAAFF ION ACCELERATOR AT THE CENTRAL RESEARCH INSTITUTE FOR PHYSICS OF THE HUNGARIAN ACADEMY OF SCIENCES, BUDAPEST

E. Pásztor, P. Kostka, E. Klopfer, Gy. Berecz,
G. Bürger, P. Gombos, B. Horváth, L. Királyhidi,
P. Riedl

Nuclear Physics Department
Central Research Institute for Physics, Budapest

SUMMARY

The present report describes the new 5 MeV Van de Graaff ion accelerator designed and built at the Central Research Institute for Physics of the Hungarian Academy of Sciences, and started in normal operation on 12. March 1970. In its present state, the equipment is suitable for accelerating protons, deuterons and He_4^+ ions; analyzed ion beams are of max. 10 μA intensity and the stability of energy of ions is /1.5 - 2.5/x 10^{-4} at the target. Design is also described, main technical data are given, and special problems of the high-pressure gas insulation and the charging system are dealt with in detail. Original measuring results are given on the harmful effects of humidity and dust contents. Mechanical and electrical designs of the ion source and its auxiliary equipment are dealt with, technical data listed, and the used type of system engineering is described. Technological and ion-optical development of the accelerator tube is outlined from a conventional homogeneous-field porcelain tube to a PVA-cemented inclined-field glass accelerator tube. Details of the ion-optical design, as well as conditioning and putting in work of the completed tube, are also discussed. Design of the complex energy stabilization system, the NMR flux -meter developed in the Institute, and the impulse width modulated stabilization system of the magnetic field are also treated. Finally, experiences gained during 6,253 hours of operation completed so far are summed up.

ÖSSZEFOGLALÁS

A cikk ismerteti a Magyar Tudományos Akadémia Központi Fizikai Kutató Intézetében tervezett, épitett és 1970. márc. 12-én üzembe állitott uj, 5 MeV-os Van de Graaff ion-gyorsitót. A berendezés jelenleg protonok, deuteronok és He_4^+ ionok gyorsitására alkalmas, a targeten max. 10 μA intenzitásu analizált és /1.5 - 2.5/ x 10^{-4} stabilitásu ionnyaláb nyerhető. A cikk megadja a berendezés szerkezeti leirását és főbb müszaki adatait, részletesen kitér a nagynyomásu gázszigetelés és a töltőrendszer speciális problémáira, valamint eredeti méréseket közöl a nedvesség- és portartalom hatásairól. Ismerteti az ionforrás és segédberendezéseinek mechanikai és villamos felépitését, adatait és ujszerü rendszertechnikáját. Leirja a gyorsitócső technológiai és ionoptikai fejlesztésének menetét a konvencionális, egyenesterü porcelán csőtől egy PVA-ragasztásu, ferdeterü üveg-gyorsitócsőig. Részletesen kitér az ion-optikai tervezésre, a kész cső trenirozására és üzembehelyezésére. Ismerteti a komplex energiastabilizáló rendszer felépitését, a kifejlesztett NMR-térmérőt és az impulzusszélesség-modulált térstabilizáló rendszert. Végül közli a gyorsitó eddigi, 6253 üzemórás müködése során szerzett üzemi tapasztalatokat.

РЕЗЮМЕ

Описывается ионный ускоритель на 5 Мэв, разработанный и построенный в ЦИФИ ВАН, пущенный в эксплуатацию I2 марта I972 г. В настоящее время с помощью установки ускоряются протоны, дейтроны и ионы He_4^+, на мишени получается анализированный пучок ионов с максимальной интенсивностью I0 мка и стабильностью /I,5-2,5/xI0^{-4}. Описываются конструкция и основные технические данные установки, подробно излагаются специальные проблемы, связанные с газовой изоляцией с помощью высокого давления и системой зарядки. Приводятся результаты измерений, проведенных для определения влияния содержания влажности и пыли. Описываются механическая конструкция, электрическая схема, технические данные и принцип новой конструкции источника ионов и его вспомогательных устройств. Излагается ход технологической и ионооптической разработки, начиная от конвенциональной фарфоровой ускоряющей трубы с гомогенным электростатическим полем и кончая стеклянной ускоряющей трубой с наклеенным электростатическим полем, склеенной при помощи PVA. Подробно описывается ионооптическая разработка, закалка и ввод в эксплуатацию готовой трубы. Описываются конструкция комплексной системы стабилизации энергии, измеритель поля, работающий на принципе ЯМР, и система стабилизации поля, модулированная по ширине импульса, и, наконец, излагается опыт, приобретенный в течение 6253-часовой эксплуатации ионного ускорителя.

CONTENTS

INTRODUCTION - BRIEF TECHNICAL DESCRIPTION

At the Central Research Institute for Physics of the Hungarian Academy of Sciences, a Van de Graaff ion accelerator has been in use from the spring of 1963 for purposes of basic research in nuclear physics [1,2]. Up to the summer of 1968, some 12,000 hours of operation were spent on nuclear research. During that period the necessity of a complete reconstruction became manifest, mainly for the following reasons:

- The progress in Hungarian nuclear research necessitated the extension of energy limits of acceleration. Owing to insulation engineering problems arising from the geometrical dimensions, this was unfeasible with the old equipment.
- It seemed to be necessary to increase the target current intensity by approximately one order.
- The good energy-resolution required for nuclear spectroscopic experiments made desirable the increase of the energy stability attained with the old equipment by approximately one order.
- In order to extend nuclear physics experiments over a wider range, acceleration of ions other than protons and deuterons /e.g. He_4^+/ seemed desirable as well.
- The need to render nuclear physics experiments more reproducible and spectra clearer necessitated the installation of a vacuum system of a higher degree of purity and with a higher pumping speed.

Many of the materials and components, as well as the engineering and technological designs incorporated in the old equipment were based on the Hungarian industrial and economic background of the fifties and could be replaced with considerably more modern counterparts. These out-of-date components and obsolete designs were the source of numerous failures which unnecessarily extended the time required for maintenance.

While measurements were made with the old equipment, reconstruction was decided upon on the above-mentioned grounds, and planning started in 1966. The concepts were drawn up, goals and specifications made in 1967. In the course of that process it became clear that the above requirements could be met by nothing short of a quite drastic treatment, i.e. a new ion accelerator had to be designed and built. After setting the task, detailed designing and construction of the new equipment was started.

Assembly of the new ion accelerator started on 15. September 1968. The voltage source was completed by 21. December 1968, and the first voltage test produced a no-load voltage of 6.34 MV. On 10. January 1969 the first /porcelain/ accelerator tube was built in, and from February onwards acceleration tests were carried out with it at normal atmosphere and then under pressure. Based on the experiences gained during these tests, a number of useful alterations were carried through on both the voltage source and the accelerator tube. With these completed, regular nuclear measurements were commenced with the new parameters on 12. March 1970 [3, 61]. The present equipment has the highest accelerating voltage in Hungary and between 12. March 1970 and 19. July 1971 completed 6,253 operating hours.

Main technical data of the new equipment are given on Table I, while the block diagram showing its general layout is presented on Fig. 1.

Table 1

Technical data of the new ion accelerator

Acceleration energy /for single-charge ions/	0.8 - 5.0 MeV
No-load voltage attained, max.	6.34 MV
Acceleration voltage attained, max.	5.28 MV
Types of particle accelerated so far	p, d, He_4^+
Energy stability	$(1.5 - 2.5) \times 10^{-4}$
Analyzed and stabilized ion current obtained at the target, max.	10 µA
Beam diameter obtained at the target, max.	1 mm
Operating pressure of insulating gas	8 - 15 att
Pressure of insulating gas, max.	20 att
Gas mixture composition	70% N_2+24% CO_2+6% CCl_2F_2(F12)
Moisture content of gas mixture, max.	50 ppm (0.05 g/kg)
Type of accelerator tube	homogeneous,inclined field
Length of accelerator tube	3,600 mm
Outer diameter of accelerator tube, max.	306 mm
Vacuum measured at bottom of accelerator tube /during operation/	$(3-6) \times 10^{-6}$ Hgmm
Total cubic capacity of vacuum system	540 litres
Stability of the magnetic field of the analysing magnet	3×10^{-5}
Deflection radius of analysing magnet	522 mm
Energy of deflectable particles, max.	11.4 MeV/amu/acu^2
Charging belt speed	24.5 m/sec
Continuous length of charging belt	8,750 mm
Width of charging belt	450 mm
Height of horizontal drift tube axis	1,360 mm
Total weight of equipment /without the equipments located in the target room/	35 tons
Power requirement of accelerator, approx.	25 kW
Hours of operation completed during 12/3/1970 - 19/7/1971	6,253

Fields of application:

- Basic research in nuclear physics for discovering the structures, behaviour and regularities of nuclei
- Application of nuclear research methods involving the use of electrically charged particles in other fields of physics and technology, e.g. for the activation analysis,determination of doping material in semi-conductors etc.

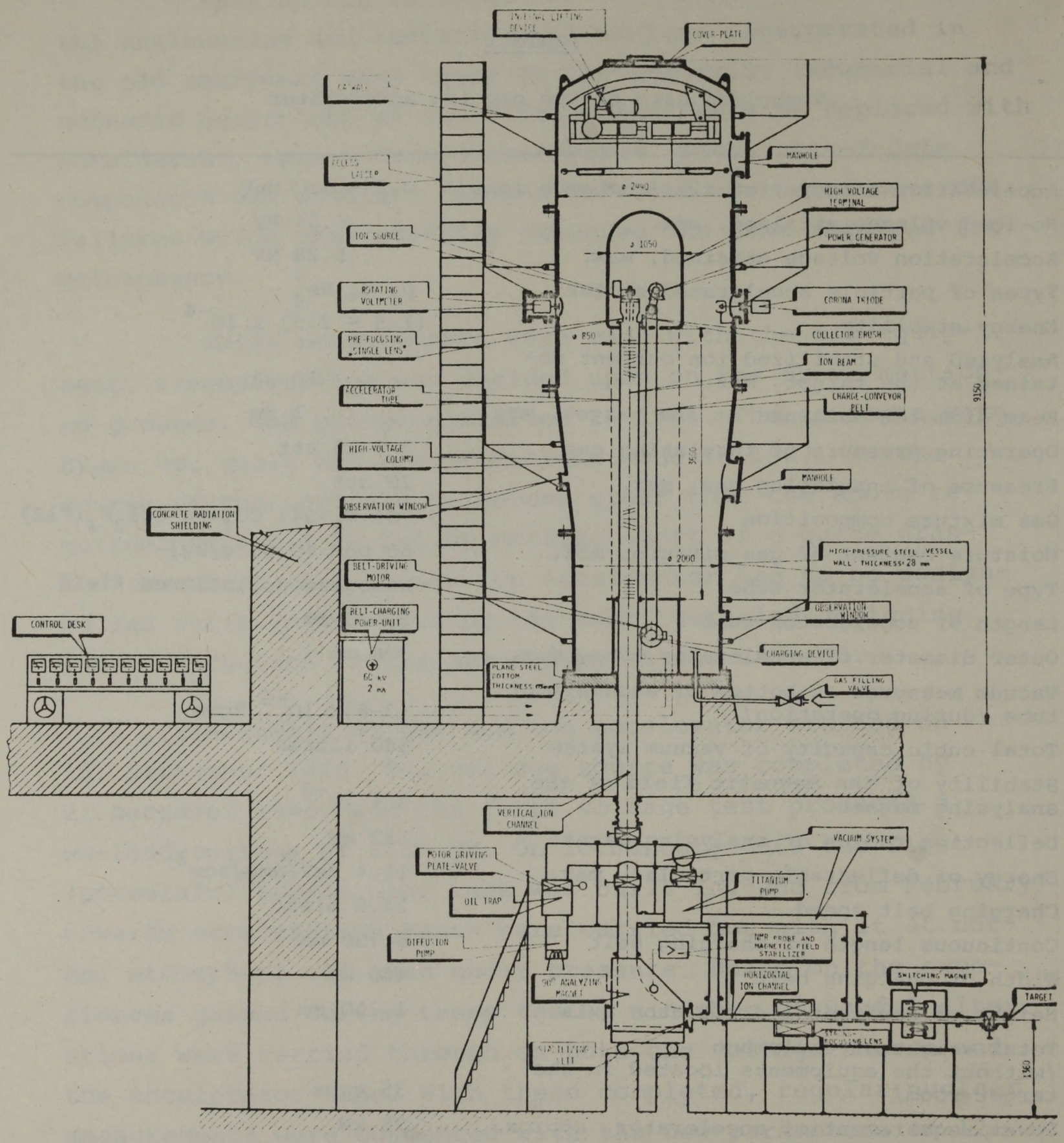

Fig. 1 General layout of accelerator

In order to attain the goals of the reconstruction program, first of all a new voltage source and accelerator tube had to be constructed to change the outdated units [2]. Accordingly, the high-voltage column, pressure vessel and high-voltage terminal of the voltage source were replaced with new units, whereas the accelerator tube underwent dimensional and technological changes.

Following from the requirement of increasing the intensity of particle current, both the ion source and the ion-optical elements coupled to it had to be improved, which involved also the reconstruction of the power supply system. The development of a long-life supply-unit family, which had been started at an earlier date, was thus completed. Increasing of the energy stability required the elaboration of the synchronizable nuclear magnetic resonance stabilizing system of the analysing magnet serving as reference. By making use of this system, the opportunities offered by the other existing stabilizing units could be fully utilized in energy stabilization. In the vacuum system, steel has been replaced with stainless steel, and ion-getter pumps have been installed - although, owing to the envisaged acceleration of He ions, the facilities for exhausting the system by means of diffusion pumps have also been retained, and even modernized.

To facilitate the design of various parts of the new generator, research and development work had to be undertaken on several lines reaching well beyond the limits of conventional engineering practice. Actual manufacture and erection were preceeded by series of laboratory measurements, much experimenting with novel types of technological and manufacturing techniques, elaboration of calculation and dimensioning methods /and where possible their adaptation for computer processing/, design of new series of circuits, and the creation of appropriate measuring and calibration facilities.

In the following chapters, detailed description of the design is given, and the subjects that received most

attention in the course of development are discussed, among others the high-pressure gas insulation, the ion source and its power supply system, the accelerator tube and the stabilization of the analysing magnet. Without aiming at completeness an account is given also of the lines of research followed previous to commencing construction.

I. DESCRIPTION OF DESIGN

1. PRESSURE VESSEL AND THE ELEMENTS LOCATED IN IT

1.1 Pressure vessel

As is generally known, electric strength of the ion acce'erator is maintained by high-pressure insulating gas [4], the pressure of which has been limited at 20 att. The pressure vessel is made up of 5 sections /Fig. 2/, due mainly to such local conditions as the lifting capacity and stroke of the existing crane etc. Maximal internal diameter of the vessel is 2,440 mm and its cubic capacity 34 m^3. The voltage source is mounted inside, on a plane bottom. The latter is 175 mm thick, weighs 5 tons, and is provided with the following passages: accelerator tube passage, observation hole for industrial TV, electric connections, cooling water and insulating gas inlets. Flexible deformation of the plane bottom occurring under internal pressure cannot be neglected. Under maximum pressure, the angle of deflection at the centre of the accelerator tube passage, 215 mm away from the centre of the bottom, was predicted by preliminary calculations to be 0.96 rad, a figure agreeing well with the actual value. This angular deflection had to be taken into consideration when adjusting the accelerator tube.

The vessel section joining the plane bottom is of 2,000 mm internal diameter. This small diameter is possible because the electric field strengths measured over the lowest section of the high-voltage column /i.e. the section next to the plane bottom/ are lower than those measured in the other sections. All five vessel sections are provided with two or

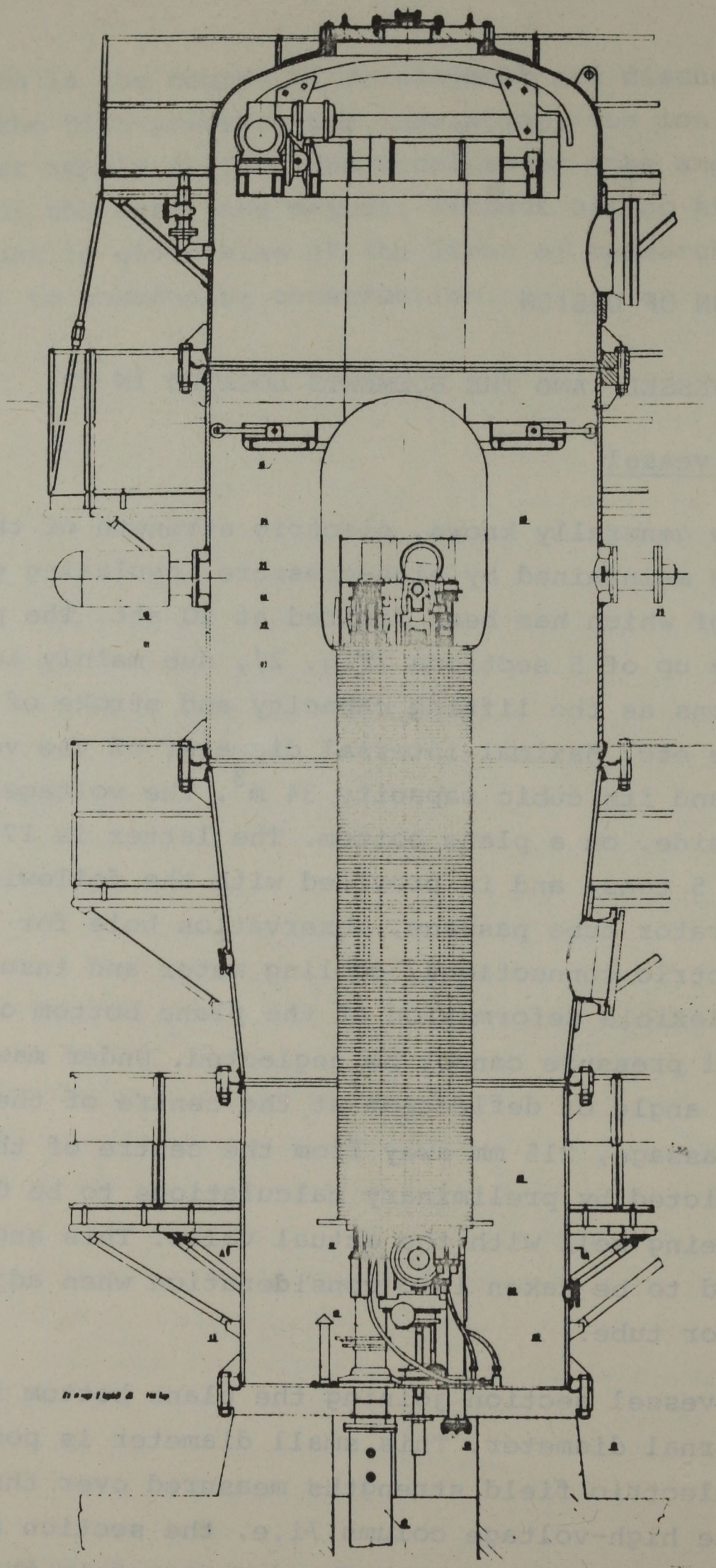

Fig. 2 Construction drawing of pressure vessel and high-voltage column

three 80 mm diam. observation apertures covered with plexiglass. Over the next section upwards - corresponding to the higher electric field strengths - the vessel diameter is enlarged to 2,400 mm and there is a 500 mm diam. manhole to facilitate maintenance. On the following vessel section are mounted the generating voltmeter and the corona triode. Since this section has to withstand the highest electrostatic field, its internal surface is covered with a polished stainless steel lining. The internal surfaces of the other vessel sections are coated with a special paint selected for this task by experiments [5]. The top section of the pressure vessel is covered by a deep-domed bottom. During regular operation, the elevator [6] is located in that section of the vessel.

Since the pressure vessel is made up of 5 sections, the bolting together of the individual units and access to inspection holes, the corona triode and other fittings are facilitated by catwalks assembled from eight segments each for easier mounting and fixed to the fastening flanges at the levels of the four upper sections.

Structural material of the pressure vessel is high--strength boiler plate /41 Ü/. Since the bolts fastening the vessel sections are made also of high-strength material /Cr Mo V 80/, it has been possible to reduce bolt size to M42, thus rendering mounting easy. The pressure vessel has been dimensioned in full accordance with the Standards referring hereto, with the exception of the plane bottom, since at the time of the designing stage of the project no Standard related yet to such bottoms. The plane bottom has been dimensioned by the so-called method of cross-sectional factor equalization [6].

A photo of the pressure vessel is shown in Fig. 3.

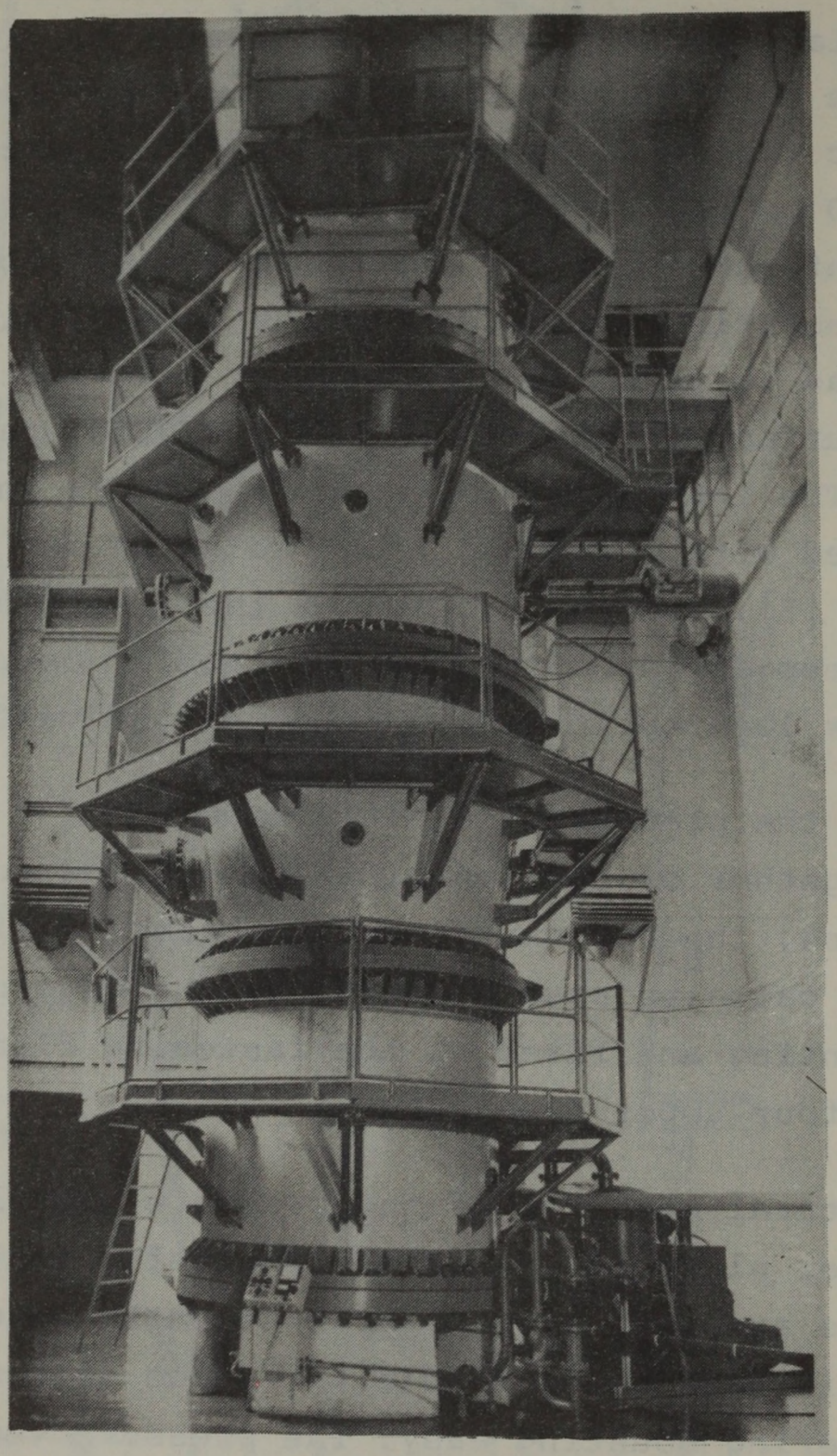

Fig. 3 General view of accelerator

1.2 High-voltage column

The column supporting the high-voltage terminal stands on four symmetrically arranged plexiglass legs fixed by conical fastenings. In order to evenly distribute the electric field strength, frames of 10 mm diam. stainless steel pipe, opening towards the accelerator tube for easy access, are fitted round each support leg at intervals of 25 mm. The charging belt is surrounded by a completely enclosed square section, into which the internal rods serving to equalize the tensions arising along the belt can be snapped. Design of the column, with the belt located inside, is shown on Fig. 4

To screen the inner space of the column from the wall of the pressure vessel, 18 mm high oval-shaped potential rings made of stainless steel can be snapped on to the four spring-type pins located on each frame. Overall dimensions of the column have been determined by electrical requirements. Its length has to agree with that of the accelerator tube, which in the present case is 3,600 mm. The electrical field strength arising between the column and the wall of the pressure vessel, as a function of the ratio of column and vessel diameters, shows a "flat" minimum. In order to reduce the field strength, the dimensions should possibly be near the minimum. With this in mind, a column diameter of 850 mm was selected for a vessel diameter of 2,440 mm /inner dia./ [7,8].

In the course of construction of the high-voltage column, the design was checked for strength in bending. As a result, the 3,600 mm long plexi-glass rods had to be reinforced at three points with some interconnecting structures the rigidity of which exceeded that of the frames. The plexi-glass rods were checked for fatigue caused by vibrations. In the course of this, fatigue measurements were made at the Aeronautics Department of the Polytechnical University, Budapest

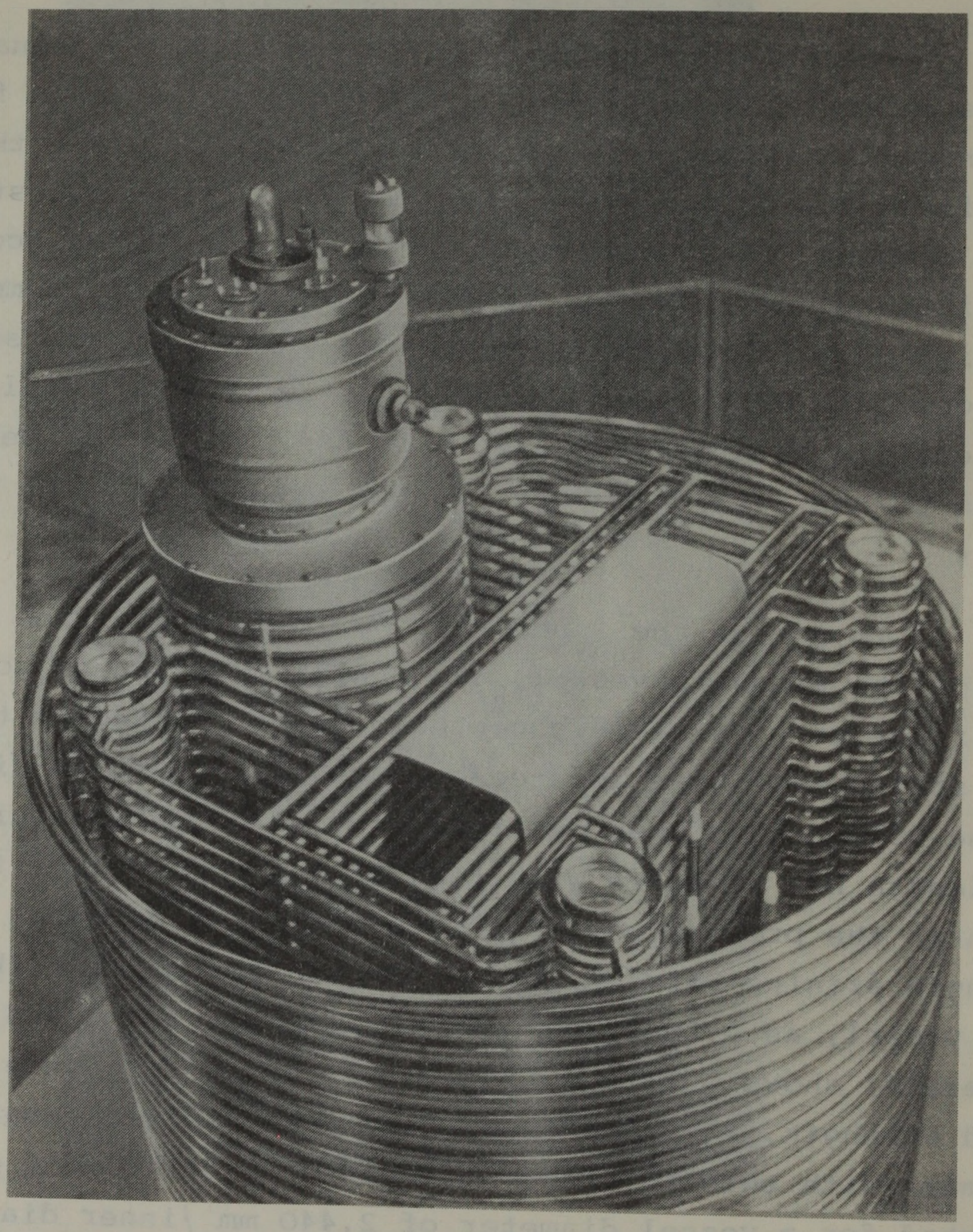

Fig. 4 Construction of insulating column

[6], where it was established that the effect of deflection coincided with that of the deflections and vibrations measured on the assembled column. Accordingly, fatigue fracture of the plexiglass is expected after 8×10^{10} deflections, which means a lifetime of some six and a half years for a max. 7,000 hours of operation per year. The columns can be replaced easily, whenever necessary.

The instruments supplying power to the ion source are switched on and off and controlled by means of dia. 10 mm plexi-glass rods. One each of those rods is located in the holes drilled in the plexi-glass legs which are mounted beside the accelerator tube. The other switching/control rods are mounted within the frame, i.e. in the high-voltage column near the accelerator tube and opposite to the tube, respectively. The high-voltage divider is also located opposite to the accelerator tube. Total value of the resistance provided by the chain is 25 GΩ . There are a total of 138 pieces in the chain, consisting of 4 resistors each embedded in a strong epoxy-resin coating facilitating easy handling. Every four- - resistor set can be loaded with 20 W each. Their value is generally 220 MΩ, with the exception of the resisitors located at the upper section of the column, where the values of the sets have been selected to suit the focussing requirements.

1.3 Charging belt drive

The charging belt drive mechanism is mounted under the insulating column. The charging belt runs over the pulleys of drive mechanism and the high-voltage terminal within the insulating column. The lower pulley is driven from both sides by a 7 kW electric motor which is coupled through flexible couplings to the ends of the shaft of the pulley; the upper pulley runs free. Since the charging belt drive mechanism is

mounted to the high-voltage column, the rotary components have been dynamically trued with special care, and appropriate attention has been paid to damping vibration [6].

Even running of the belt requires a tensioning force of at least 300 kp per strand, as well as tiltability of the lower pulley. Both these requirements are met - even when the pressure vessel is closed - by means of a power-driven mechanism. The speed of belt tensioning is 64 mm/minute, and that of pulley tilting 13.5 mrad/minute. The degree of belt tensioning can be measured by means of a force meter developed especially for this purpose and coupled to the holder of the lower pulley. Tensioning force is measured by sensing the deformation of a spring and establishing the change occurring in inductivity.

The belt pulleys are slightly crowned, their nominal diameter being 160 mm. The outer surfaces are hard chromium-plated and ground. Pulley speed is 2,930 r.p.m., producing a belt travel speed of 24.5 m/sec.

1.4 High-voltage terminal

A frame structure made up of vertical support members and horizontal plates, on which the auxiliary electronic and other equipment of the ion source are mounted, is located on the plate supporting the high-voltage terminal and closing the column at the top, and at the same time the internal space of the terminal /Fig. 5/.

At one of the levels of the frame structure is the supply generator, supporting a fan. Its function is to supply the power to the ion source. The generator is driven by the upper belt pulley through a V-belt. The fan mounted on the supply generator has two functions: cooling the entire internal space of the terminal by change of gas, and providing

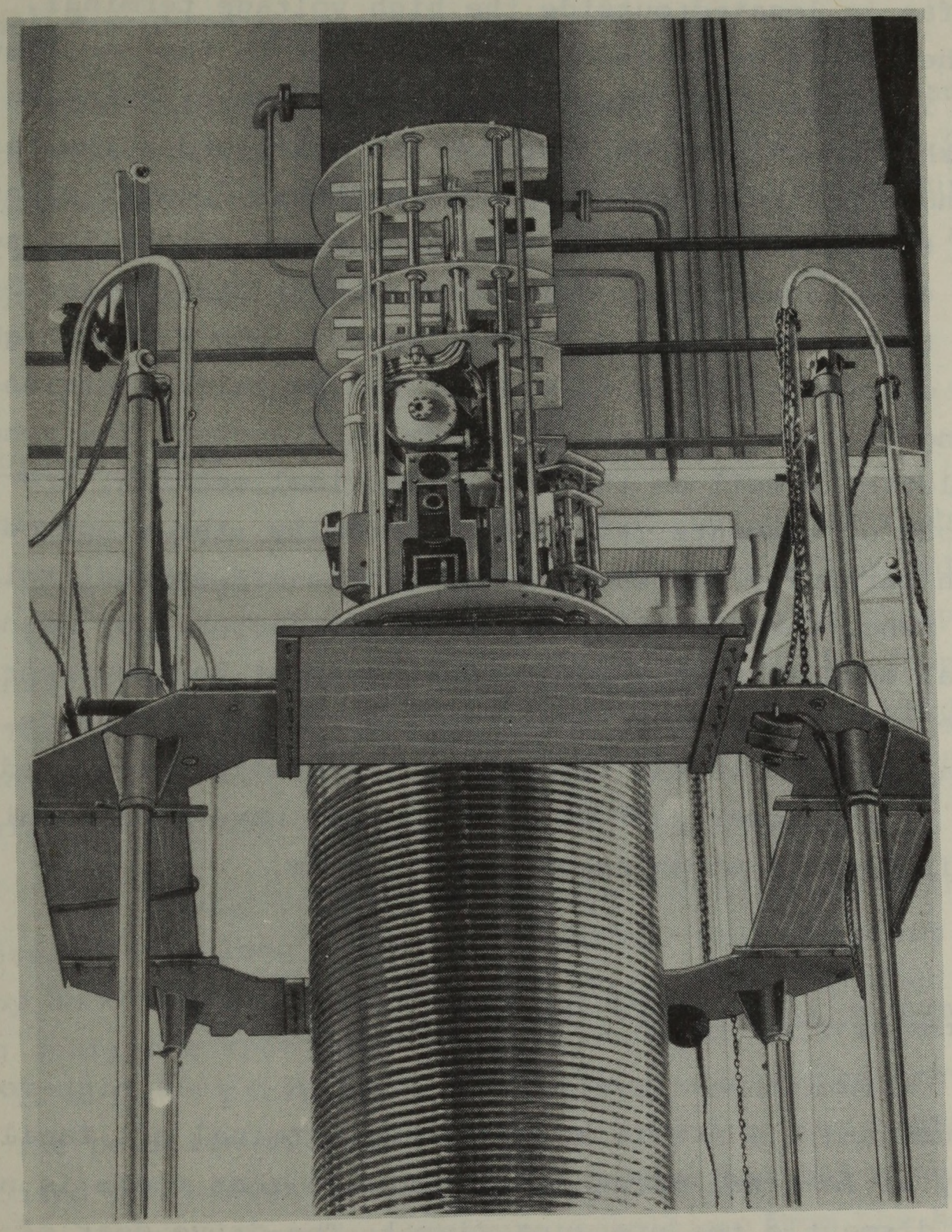

Fig. 5 Internal construction of high-voltage terminal

an adequate cooling for the ceramic triodes of the oscillator and the glass bulb of the ion source. Accordingly, the inlet of the fan is located outside the high voltage terminal, while the gas is delivered from the outlet to the oscillator and the ion source via plastic tubes. The gas circulation established in this manner between the space under the terminal and other parts of the pressure vessel is sufficient to keep the temperature in the neighbourhood of the ion source down to 42°C, even though the internal heat dissipation below the terminal generally reaches approx. 600 W. The high-voltage electrode itself is made of 1.5 mm thick stainless steel and is 1,600 mm high, 1,050 mm in diameter. The spherical calotte,as well as the lower spherical section, are welded out of segments /Fig. 2/. Externally, the electrode has been carefully polished. Inside there are several reinforcing ribs. The electrode has been manufactured by means of a special manufacturing process developed at the Engineering Department of the Central Research Institute for Physics. The spherical calotte at the top and the carefully calculated profile of the lower part of the terminal have been machined to specifications to an accuracy of ± 1 mm.

1.5 Elevator in pressure vessel

Maintenance and repair of the 3.6 m tall high-voltage column and 1.6 m tall high-voltage terminal are facilitated by an internal maintenance lift, so that there is no need to dismantle the pressure vessel. The drive gear of the elevator and /during acceleration/ the annular lift platform are housed in the upper dome of the vessel. In use, the platform can be moved down the voltage column and the high-voltage electrode as far as the level of the pressure vessel manhole: its outer diameter is 2.040 mm and its inner diameter 1.100 mm. The platform is prevented from horizontal swinging by 4 roller-type arm braces spaced at 90 degrees around the

periphery. The electric field is protected from deformation during acceleration by a screening plate of the appropriate bend radius mounted on the bottom of the platform.

Load carrying capacity of the lift is 300 kp, and speed of travel 1 cm/sec. It can be controlled by means of push-buttons mounted on the platform and on the outer surface of the pressure vessel. Labour safety is ensured by the appropriate safety and signal equipment.

1.6 Corona triode

The corona triode assembly [9] serving for stabilizing of high voltage produced by the generator is located opposite the high voltage terminal, on the mantle of the pressure vessel. The assembly can be moved along the horizontal axis. The head, consisting of a needle holder and a grid cap, is located in a high-pressure chamber, whereas the moving mechanism is mounted outside the chamber.

The corona triode head can be radially moved in the pressure vessel along a length of 500 mm. This movement is made by an electric motor Type VTP 114/4 acting through a reducing gear; the speed of travel produced is 23.5 mm/min. There is a limit position switch at each end of the travel path. The position of the head is indicated on the control desk based on through sensing by a 10-turn helical potentiometer. In order to prevent seizure resulting from the horizontal arrangement, the head runs along a roller-type guideway. The drive gear is protected from breakage by a spring-loaded claw coupling.

Independently of the above-mentioned mechanical moving, the corona needle assembly and the grid cap can be also manually positioned to an accuracy of 0.02 mm, even when the pressure vessel is closed. This serves for adjustment of the

amplification factor of the corona triode acting in the stabilizing circuit. The needle holder accommodates eight ICH-80 sewing-machine needles. The needle holder can be replaced with ease. The grid cap is made of polished stainless steel.

1.7 Accelerator tube

The most important component of the high-voltage section is the accelerator tube, which is located parallel to the axis of the high-voltage column, offset at 215 mm.

In conformity with the structure of the high-voltage column, the accelerator tube consists of 3 parts. Every part ends in a steel end flange, and is joined to the following part by a rubber seal. Overall length of the accelerator tube is 3,600 mm, and overall diameter 306 mm.

Each accelerator tube part consists of glass insulating rings and aluminium electrode support rings, cemented together with polyvinyl acetate to form a sandwich-like structure. The replaceable VD50 alloy accelerating electrode of each section is a sheet held through its own flexibility in the inner groove of the electrode support. There are two types of electrode: one has the normal to its face aligned with the axis of the tube, the other type has its normal inclined at an angle of 11 degrees to this axis. The central bores of the electrodes located perpendicular to the axis are circular, with a diameter of 30 mm, whereas those of the inclined electrodes are of 30 x 60 mm /Fig. 6/. The electrode support rings are spaced at 25 mm, measured between their centre lines. In the lower and upper tube thirds there are 47 insulating rings each, and in the central third part 46 rings, making a total of 143 accelerating electrodes incorporated in the tube. On the outer rims of the electrode support rings overhanging the glass insulators high-voltage screening rings are mounted, into the grooves of which the

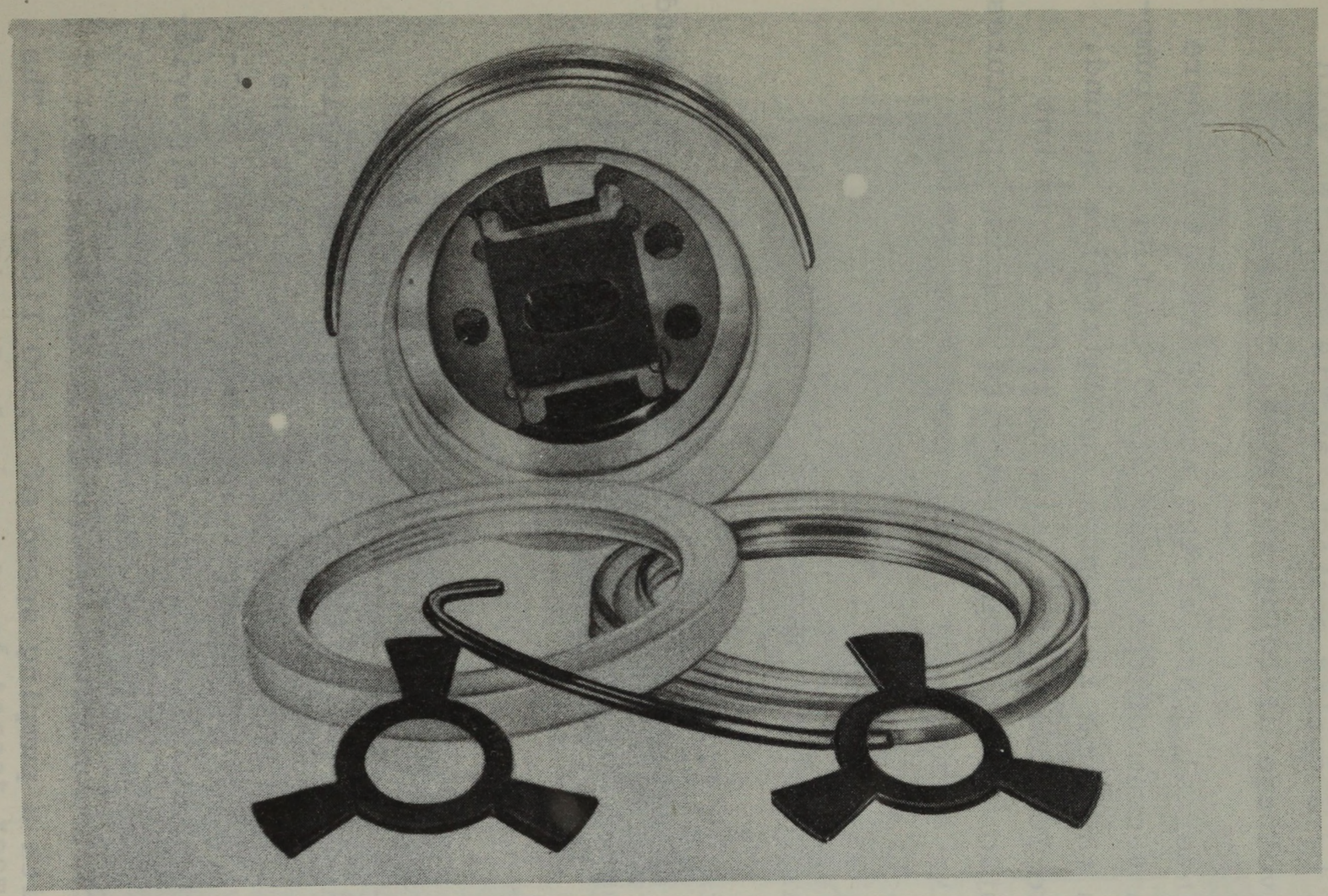

Fig. 6 Design of accelerator tube

spark gaps protecting the electrodes against breakdown. are fitted; there are 8 spark gaps for every electrode. Each electrode support ring is coupled to the column frame located at the same level by a spring contact, and is supplied with voltage from the voltage dividing resistor.

In the internal space of the accelerator tube there is at all times a vacuum of the order of 10^{-6} mm Hg. The pumping speed through the tube is approx. 15 litres per second. Since the aperture located in the axis of the tube is not enough for exhaustion, there are a number of pumping apartures in a labyrinth-like arrangement in the electrode system.

2. ELEMENTS LOCATED OUTSIDE THE PRESSURE VESSEL

The units of equipment located in the target room serve partly for transferring the accelerated particles towards the target and partly for producing the necessary vacuum /Fig. 7/.

2.1 Vacuum system

The vacuum system of the generator, the schematic representation of which is shown on Fig. 1, serves for the pumping of partly the accelerator tube, and partly the sections located around the target. The vacuum system is provided with two types of pumping system, one of them containing 2 parallel-connected ion getter pumps [10], and the other a diffusion pump with a pumping speed of 3,500 litre/sec. The individual sections of vacuum system are separated by gate valves. For fore-vacuum exhaustion of these, and also to provide a fore-vacuum for the diffusion pump, two DUO 25 rotary pumps manufactured by the Balzers Gruppe are employed. In order to prevent the backward flow of oil vapours from the diffusion pump, an oil trap containing a freon-filled refrigerator and a liquid nitrogen cold trap have been inserted

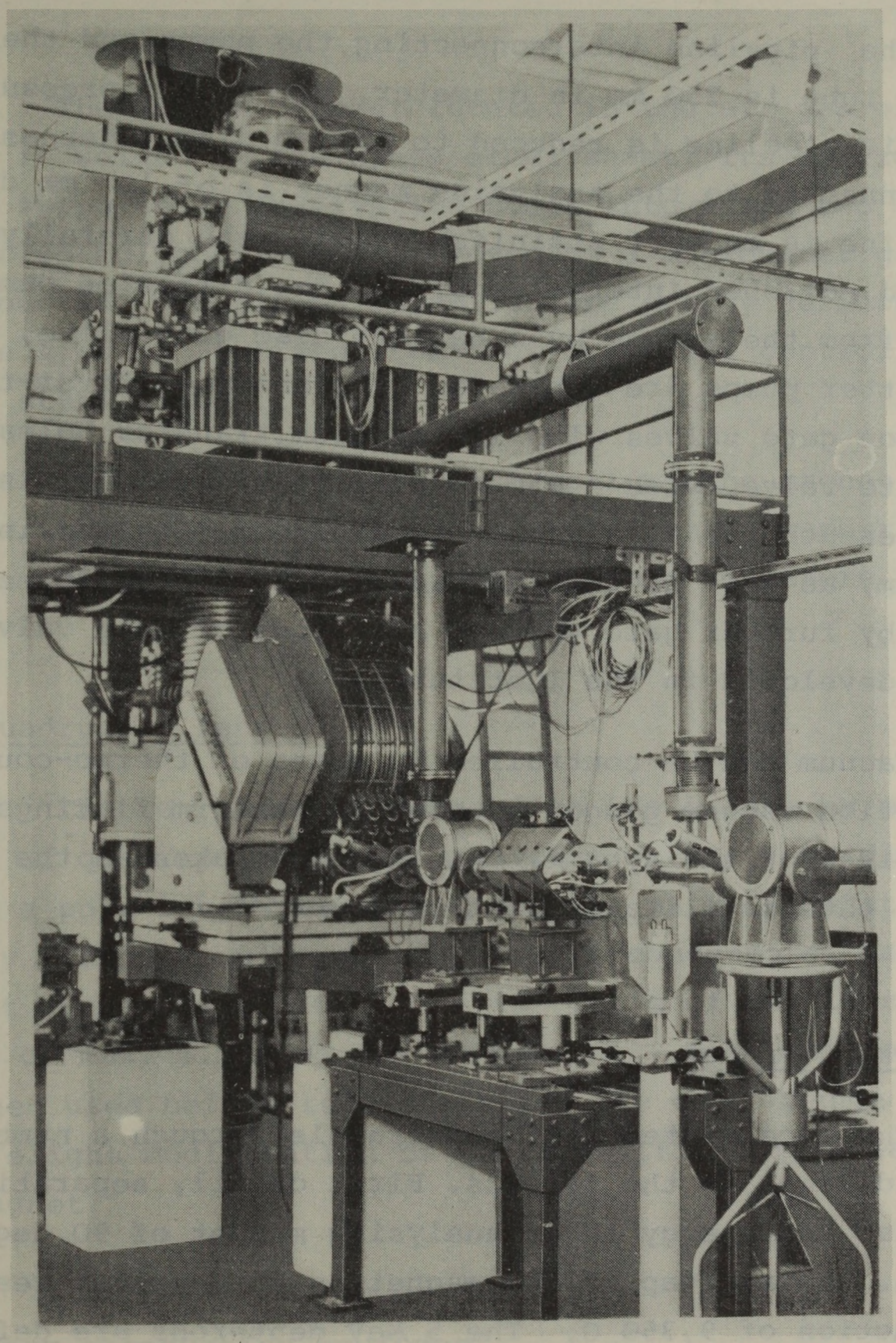

Fig. 7 Equipments of target room

into the system. The rotary pumps also operate through a liquid nitrogen cold-trap.

The pipeline interconnecting the pumps and the accelerator tube is 250 mm in diameter. Within the pressure vessel, this pipeline is reduced to 180 mm diam. whereas the section connected to the analysing magnet is of 100 mm diam. The pipeline is made of stainless steel, with carefully cleaned and polished internal surface. The diffusion pump is separated from the system by a Balzers disc gate valve, and the ion getter pumps are separated by mechanical lever-type quick-action gate valves with 160 mm diam.transfer holes. A similar gate valve, with a 250 mm diam.transfer hole, is mounted beneath the accelerator tube. The drift tube in the target room, as well as the individual target facilit are separated by further gate valves. All types of gate valve have been developed in the Institute.

Vacuum can be controlled by means of thermo-couple and ionization vacuum gauges mounted in uniform fittings at several points of the system. Readings are taken in the control room, thus facilitating central control.

2.2 Analysing magnet

The accelerated ion beam travels through a number of important devices to the targets. First of all, separation is made by mass and energy in an analysing magnet of 90 deg. deflection. The air gap of the magnet is 25 mm wide, resulting in an induction of 9,350 G. The 5 MeV deuterons are deflected at a radius of 522 mm. Maximal excitation is 25.000 amper turns. The coil is made up of water-cooled sheets and self--carrying coil elements forming a sandwich-like structure. The coil is supplied with power by a 6 kW 25 A motor-generator aggregate.

The magnet, weighing approx. 3.5 tons, is supported by a strong stand which is in turn, supported by concrete

legs. The stand has been designed to allow shifting of the magnet in three directions and tilting and turning about three axes.

The vacuum chamber located in the air gap of the magnet is welded of stainless steel sheet. Its horizontal outlet supports an observation block into which two insulated and cooled molybdenum plates moved by a micrometer gauge have been mounted. The plates establish the energy defining gap, and the signals received from them serve for controlling the energy stabilizing circuit.

In the course of reconstruction, the magnet was provided with a new coil, support stand, vacuum chamber and slit assembly; its core remained the same as before.

2.3 Quadrupole lenses

The ion beam is focussed on the target by means of a pair of quadrupole lenses provided with a lens diameter of 40 mm, a pole length of 390 mm for the pair. Excitation is made by a supply unit made up of semi-conductors having a current stability of 10^{-3}. The 4Ω coils of the lenses apply a load of max. 4.5 A on the supply unit. This pair of lenses had been used before reconstruction the only change to them being slight modification of their positions in relation to the magnet.

2.4 Beam observation equipment

The ion beam can be observed by instruments and visually alike. For visual observation, quartz plates can be pushed into the path of the ion beam before and after the analysing magnet, after the quadrupole lens and in the target channels. Position and focussing of the ion beam can be controled during acceleration by means of a rotary beam indicator [11] device located after the quadrupole lens.

2.5 Switching magnet

The switching magnet [2], which had been in use also before reconstruction, serves for distributing the ion beam to 3 measuring stations. At an excitation of 10,000 G, 5 MeV deuterons are deflected at 40 deg., plus or minus. In this manner, 3 target positions can be established. This magnet is especially suitable for operating new the target fittings located at a distance of approx. 1 m, since even under maximal excitation its field can not interfere with nuclear measurements or the functioning of the detecting instruments. The magnetic field strength measured at the outer surface of the magnet has not exceeded several 10 G.

3. LAYOUT

3.1 Generator room

The accelerator equipment has been erected in an existing building [12], which had accommodated the previous generator. The position of the ion beam remained essentially the same as before. Yet even though dictated from the start by static strength considerations inherent in the given structure of the building, with no possibility of changing it, this layout caused no problems. Height of the building was similarly given, together with the lifting gear of the pressure vessel. Consequently, both the height of lifting and the lifting capacity suited the parameters of the former generator. By constructing the pressure vessel from several sections it was possible not only to make full use of the above conditions, but to turn them into advantage in both mounting and handling the equipment. The generator room is 12.6 m long, 9.61 m wide and 15.0 m high. The overhead runway of the pressure vessel lifting mechanism is located 13.5 m high, and the crane for mounting works runs 11.0 m high. By means of the above two erecting facilities, as well as rollers and rails, mounting and repair can be undertaken at practically any point of the

generator room. Experience has proven that the present floor area is sufficent to perform any work under normal conditions.

3.2 Target room

Nuclear experiments are carried out in a 12.6 x 8,5 m room located under the generator room. The target room is accessible directly from the generator room through a short flight of steps, and indirectly through a "Z" shaped protection gate from the main staircase of the building. Both the target room and the generator room are shielded off from the adjoining rooms by 1 to 1.6 m thick concrete walls that offer adequate protection even at a yield of 10^{12} neutron/sec. In the course of experimentation it became clear that the nuclear experiments require more area than was available at the time, thus the construction of two new rooms of 13 x 13 m^2 and 6 x 8 m^2 floor area, respectively, has been started. The new rooms are expected to be completed in the near future and will adjoin the present room through a 2 x 5 m^2 aperture to be made on the existing wall.

3.3 Control room

The generator is controlled from the control room, from which the generator room can be approached through another protection gate. Cable ducts run in the floor both within the control room and in the directions of the generator room and the target room. The cable ducts accommodate the control, test and actuating cables.

3.4 Measuring rooms

The measuring rooms accommodating the electronic instruments required for nuclear experiments are adjoining the target room. The measuring stations are interconnected with

the measuring instruments by cable ducts running along the walls. These accommodate the signal and other cables running into the measuring centre used for multi-parameter measurements and the other two measuring rooms, respectively. In the measuring centre there are a small computer Type TPA 1001, a 4096-channel analyzer and the auxiliary units required. Over and above these instruments, a 1024-channel analyzer, one or more 512-channel analyzers, analog circuits and various detectors are also available.

3.5 Communication system

Besides the control and power lines closely associated with the operation of the generator, also regular communication has been established between the above-mentioned rooms. This system consists of two amplifier channels, as well as a sufficient number of microphones and loudspeakers to facilitate the establishment of any variation of verbal communication between the rooms concerned. This applies also to the vessel of the generator, where communication can be made by either loudspeaker or headpiece.

II. HIGH-VOLTAGE PROBLEMS

1. GENERATION OF HIGH VOLTAGE

A precondition of faultless functioning of the generator is that high voltage required for ion acceleration must be safely produced with a minimum of fluctuation also without the use of the energy stabilizing system. It is not sufficient to combat the problems arising from the increasing dimensions of the equipment and the ever higher voltages [13, 14, 15] by maintaining electrostatic field strength as low as possible. It is also necessary to examine the factors influencing the insulating capability of the insulating gas /e.g. humidity content, gas composition, surface finish of the electrodes/ in order to generate reliable voltages. The geometrical dimensions of the high-voltage column and the high-voltage terminal have been determined in accordance with the designs generally adopted for electrostatic installations [16, 17] and specially applied for electrostatic accelerators [18, 19]. The special tests carried out on the insulating gas will be dealt with later on.

Stability of the high voltage may be endangered even if the high-voltage insulation between the high-voltage column and the earthed wall of the pressure vessel fully meets the requirements, since it is particularly influenced by the processes occurring within the high-voltage column. The discharges taking place not only in the accelerator tube but also along the column may result in voltage surges which simply

cannot be compensated by the stabilizing system and thus lead to alteration in the ion beam position, especially in an inclined field accelerator tube.

The charging belt of the generator has been left unchanged, but care has been taken to carefully adjust and control its running /belt tensioning mechanism, measuring of tensioning force, observation facilities etc./under the operating conditions provided by the novel design. The charging mechanism, on the other hand, underwent some significant changes in the course of reconstruction in order to improve surface uniformity of the charge. Another advantageous change achieved by the new design is the improvement in the stability of the voltage dividing resistor.

1.1 Insulating gas

As mentioned before, the voltage strength of Van de Graaff generators is particularly influenced, besides by the geometrical design, by the dielectric strength of the insulating gas, itself dependent on a number of factors, and also by the surface conditions on the high-voltage electrodes.Accordingly, tests have been carried out on the humidity content, the drying of gas influencing it, surface finish of the high-voltage electrodes, as well as the effects of dust content and gas composition. Although many data have been published on this subject [13, 14, 15, 20], during the construction of the generator a number of questions had to be cleared by obtaining concrete data on the spot.

The effect of humidity content of the gas on dielectric strength has been studied by several authors [21, 22 et al.]. Since, however, these tests were not sufficiently extended on conditions under pressure, detailed measurements have been performed in this respect. The test equipment required - an evacuable and pressurizable vessel with a high-voltage electrode, and a measuring equipment for the de-

termination of humidity content - had been prepared beforehand [23] . Great care was exercised in calibrating the hygrometer; the calibrations were made down to a dew point of -50°C over the pressure range of 1 to 15 att. It was found that the differences obtained between the measured and actual dew points depended on the design of the freezing vessel. By suitably modifying the design, good agreement of the measured and actual values was achieved.

Breakdown tests were performed in the test vessel filled with gaseous N_2 and $N_2 + CO_2$ gas mixture, respectively, with various absolute humidity contents. Thereafter, tests were carried out in a homogeneous field with plane and dia. 60 mm Rogowsky electrodes, at a gas temperature of $\vartheta = 20°C$ and under pressures of 6 and 10 att. Test results are shown on Fig. 8. "U" stands for the breakdown voltage obtained at the humidity content given on the Figure, and "U_o" for the breakdown voltage associated with an absolute humidity content of x = 0.1 g/kg; the latter value was chosen for its easy evaluability. As apparent from the measurements, the ratio of U to U_o is independent of pressure, being dependent only on the absolute humidity content of gas. Practically the same results were obtained in nitrogen and N_2 + + CO_2 mixture. The absolute value of tension, of course, depends on the gas composition and the pressure applied.

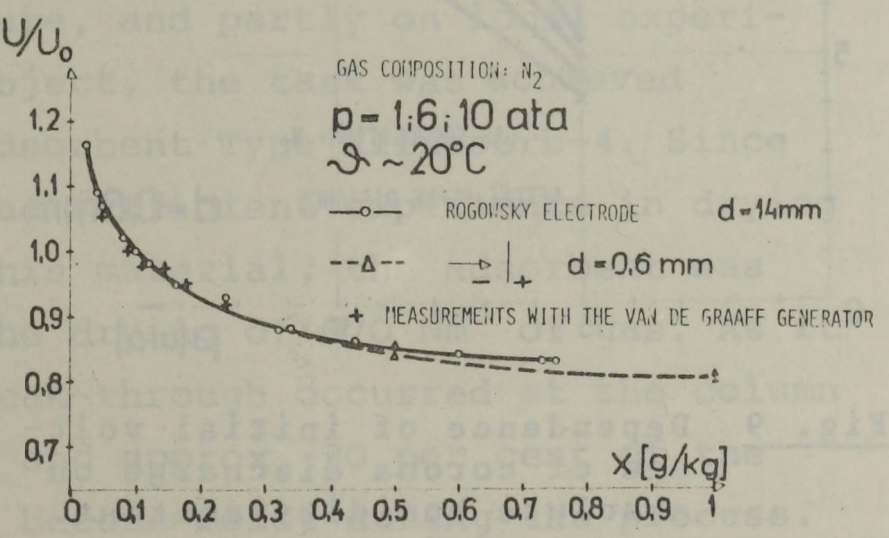

Fig. 8 Variation of breakdown voltage as a function of absolute humidity content of gas

The tests were extended also to an inhomogeneous field. By arranging needles of negative polarity opposite a plane of positive polarity, not only could the change in breakdown voltage be examined as a function of the humidity

content and pressure of the gas, but the entire characteristic of the corona discharge /I = f/U// and observations on its formation could also be made in the course of the individual measurements. One of the most important observations in this respect was that the initial voltage of the corona discharge rose with increasing humidity content /Fig. 9/, until the percentile change in breakdown measured at the tested gaps completely coincided with the results obtained in the homogeneous field.

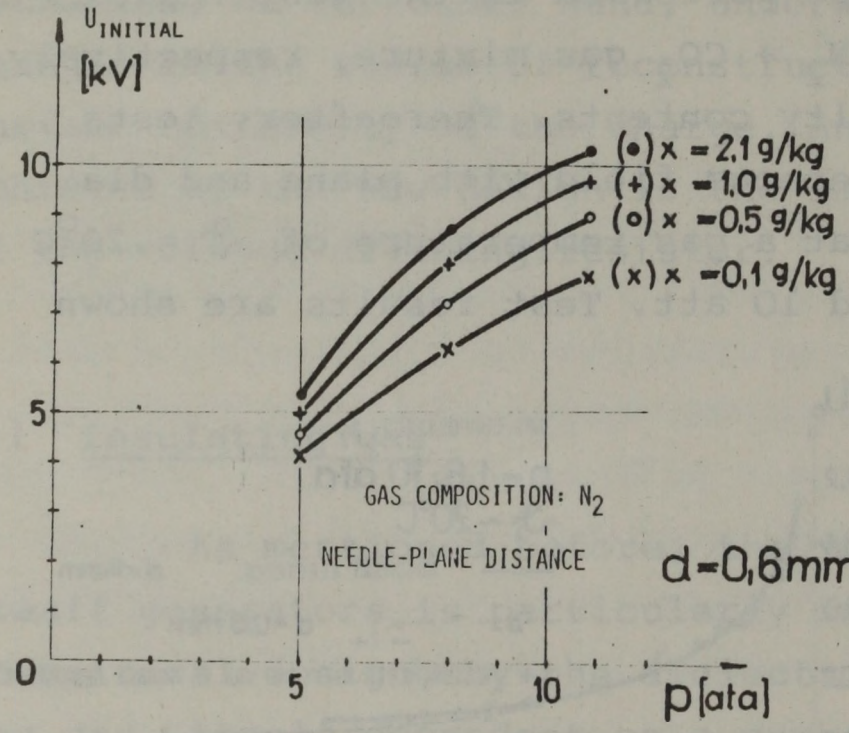

Fig. 9 Dependence of initial voltage of corona discharge on absolute humidity content of gas

With the knowledge of the correlated data of absolute humidity content, gas composition and gas temperature obtained during the several years of operation of the old accelerator, a significant amount of information was available also on the conditions prevailing with a large spark gap. These data coincided well with the measurements obtained with the test vessel, and agreed with the experiences gained with the new generator.

All the above test results have unequivocally proven the fact that breakdown voltage depends on the changes occurring in absolute humidity content, the voltage produced at a given spark gap being the higher the lower the humidity content of insulating gas. This effect is of special importance if $x > 0.1$ g/kg. If, on the other hand, $x < 0.1$ g/kg, breakdown voltage depends hardly at all on absolute humidity content.

The above data emphatically stress the necessity of gas drying for Van de Graaff generators, indicating also quantitative requirements. The reduction of humidity content required the solution of a complex problem. First, drying of the gas charged into the generator had to be solved, and second, it had to be seen that no adsorbed humidity remained in the vessel and on the internal surfaces of the equipment previous to gas charging. Although the insulating gas used contained approx. 70 % N_2 + 24 % CO_2 + 6 % Fl2, the drying process was dimensioned to suit the characteristics of the commercial nitrogen, since humidity content of the mixture was determined mainly by the largest component, N_2. Owing to the very high price of "extra dry" gas, which is almost out of the question in this country, the facilities necessary for gas drying were established. Based partly on examples quoted in technical literature, and partly on local experiences [25] gained on the subject, the task was achieved by using molecular filter adsorbent Type Klinosorb-4. Since not even the Manufacturer had sufficient experience in drying large volumes of gas with this material, the adsorbent was examined after completing the drying of 670 Nm^3 of gas. As it turned out, the level of break-through occurred at the column height originally expected, and approx. 30 per cent of the 3,200 g filter material had become moist during the process. Actual drying capacity of the material was established at 6.4 per cent. By means of the outlined system it was possible to dry the commercial gas to a humidity content of $x = 0.0003$ g/kg.

In the course of the operation test, also the regeneration of the molecular filter was completed. Previous to regeneration, the position of break-through level had been clearly visible, since the colour of the molecular filter having no more free drying capacity had by then changed from the original lilac color. Regeneration was achieved by heating the absorbent to approx. 400 ^{o}C in a furnace, filling it in hot condition into the filter cylinder, and pumping the latter at once to a vacuum of $p < 1$ mm

mercury. The regenerating effect of the heat treatment was clearly visible from the colour of the molecular filter, which turned back to lilac.

Besides drying the gas in the above manner, it is necessary to see that the dried gas be prevented from getting moist again on account of any humidity remaining in the atmosphere of the vessel to be filled. The latter is dried by evacuating it, together with the storage vessels, to 3×10^{-2} mm Hg by means of a pump aggregate with a pumping speed 2×175 n^3/hour. According to our experiences, this vacuum has to be maintained in the vessels for 4 hours in order to free the internal surfaces from the adsorbed humidity.

The effect of humidity contained in the insulating gas is twofold: it partly determines insulating characteristic of the gas, and partly - by being adsorbed on the surfaces - interferes with the voltage strength of the surfaces. Regarding this, data have been obtained by voltage measurements performed on the test vessel and the generator. Over the usual pressure range, the voltage strength of the generator has been found to be proportional to $\sqrt{p}$. If the humidity content of insulating gas is $x > 0.04$ g/kg, this proportion does not apply, and voltage strength of the generator drops by a multiplication factor corresponding to quotient F. On Fig. 10 a

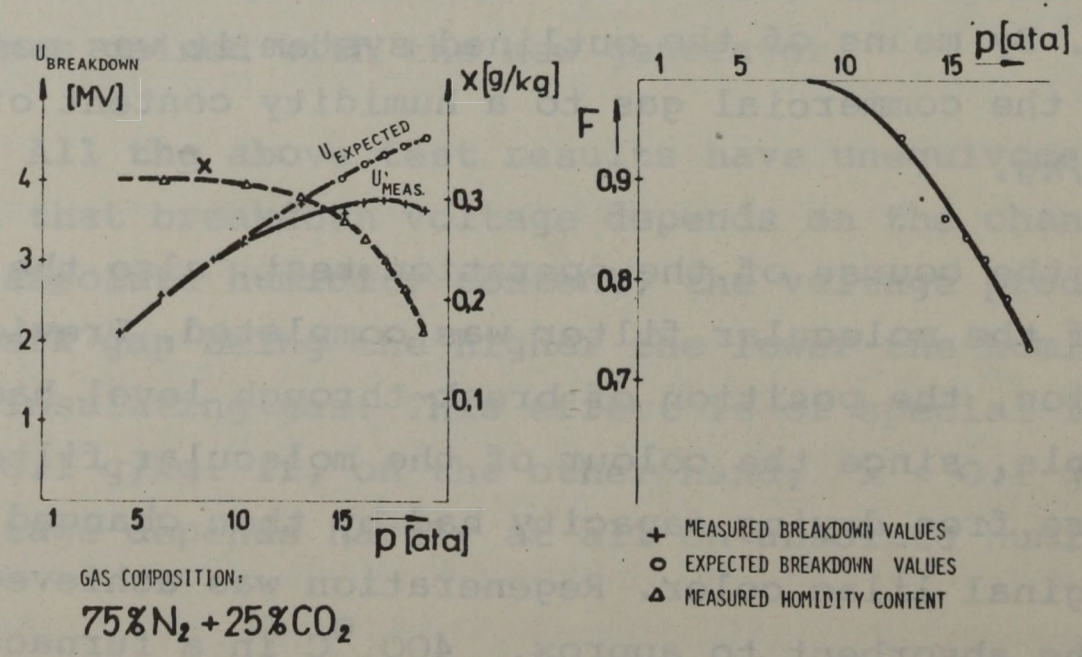

Fig. 10 Anomalous behaviour of breakdown voltage

diagram illustrating this phenomenon is shown, where U_{meas} stands for the measured breakdown voltages, U_{exp} for the values expected on the basis of proportionality to $\sqrt{p}$, and x for the absolute humidity content of the gas. The ratio obtained between the measured and expected breakdown voltages indicates a higher degree of interference than originally expected from the knowledge of the humidity content. The drop occurring in the humidity content of gas with the increase of pressure deserves mentioning, since the gas delivered into the system had a constant humidity content. It follows that with increasing pressure water must have been adsorbed in the generator and so led to a drop in the actual breakdown voltage in relation to the expected value. From the curve of Fig. 11, taken with a significantly drier insulating gas, it is apparent that there is no longer any difference between the measured and expected breakdown voltages. The data for both this and Fig. 10 were obtained with a vessel whose internal wall surfaces had been coated with nitro-silver paint applied on a red lead base coating. Since, however, the latter coating had a detrimental effect on the generator, model-scale tests were carried out with various coatings, using gases at a pressure of p = 7.5 att with an absolute humidity content of x = 0.05 g/kg and a relative humidity content of 100 %. For one of the investigated paints, the value of breakdown voltage obtained in moist conditions was 45 to 66 per cent of the value got in the

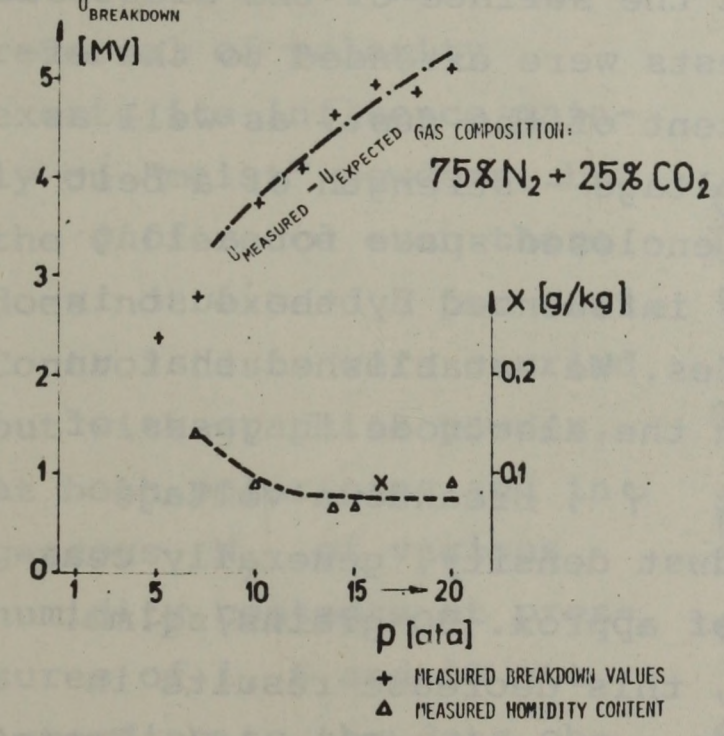

Fig. 11 Breakdown voltages obtained after careful drying

case of dry gas. The three-component protective coating finally chosen for the internal surface of the generator shows a difference of not more than 2 per cent between the moist and dry values [5]. The most critical vessel element, the cylinder located opposite to the high-voltage terminal, has been covered with stainless steel sheet. Besides the above aspects, this coating serves also to prevent the surface from damages caused by possible breakdowns.

The effect of dust content on spark discharge in normal atmosphere has been investigated also by other authors [13, 27, 28], but as far as we know, nobody has dealt with this phenomenon under pressure, as a consequence of which tests were performed up to 10 att [63] in the course of which the effect of the dust settled on the surface of the electrode was examined. Subsequently the tests were extended to the effects caused by the moisture content of the dust, as well as the pressure and polarity. The voltage - strength of a belt - generator that is operated in an enclosed space for a long period of time may be particulary influenced by the dust inevitably settling on the electrodes. We established that under the effect of dust applied on the electrode in gases of various relative moisture content φ , breakdown voltage tended to drop as a function of dust density, generally ceasing to decrease above a density of approx. 30 grains/sq.mm. In relation to various materials, this decrease results in voltage drops ranging from 3 to 10 per cent /Fig. 12/. Grain size of the dust represents in this case changes of several per cent. On testing dusts of various humidity content, it was also found that the effect of the humidity content adsorbed by the dust applied on the electrode is sufficient to decrease breakdown voltage in some cases by as much as 35 per cent for "moist" dust, whereas the same effect hardly reaches 10 per cent for "dry" dust /Fig. 13/. The above measuring data underline also the effect of the specific resistance of dust grains. As long as dust is an effective insulator, a voltage drop of

approx. 5 per cent is observed. However, with the conductivity of the dust increasing, e.g. as in the case of powdered sugar which, although having a high specific resistance, is water-absorbent and thus gradually becomes conductive/ or other conductive powders /e.g. graphite/, breakdown voltage gradually decrease by as much as 25 or 35 per cent. Also the reversal of polarity exerts its influence mainly on "moist" powders, but the difference even there does not exceed 5 per cent. Control tests were carried out with graphite powder, at both polarities and in gaseous N_2 of various humidity contents at pressures of 1, 6 and 10 att. According to the data obtained, the ratio between U and U_o was independent of the pressure, depending entirely on the humidity content of gas /Fig. 14/. These tests yielded data not only on the effect of dust on breakdown voltage, but also on the greater voltage decreasing effect of "moist" powders. Accordingly, the drying of gas plays an important role in respect to this factor too.

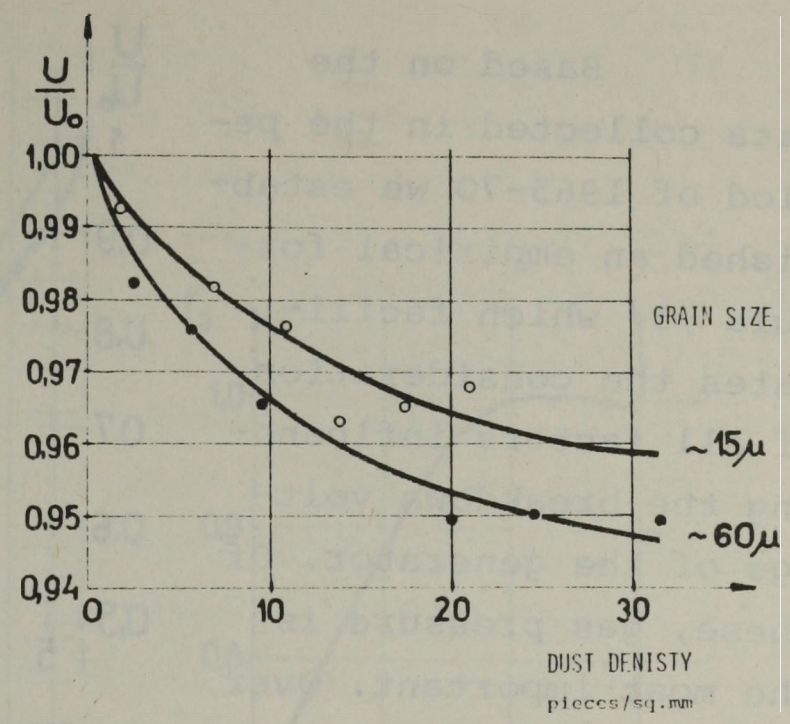

Fig. 12 Effects of various sizes of dust particle on breakdown voltage

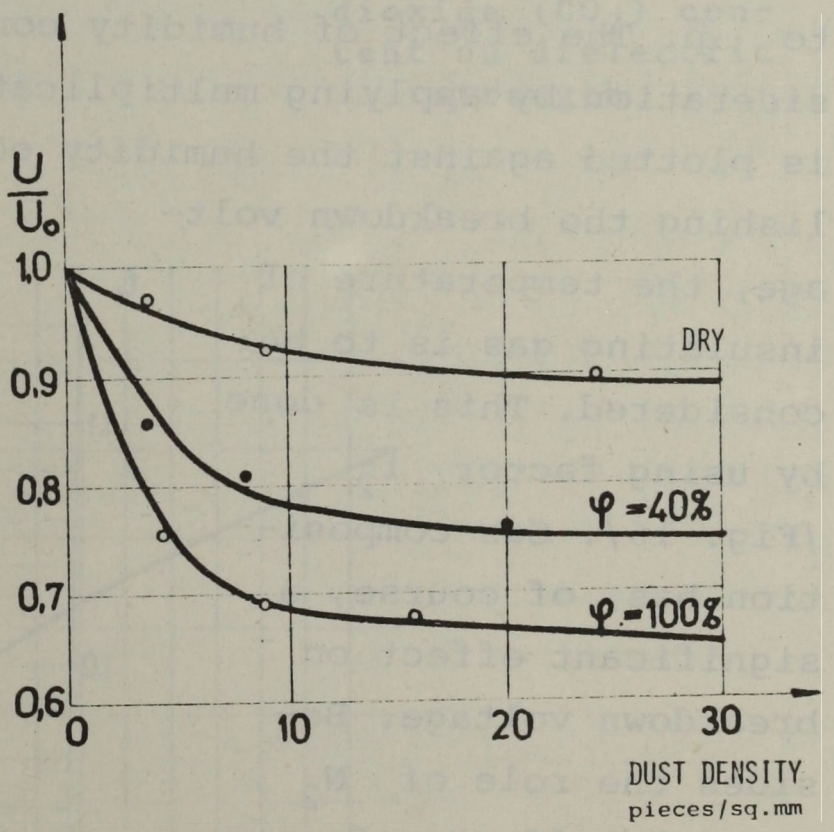

Fig. 13 Effects of graphite particles of various humidity content on dielectric streng

Based on the data collected in the period of 1965-70 we established an empirical formula /1/ which facilitates the consideration of all factors influencing the breakdown voltage of the generator. Of these, gas pressure is the most important. Over the usual pressure range /p > 5 att/, the breakdown voltage was to a good approximation proportional to $\sqrt{p}$. The effect of humidity content may be taken into consideration by applying multiplication factor f_1; the latter is plotted against the humidity content on Fig. 15. In establishing the breakdown voltage, the temperature of insulating gas is to be considered. This is done by using factor f_2 /Fig. 16/. Gas composition has, of course, a significant effect on breakdown voltage. Besides the role of N_2, also the effects of CO_2 and F12 gases have been separately investigated. The test results obtained are shown on Figs. 17 and 18. The effects of the factors obtained in this manner are summed up in the correlation

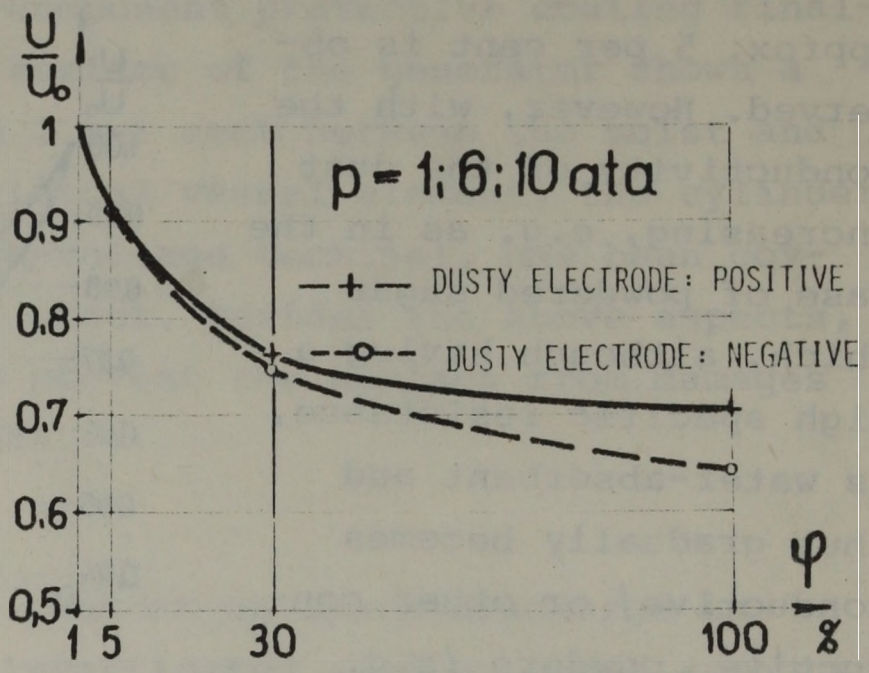

Fig. 14 Effects of graphite particles of various humidity content on dielectric strength at various pressures

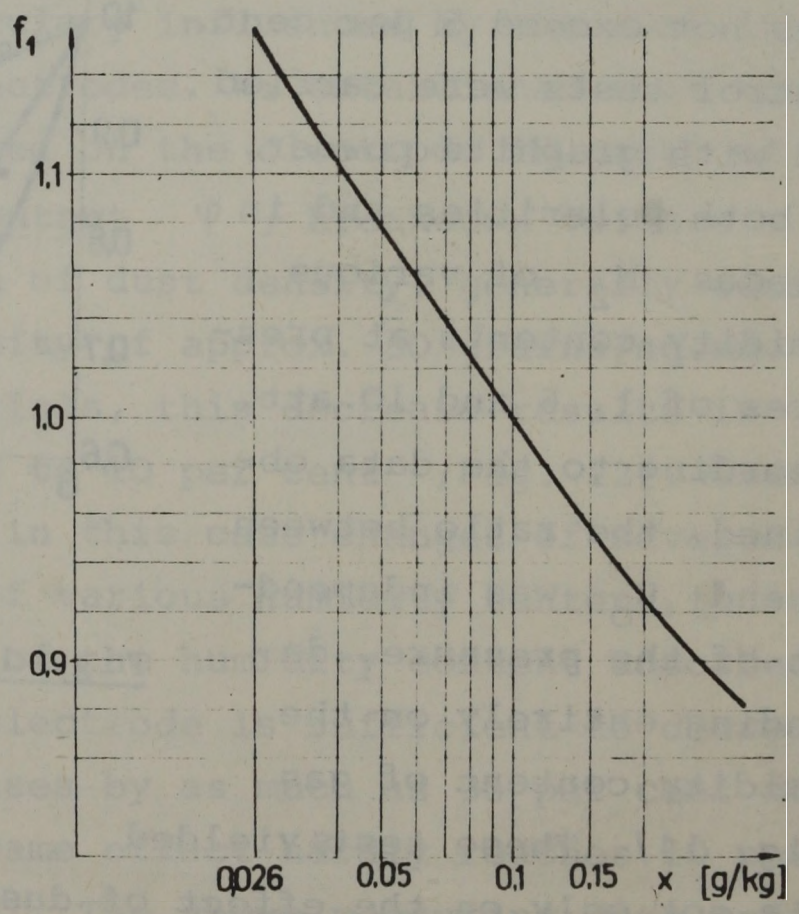

Fig. 15 Effect of absolute humidity content on dielectric strength

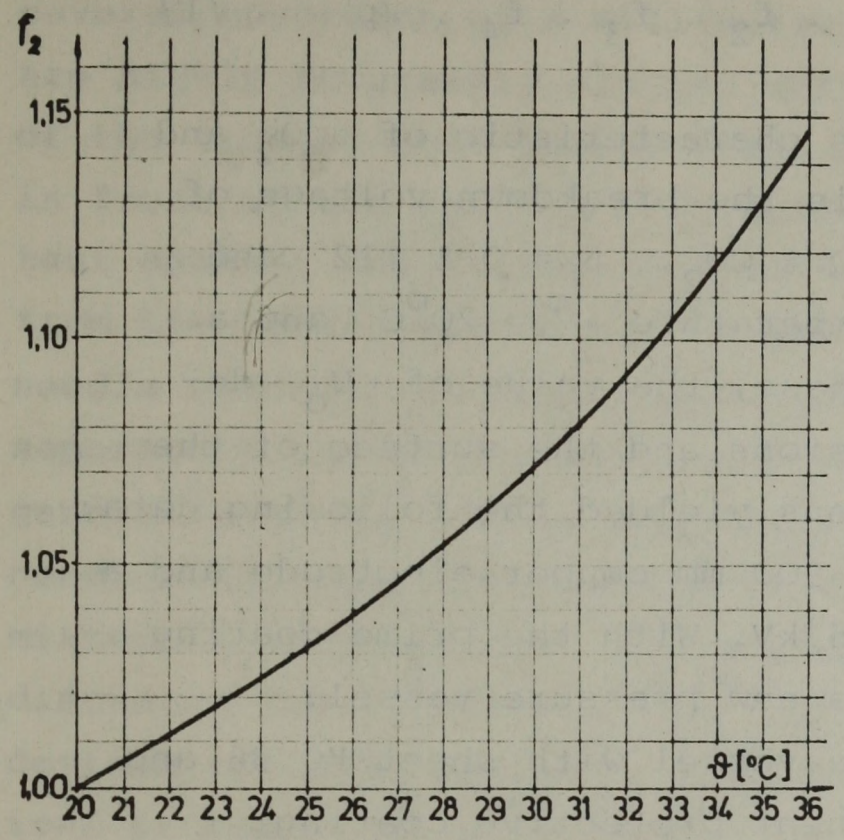

Fig. 16 Effect of gas temperature on dielectric strength

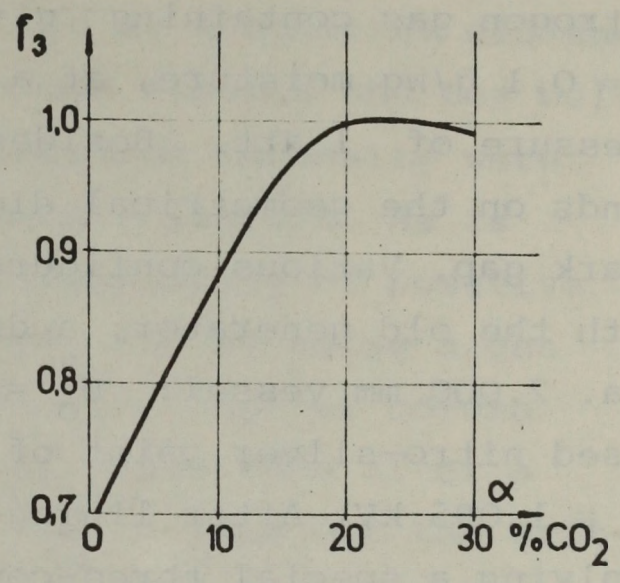

Fig. 17 Effect of carbon dioxide (CO_2) content on dielectric strength

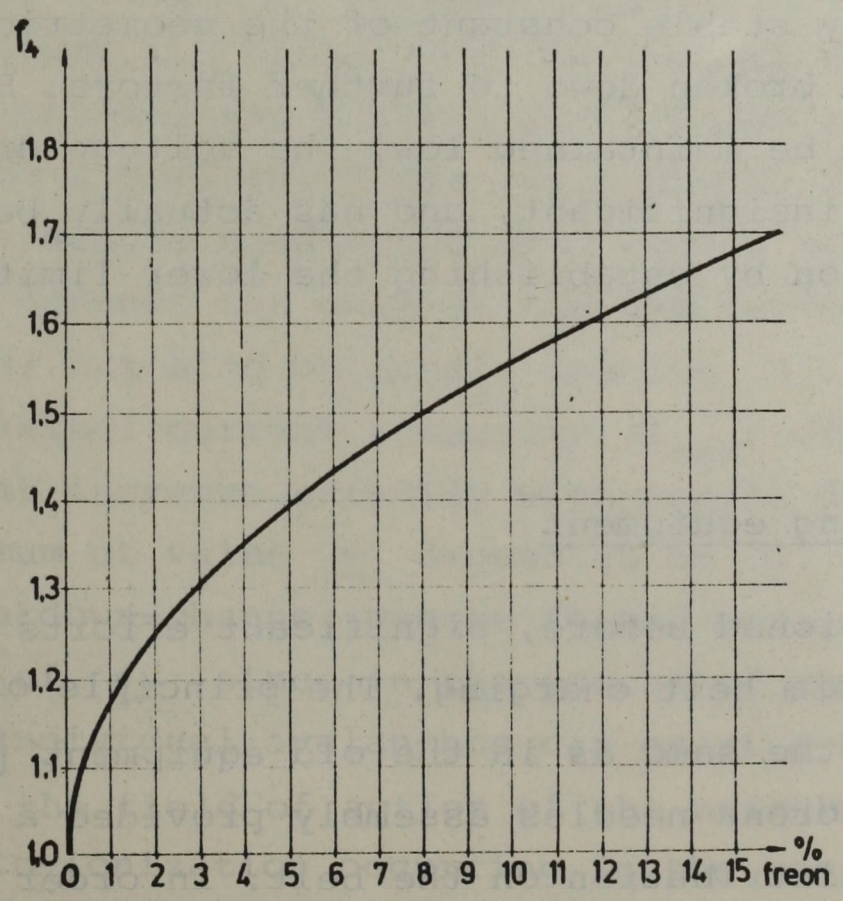

Fig. 18 Effect of freon (F12) content on dielectric strength

$$U_{breakdown} = U_o \cdot f_i \cdot f_2 \cdot f_3 \cdot f_4 \cdot \sqrt{p} \qquad /1/$$

where f_3 and f_4 are factors characteristic of CO_2 and F12, respectively, while U_o is the breakdown voltage of nitrogen gas containing α = 20 % CO_2, β = 0 % F12 and x = 0.1 g/kg moisture, at a temperature $\vartheta = 20^oC$ and a pressure of 1 att. Besides these, the value of U_o depends on the geometrical dimensions and the surface of the spark gap. Various configurations yielded the following data: with the old generator, a dia. 900 mm copper electrode and a dia. 2.000 mm vessel: U_o = 835 kV. With the prime coating based nitro-silver paint of the new pressure vessel: U_o = 1.095 kV. After lining the vessel with sheet KO 36 and applying a special three-component protective coating: U_o = 1.140 kV. The above values of U_o have been obtained to an accuracy of $\pm$ 5 per cent, from the data collected on the old and new generators between 1963 and 1971.

Under given geometrical and surface conditions, U_o is a sufficiently stable constant of the geometrical configuration not to be broken down to further factors. Since humidity content is to be maintained low, the voltage drop arising from dusting is insignificant, and has actually been taken into consideration by establishing the lower limit of the U_o.

1.2 Belt charging equipment

As mentioned before, significant efforts were made to achieve uniform belt charging. The principle of charger design remained the same as in the old equipment [2]. The new fitting of the corona needles assembly provided a much more uniform charge distribution on the belt. In order to adjust the needles to a very high degree of accuracy, they are embedded in a cast made of Araldite epoxy-resin. The gaps between the needles are spaced very precisely with an accuracy of

several hundredth of a millimetre. The top points of needles are highly accurately aligned with a line similar to the shape of the crowned belt pulley /Fig. 19/. The needles are mounted in front of the earthed belt pulley, where the belt is pulled taut against the pulley well so as to be at a constant distance from the needle assembly. The gap between needles and the belt, needle spacing,and distribution of discharge intensity were separately tested for several protecting resistors. As is generally known, with a configuration consisting of positive needles and negative counter-electrodes, and by using a gas mixture as regularly in the generator, the range of corona discharge occurring as a function of pressure ends after a certain critical pressure [13]. In order to find out the critical pressure, we already carried out previously tests at the selection of needles Type 80/287 WK, manufactured by ICH [2]. Those tests were later on extended also on gas mixtures containing Fl2 as well; the humidity was $x < 0.04$ g/kg in these cases. As apparent from our measuring data shown on Figs. 20 and 21, critical voltage is reached at values of $\underline{p}$ and $\underline{d}$ which are the lower the higher the Fl2 content of gas. Based on these data, optimal gap between the needles and the belt turned out to be 2 to 3 mm. These tests had to be performed not only with a single needle but also with a needle assembly. Optimal charge depends not only on the gap between the needles and the belt /d/ but also on needle spacing /s/. We were able to show that maximal current intensity /I_{max}/ of the needle assembly did not increase steadily with needle density but reached a maximum at value $\underline{s}$ depending on $\underline{d}$. /See Fig. 22/. Namely, the breakdown-channel can be formed more easily at smaller values of $\underline{s}$, since in the course of the preliminary discharge the individual avalanches can exert a higher degree of activity in the field of action of the neighbouring needles, due to the photo-ionization occurring in the gas. This is, however, hindered by the fact that with the needle spacing reduced, resulting in certain geometrical changes, electric field intensity triggering off the discharge tends to drop. The simultaneous occurrence of the two effects results in the

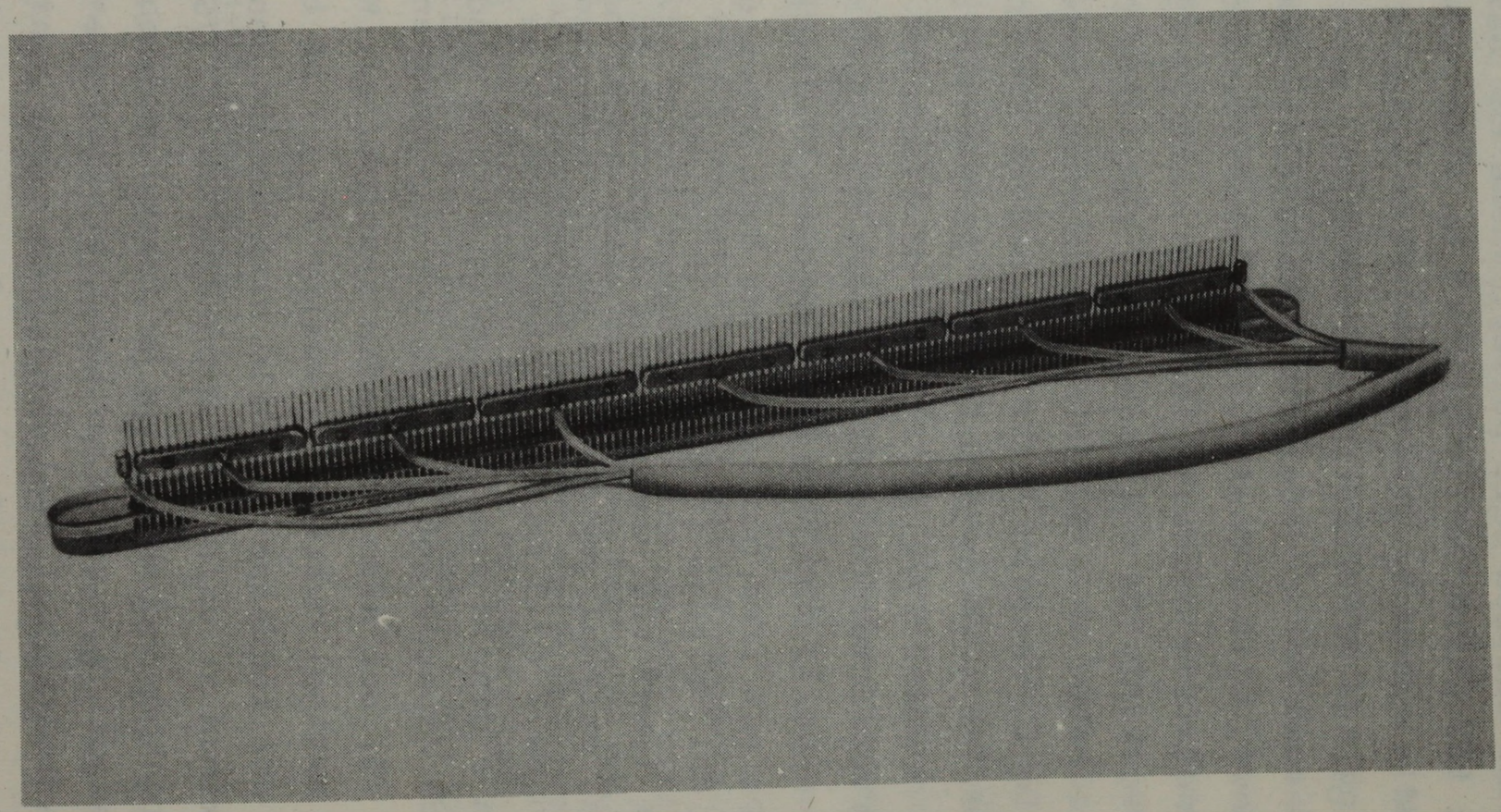

Fig. 19 Charging needle assembly

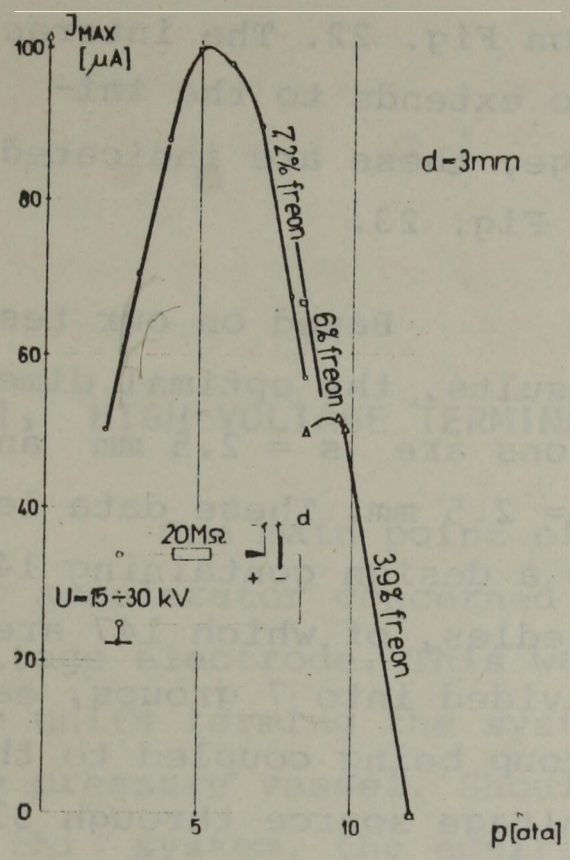

Fig. 20 Effect of freon(F12) content on corona discharge

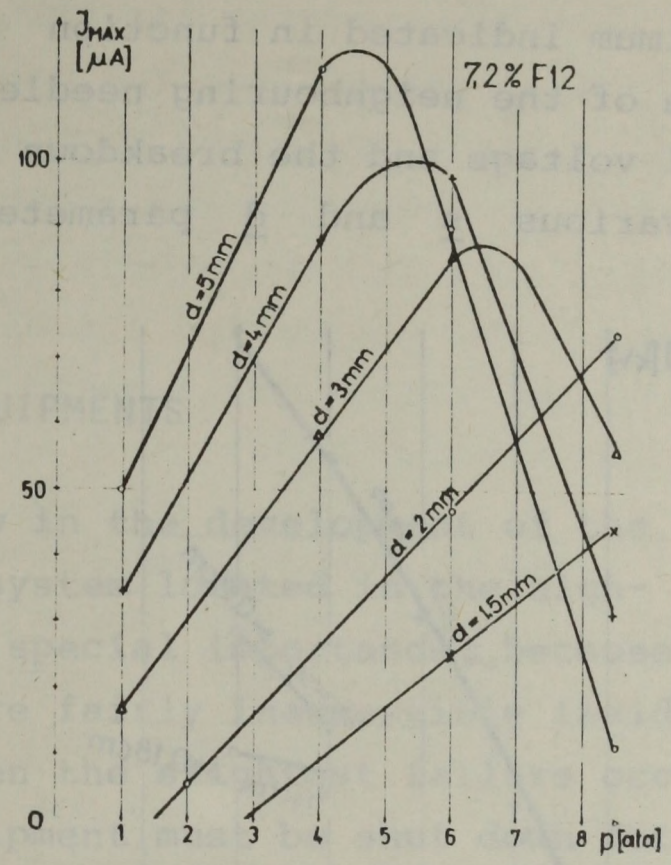

Fig. 21 Corona discharge characteristics obtained with constant freon (F12) content and various needle plane distances

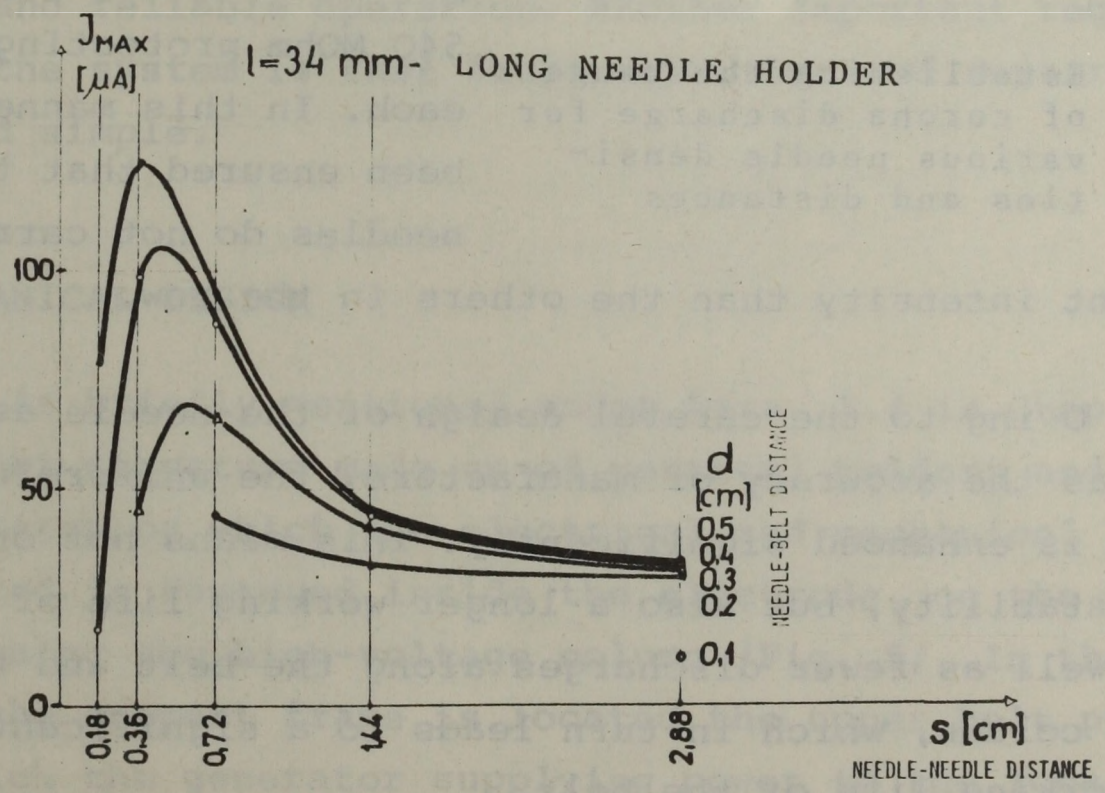

Fig. 22 Effect of needle density on total current of charging needle assembly

optimum indicated in function s/d on Fig. 22. The interaction of the neighbouring needles also extends to the initial voltage and the breakdown voltage, these are indicated by various s and d parameters on Fig. 23.

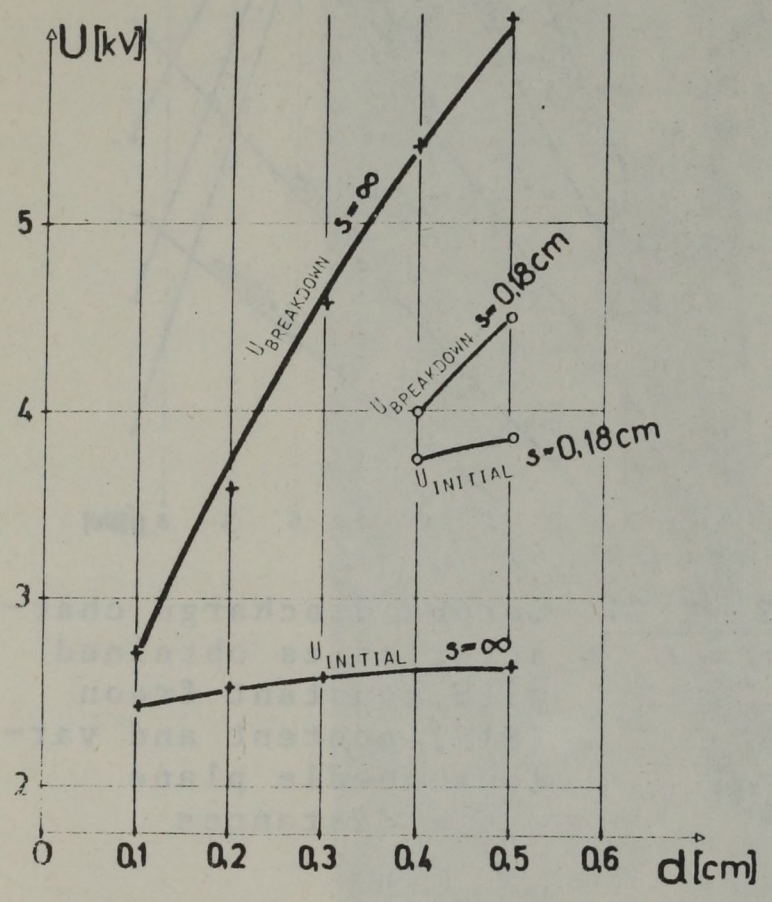

Fig. 23 Establishing the range of corona discharge for various needle densities and distances

Based on our test results, the optimal dimensions are s = 2.5 mm and d = 2.5 mm. These data led to a design containing 149 needles, of which 147 are divided into 7 groups, each group being coupled to the voltage source through 33 MOhm protecting resistors. The two outer needles of the row, which have only one neighbour each, are in a special position and thus provided with a separate 540 MOhm protecting resistor each. In this manner it has been ensured that the outer needles do not carry a higher current intensity than the others in the row.

Owing to the careful design of the needle assembly, as well as the accuracy of manufacture, the uniformity of belt charging is enhanced significantly. This means not only better voltage stability, but also a longer working life of the needles as well as fewer discharges along the belt and the high-voltage column, which in turn leads to a significant increase in the working life of the belt.

III. HIGH-VOLTAGE TERMINAL EQUIPMENTS

One main point of view in the development of the new accelerator concerned the system located in the high-voltage electrode. This was of special importance, because the units forming the system are fairly inaccessible inside the pressure vessel. Should even the slightest failure occur in thi ; system, the entire equipment must be shut down for about 12 hours. Moreover, the units operate under heavy conditions, their adjustment is made by remote control, bridging a potential difference of 5 MV, and their functioning must also be remotely controlled. Besides meeting the requirements made on them, the individual units must be capable of lasting and reliable operation. Another important requirement made on the system is that fault detection and repair be both quick and simple.

1. MECHANICAL DESIGN

As briefly mentioned under Para. 1.4 in Chapter I, the support structure made up of vertical holders and horizontal plates, on which the electrical and mechanical fittings are mounted, is fastened inside the electrode, on the base plate closing the high-voltage column /Fig. 5/. In the lower part of the support frame is located the upper belt pulley, above which the generator supplying power to the local network is mounted. Beside the generator, towards the accelerator tube, are located the two steel bulbs supplying gas to the ion source. On the other side of the generator there are two 600 W variacs and, slightly offset to another level, four 250 W variacs. On both sides of the accelerator tube there

are 3 switches, serving for switching on and off the various voltage sources from the control desk. Both the switches and the variacs are moved by plexi-glass rods. Four rods linked to the switches are located on both sides of the accelerator tube and two others in the bores of the two plexi--glass columns supporting the high-voltage column. The rods turning the variacs are located on the side opposite to the accelerator tube [26].

Above the aforementioned assemblies, there are three horizontal plates on the support frame. In this manner three levels have been formed for accommodating the racks in which the electric units are mounted. The levels can accommodate four 150 x 205 x 200 mm and two 150 x 205 x 300 mm racks each. At one side of the support frame there is an U-shaped cut-away section for the removal of the accelerator tube.

2. ELECTRIC SYSTEM

2.1 Block diagram

The block diagram of the system located in the high--voltage terminal is shown on Fig. 24. The present system comprises the power supplies required for the acceleration of protons, deuterons and He_4^+ ions . Accordingly, the power supplies operate the radio-frequency ion source and supply the pre-focussing lens located at the input of the accelerator tube. These units do not, however, fill the entire space available at the three levels of the support frame, but occupy only the racks at the first level and a single rack at the second level.

2.2 Program facilities

By adopting the rack system, our aim was not only to establish self-contained units from both electrical and me-

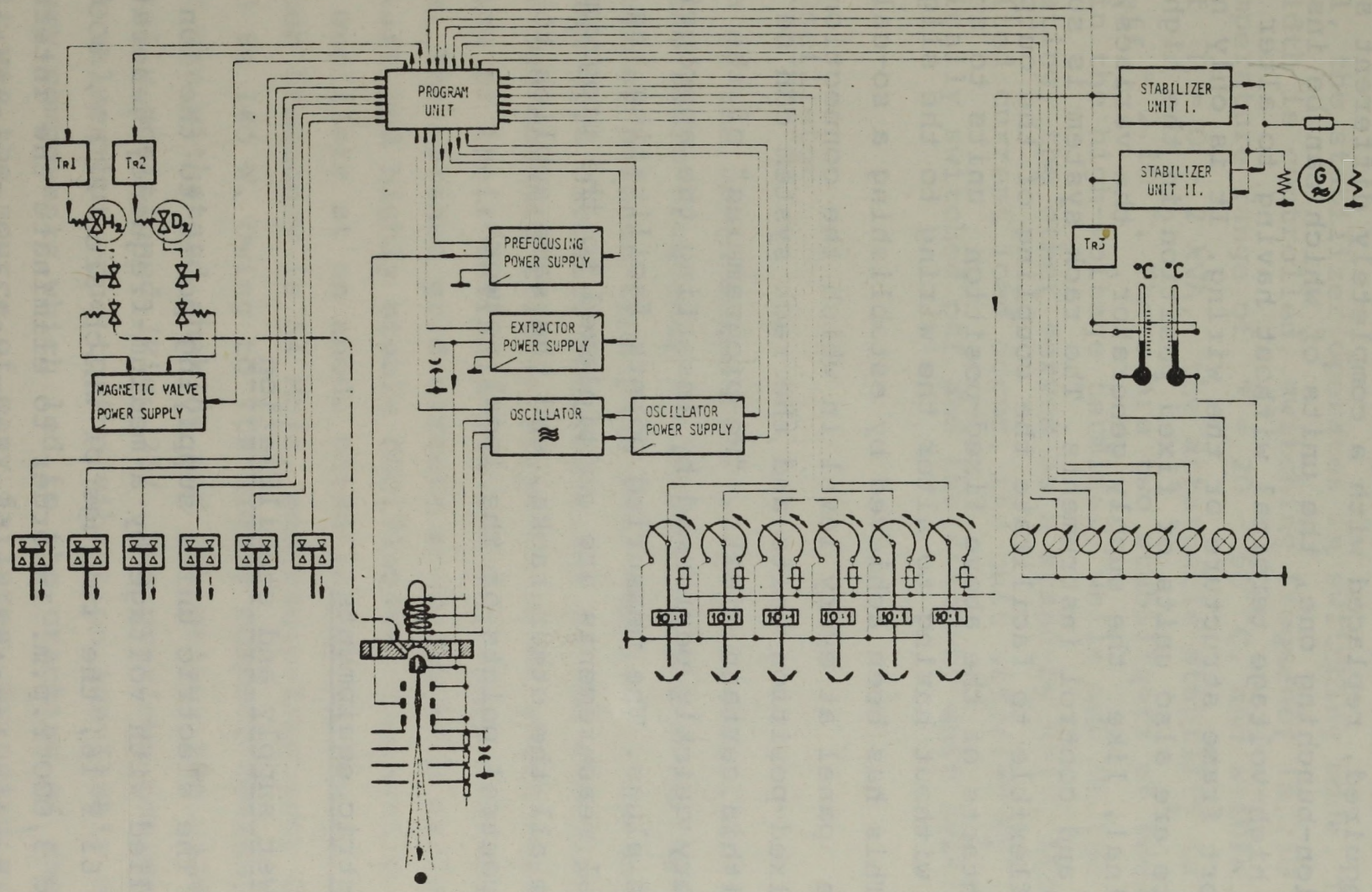

Fig. 24 Block diagram of the system located in the high-voltage terminal

chanical points of view, but also to ensure the interchangeability of the racks both within and between the individual levels of the support frame. Owing to this design, the system can at any time be complemented with units mounted in racks or, if required, replaced with a completely different system, e.g. an ion-bunching one, the units of which can be inserted into the high-voltage terminal without having to alter either the support frame structure or the wiring. It is only natural that there are also units of fixed position in the high-voltage terminal, like the supply generator, the variacs, switches and control instruments. The rack system is sufficiently flexible to facilitate the coupling of the output and input contacts of the above fixed-position units to any rack position without having to alter the wiring to the slightest extent. This has been achieved by establishing a so-called programme panel at every level in which the connection points of the fixed-position units and the rack system can be easily varied within certain limits. "Re-programming" of the system can be very quickly performed by inserting the appropriate programme plugs. The measuring points facilitating the taking of control measurements are multiplexed to the programme plug from all the other racks, and the same applies to the voltage control points of the local network.

2.3 Electric equipments

2.3.1 Power supply and stabilization

The electric units supplying power to the ion source are supplied with voltage by a medium-frequency generator Type ZNH 63 F 16, the ratings of which are 220 V, 800 c/s, 2 kVA and 3,000 r.p.m. In order to eliminate the interaction of the circuits located in the terminal and compensate the effects of possible speed variations, the local network has been stabilized. The voltage supplied by the generator is rectified by a cuprox rectifier in the stabilizer, by means of which an effective value first stabilized, then compared

to a constant voltage; thereafter, excitation of the generator is controlled by means of an amplified signal obtained from the difference between the actual and the constant voltage. In order to cut down heat generated in the high-voltage terminal, the stabilizer operates in switching mode. The pulse width is controlled, switching frequency is 250 c/s. In a temperature range of ϑ = 20 - 50 °C, and within a load range of P = 0 - 2 kVA, the attainable stability is $\Delta U_{eff}/U_{eff} = 2.10^{-2}$. There are two stabilizers of identical design in the high-voltage terminal; while one of the units is operating, the other serves as a stand-by unit. Should a pre-limited current load occur, the unit affected by it is automatically switched off and the stand-by unit switched on.

2.3.2 Oscillator

Of the units shown on Fig. 24, the oscillator exciting the radio-frequency ion source is the most important. The so-called balance-type push-pull oscillator operates in an earthed grid circuit. The valve set of the oscillator consists of two ceramic triodes /Type GS 90 B/ which were selected in view of their reliable functioning under external overpressure. The earthed grid circuit provides both reliable quick start and highly stable oscillation. The system can already oscillate at an anode potential of as low as 300 V. Oscillator frequency is 54 Mc/s, and radio-frequency output obtained is 140 W. Owing to its highly compact design, the oscillator can withstand shaking and vibration; the valves are horizontally positioned /Fig. 25/. The previous design included vertical valves but, due to the vibration inevitably caused by the rotary components,which led to the cracking of the cathode paste, it was the source of many failures. By using a horizontal valve arrangement, this defect was cured. By means of the air condenser feed-back, the oscillator system can be balanched out, and the cathode current and heating-up of the valves equalized. The coupling-out coil of the oscillator can be adjusted

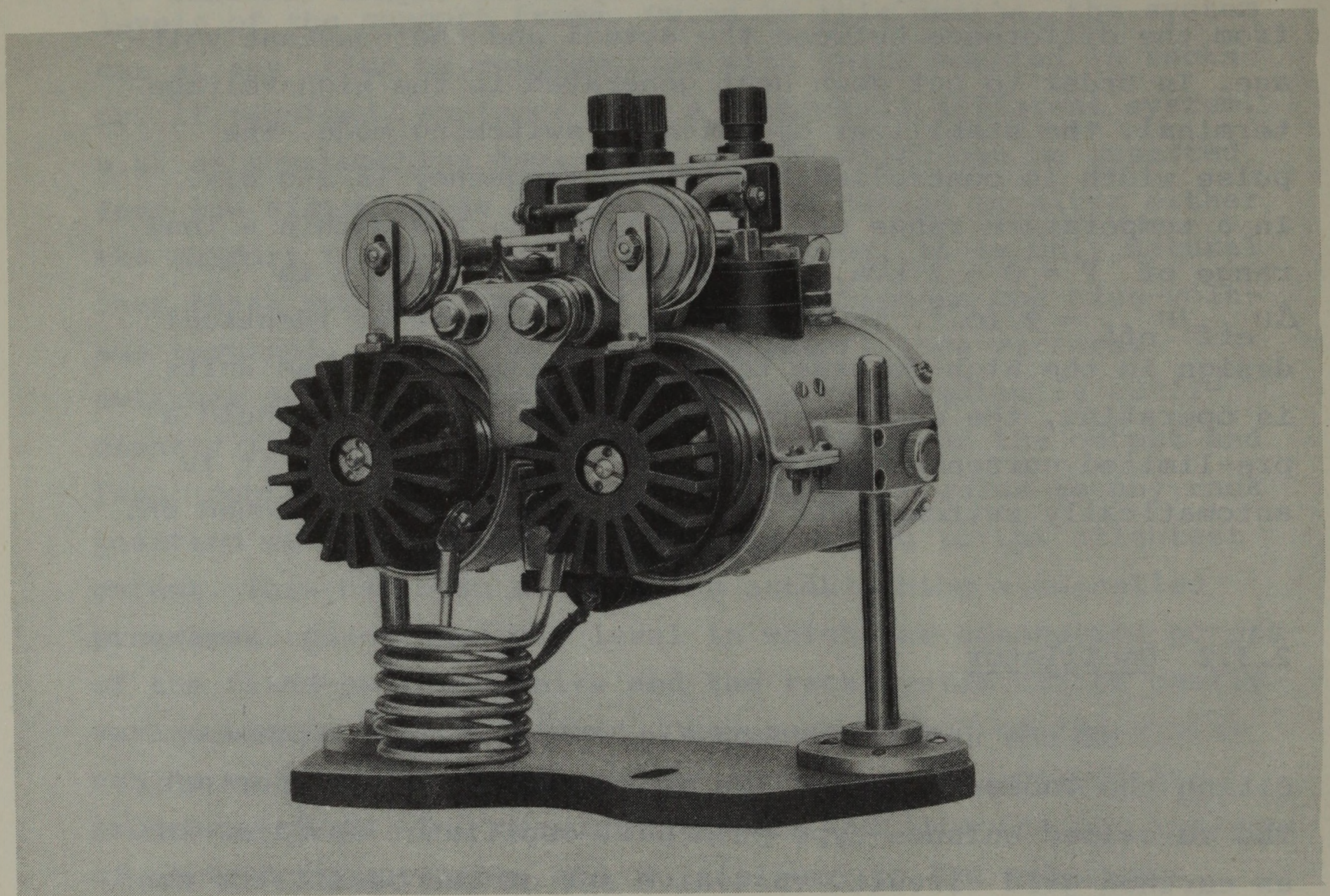

Fig. 25 Oscillator of ion source

in any direction in relation to the bulb of the ion source. Since this coil is mounted in a fixed manner on the oscillator tubes, the entire oscillator can be moved both vertically and horizontally. The components have been treated to withstand corrosion caused by the CO_2 and Fl2 atmosphere. Optical blackpaint of the cooling fin serves for improving heat transfer which can be also helped by the cooling fan mentioned under Para. 1.4 in Chapter I.

2.3.3 D.C. voltage supply units

Of the supply units, the one supplying anode voltage to the oscillator is the most important /Fig. 26/. This unit supplies 0 - 1500 V and 0 - 250 mA. It is designed in a voltage doubling circuit. The transformer associated with this supply unit is made of HIPERSIL strip iron, and loaded with max. 4 kGs at 800 c/s. In this manner, losses are kept very low. Rectification is made by a silicon diode chain consisting of 2 x 4 diodes Type BY 238, and provided with a parallel--connected protective resistor chain. The unit is protected against any high-frequency effect that might find its way back to it by a protective capacity chain located at the output end and a high-inductivity choke coil incorporated into the anode lead going to the oscillator.

The function of the extracting voltage supply unit is to generate the voltage required for extracting the positive particles from the ion source plasma. This voltage source is of negative polarity, and can be continuously controlled during regular operation over the range of zero to 6 kV. Since the last piece of the high-voltage dividing chain of the accelerator is directly connected to the hot point of this unit, a protecting spark gap is coupled to that point. Its function is to protect the supply unit and the extracting system of the ion source from transients possibly occurring in the case of high-voltage breakdowns.

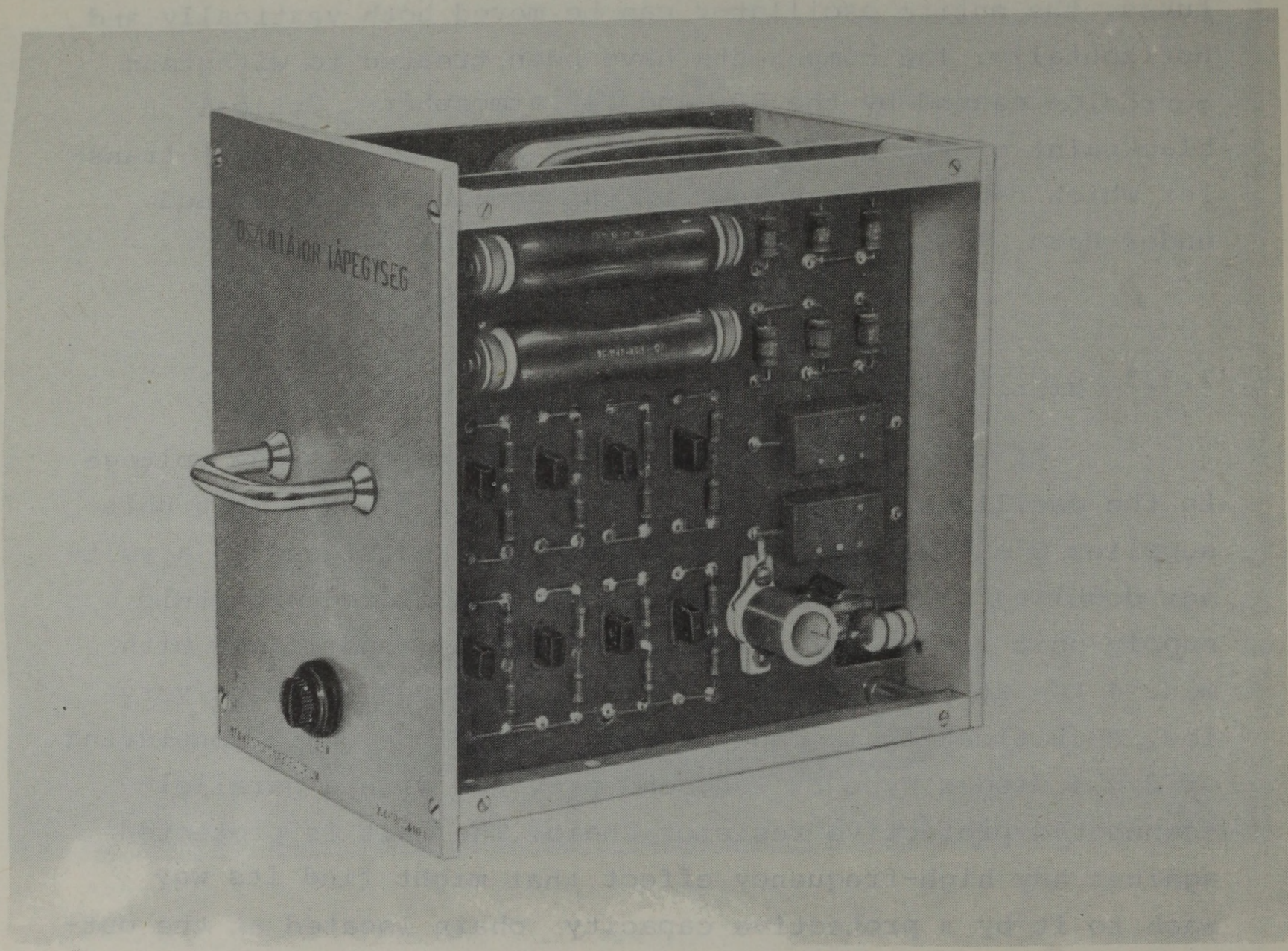

Fig. 26 Anode and heating voltage supply unit of oscillator

The supply unit of the pre-focussing lens is shown on Fig. 27. This power supply can be continuously controlled between zero and 20 kV d.c. and supplies voltages of negative polarity. Owing to the highly compact arrangement of the unit, we have designed its transformer with the utmost care. The primary and the secondary coils have been separately moulded in casting resin Type Araldite E under vacuum. The coil-cores are made of glass-fibre reinforced plastic, with HIPERSIL iron cores. The secondary coil supplies power to a voltage doubling rectifier made up of two silicon diodes.

The valves controlling gas delivery to the ion source are supplied with heating voltage by a 50 W transformer each. At the secondary ends of the transformers there are an 1 V/ 20 A and a 15 V/ 2 A coil each. The high current intensity coils serve for directly heating the palladium tube of the Pd valves used for the acceleration of protons and deuterons, whereas for accelerating He_4^+ ions the Pd valve is replaced with a bimetal valve, the heating current of which is supplied by the low current intensity coils of the transformer. The bimetal valve is indirectly heated. In order to shorten the supply cables of the high current intensity coils, the transformers are located in the vicinity of the valves associated with them. The primary ends of the transformers are coupled to the power supply alternatively through the contacts of one of the switch channels. The latter serves also for switching the excitation of a cut-off magnetic valve used for separating the Pd valve from the gas inlet, /see under Para. 3.2 in Chapter III/. The latter circuit is a full-wave bridge rectifier scheme.

The most important data of the supply units are summed up on Table II.

The supply units are mounted on individual racks. This is apparent from Fig.s 26 and 27, illustrating the supply units of the oscillator and the pre-focussing lens, respectively. The other supply units are mounted in similar racks.

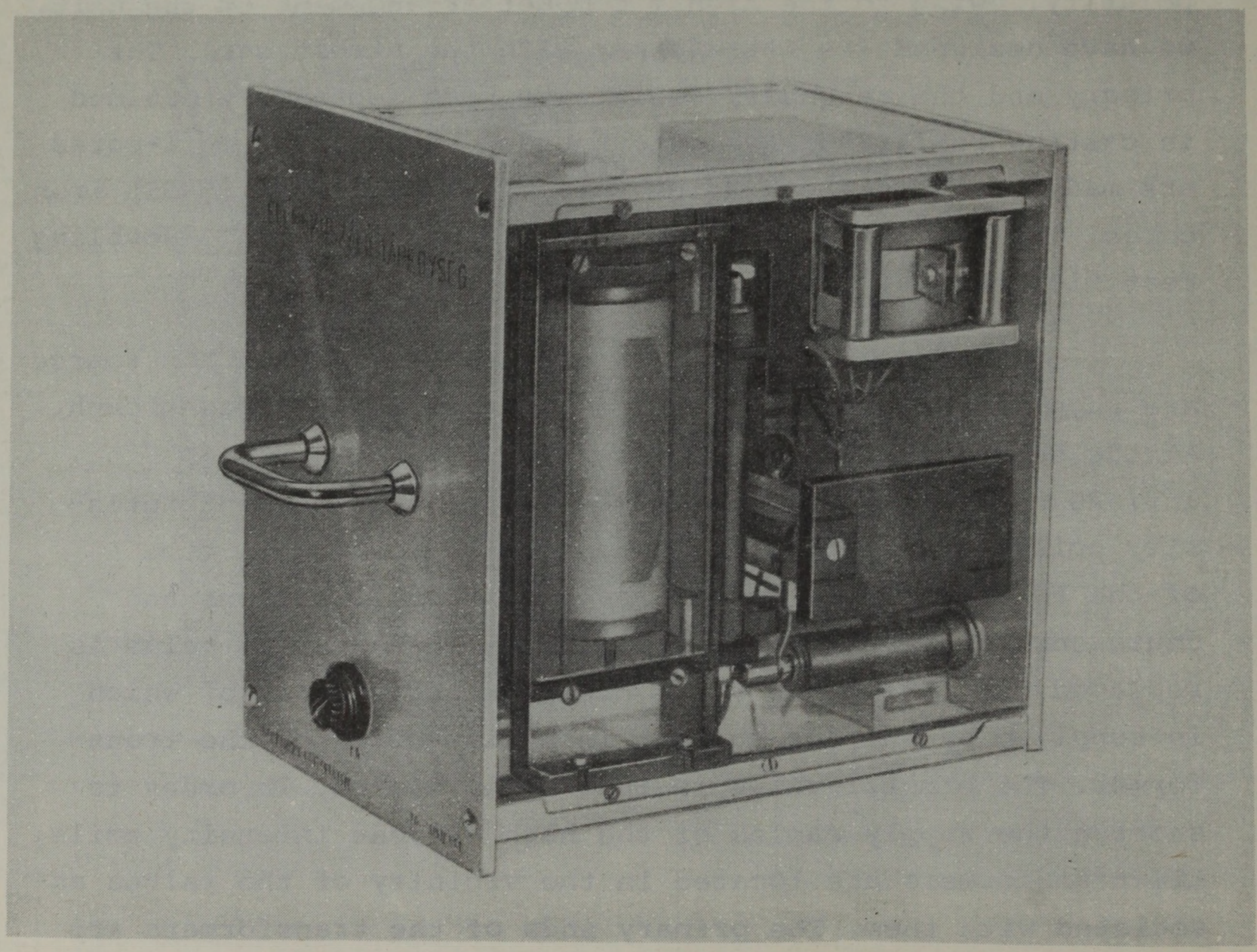

Fig. 27 Supply unit of pre-focussing lens

Table II

Units	Parameter	Values	Remarks
1./ Oscillator	anode voltage cathode current frequency RF output	1.400 V d.c. 200 mA 54 MC/s 140 W	
2./ Oscillator supply unit	input voltage outpout voltage ripple max. current polarity no-load voltage load voltage loading current output	0-220 V/800 c/s 0-1.500 V d.c. 1.5 per cent 250 mA positive 1.750 V d.c. 1.400 V d.c. 200 mA 280 W	variable /under a load of 250 mA/
3./ Extracting voltage supply unit	input voltage . output voltage polarity max.current ripple	0-220 V/800 c/s 0-6 kV d.c. negative 15 mA 0.6 per cent	variable /under a load of 14 mA/
4./ Pre-focusing voltage supply unit	input voltage output voltage polarity max.current ripple	0-240 V/800 c/s 0-20 kV d.c. negative 0.5 mA 0.65×10^{-3}	variable /under a load of 0.5 mA/
5./ Pd valve heating	input voltage output voltage max. current /output/	220 V/800 c/s 1 V/800 c/s 20 A	variable
6./ Magnetic valve supply unit	input voltage no-load voltage polarity max. current operation data	220 V/800 c/s 13 V d.c. positive 2.5 A 9 V/1.63 A	not variable
7./ Thermal expansion valve heating	input voltage output voltage max. current /output/	220 V/800 c/s 15 V/800 c/s 2 A	variable

3. RADIO-FREQUENCY ION SOURCE

3.1 Ion source

We use a Bayly and Ward type high-frequency ion source /Fig. 28/ with the generator. The design of the ion source has been suited to the characteristics of the Van de

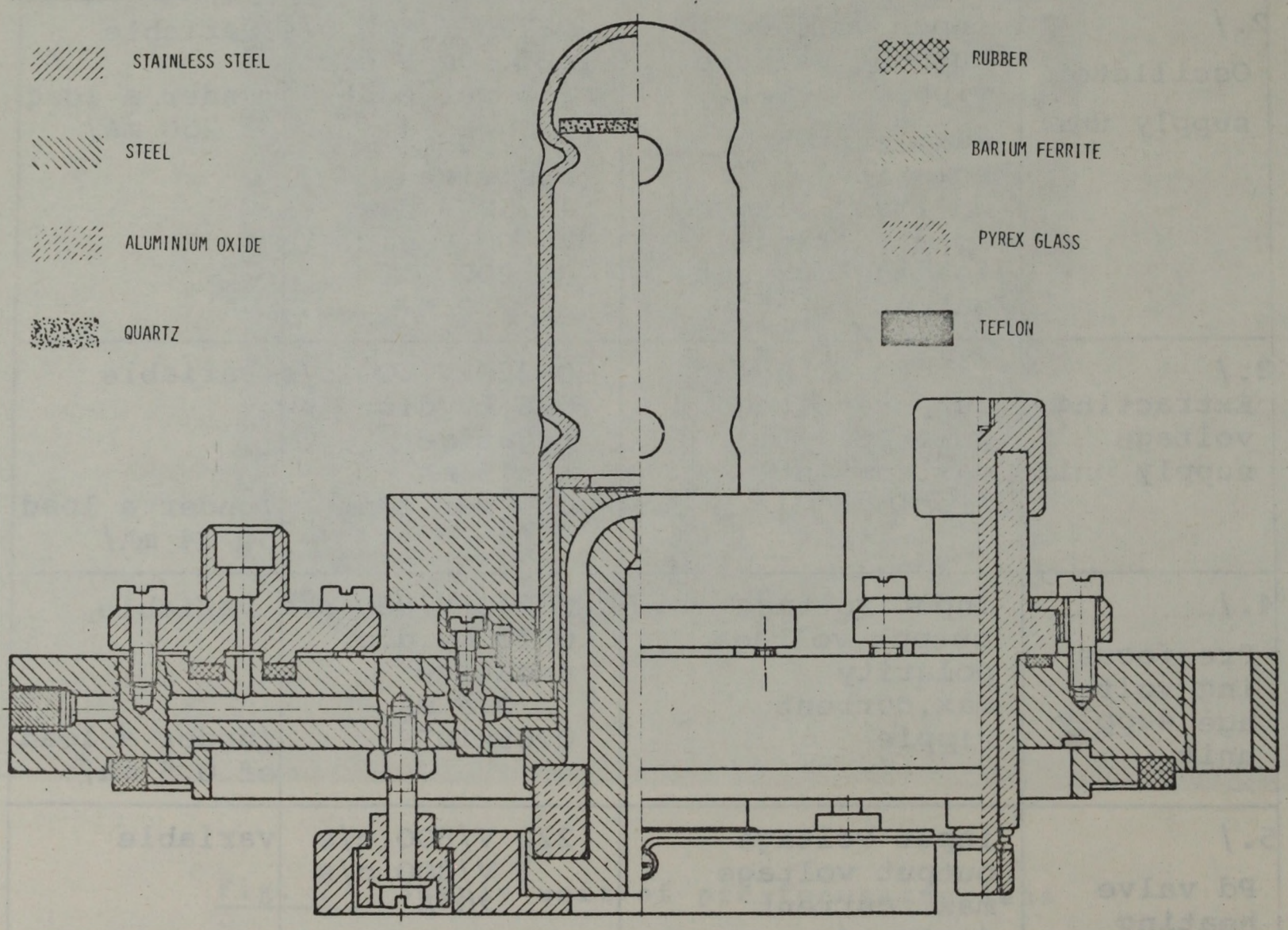

Fig. 28 Radio-frequency ion source

Graaff generator. This required the modification of the ion sources used previous to the reconstruction [2, 30]. The new design allows the replacement of the whole extracting system, accommodated now in a cartridge-like casing. The system consists of three carefully finished components /anode, insulating ring and extracting electrode/, which have been hot-compressed together. This method of assembly ensures accurate aligning, vacuum-tight sealing and good replaceability

of the extracting system. The extracting assembly is merely slipped into the seating provided on the base plate, and fastened there by means of a clamping ring. Bore diameter of the extracting electrode is 0.8 mm, and length 6 mm. The distance between the anode and the extracting electrode is 5 mm. The half-cone angle of the beam leaving the source is limited to 60 mradian by the lower edge of the extracting electrode. As a function of the extracting voltage, current intensities of the ion source are given for protons and He_4^+ ion on Fig. 29, at an oscillator voltage of 1.300 V, an oscillator anode current intensity of 200 mA and a gas consumption rate of 2 normal cm^3/hour. The ion beam contains 70 per cent of atom ions.

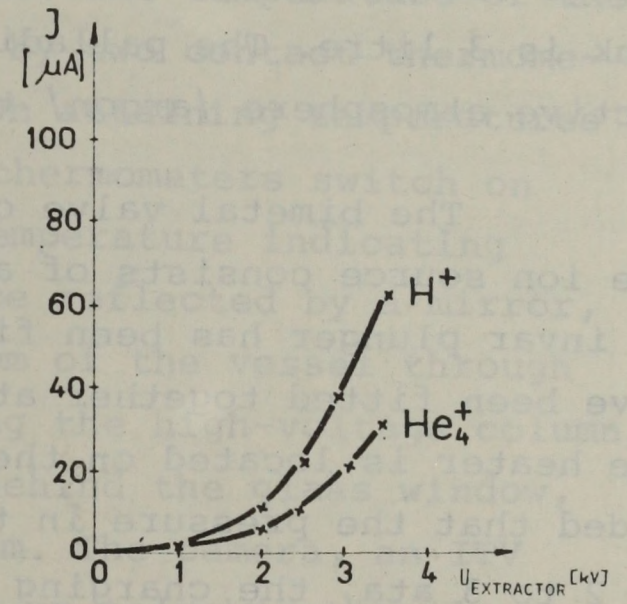

Fig. 29 Characteristic of ion source

The ion source is used also for producing He_4^+ ions. In relation to the intensity of the hydrogen beam, helium beam intensity is cut by 30 per cent at identical oscillator adjustment and extractor parameters. During calibration we found that the helium beam contained hydrogen ions as well. This was caused by partly the contaminating hydrogen and partly the hydrogen diffusing from the surfaces of the ion source in contact with the gas. In the course of the measurements we found that the hydrogen content gradually decreased. Acceleration of helium ions caused no problem with the generator.

3.2 Gas supply to the ion source

Hydrogen and deuterium gas supply to the ion source is controlled by a direct-heating palladium valve. Under operating conditions, the palladium valves are subject to ambient

temperatures reaching 40 or 45 ^{o}C, consequently in order to ensure reliable gas charging the dimensions of the palladium tube had to be so selected as to limit the rate of gas delivery to 0.5 normal cm^3 per hour at the above-mentioned ambient temperatures. The palladium tube selected for this purpose is 1.6 mm in diameter, 17 mm long and has a wall thickness of 0.4 mm. Provided that the pressure in the gas tank is at the usual level of 2 to 3 ata, the charging of 2 normal cm^3 gas per hour requires approx. 8 W. The lifetime of the valves is several thousand hours. Owing to the specially-shaped fastening,the thermal stress arising along the axis of the palladium tube is sufficiently uniform not to result in any damage caused by local overheating. Volume of the gas storage tank is 3 litre. The palladium tube has been welded in a protective atmosphere /argon/ to the top panel of the gas tank.

The bimetal valve controlling helium gas delivery to the ion source consists of a stainless steel sleece into which an invar plunger has been fitted by grinding. The two parts have been fitted together at a temperature of 140 ^{o}C. The heater is located on the outer side of the valve. Provided that the pressure in the gas tank is at the usual level of 2 to 3 ata, the charging of 2 normal cm^3 gas per hour requires approx. 10 W. Similarly to the palladium valves, this valve is also incorporated in the gas tank, and the dimensions are identical with those of the palladium-valve tanks as well.

Between the palladium valves and the ion source a metal-sealed gas line is used. Two bottles can be mounted simultaneously, each with an electromagnetic cut-off valve located in the supply lines connected to the ion source [31]. By means of this two-bottle arrangement we could make possible to operate the ion source alternately with hydrogen and deuterium gas without having to dismantle the generator tank. The function of the cut-off valves is to ensure that only the type of gas required is delivered into the bulb of the ion source. The generator tank has to be dismantled, however, when using a helium bottle, since this type of gas supply requires the

mounting of a direct pipe line between the bimetal valve and the ion source, without a cut-off valve.

4. CONTROLS

4.1 Industrial TV network

The voltages and currents adjusted in the high-voltage terminal are controlled by means of six 100 μA vibration-resistant instruments. These instruments are mounted in a small box providing dial illumination: the scales are downwards in the cut-away section located between the plexi-glass rods moving the toroidal transformers. The temperature of the high-voltage terminal is controlled by two contact thermometers located level with the racks. On attaining temperatures of 40 and 45 ^{o}C, respectively, the thermometers switch on pilot lamps. The instruments, the temperature indicating lamps and the image of the ion source reflected by a mirror, can be observed from the plane bottom of the vessel through a long cut-away section running along the high-voltage column. At that point,there is a TV camera behind the glass window, on the outer side of the plane bottom. The camera, an ITV 11-7/A provided with a Zeiss 1:4/300 mm teleobjective lens, transmits the picture picked up through the glass window to a Minivizor receiver Type ITV 18-8. The latter is mounted on the control desk, thus making possible observation of both the instruments and the image of the ion source.

5. SOME TECHNOLOGICAL COMMENTS

The components mounted in the high-voltage terminal are subject mainly to the following harmful loads: repeated cycles of evacuation and compression /to a vacuum of 5 x 10^{-2} mm mercury and a pressure of max. 20 ata, respectively/, ambient temperatures of 40 to 45 ^{o}C, constant vibration at a frequency in the range of 4 to 50 c/s. These vibrations cause

at certain points gravities reaching 5 g. Further we have a gas atmosphere containing agressive CO_2 and F12. In order to meet these high requirements, the sensitive components like electrolytic and other large-size capacitors, measuring and high-voltage resistors, transformers were moulded in casting resin and mounted in a compact, robust and vibration - resisting manner. Whenever it was possible, printed-circuit panels were adopted. All components were given some appropriate surface treatment /chromium plating, oxidation, tinning etc./. Owing to the high ambient temperatures encountered, there are only silicon-based semiconductors are utilized in the circuits.

In order to decrease the dimensions and iron losses, the transformers are made with HIPERSIL iron. In this manner we achieved e.g. that at a power supply of 800 c/s a no-load current of 24 to 28 mA flows through the 600 W variacs, while the total loss is 5.4 W/kg; for the 250 W variacs, no--load current is 6 to 10 mA, and the total loss 1 W/kg. These iron cores had been measured before final coiling, and only the ones showing the lowest losses were used.

The above units were subjected to special tests after manufacture. All of them were operated for 12 hours under rated voltages and loads in a drying box heated to 60 ^{o}C. After moulding and previous to building-in, the components were subjected to several cycles of exhaustion and compression in a test vessel. Only the components withstanding the tests were incorporated in the equipment. Over and above these tests, the oscillator was subjected to a 12-hour vibration test, after which the supply unit and the oscillator were repeatedly tested under rated load by applying the full anode voltage in one step. Previous to building-in, the measuring instruments of the terminal were tested both in a drying box and a vibrating bench.

Not only the electric components were tested before assembly. The ion sources were tested for vacuum and electrical functioning on a test stand, and thereafter subjected to a pressure test as well.

Duplicates of both the oscillator and the various supply units have been manufactured. While the first units are being continuously operated in the equipment, the second ones serve as stand-by units. The rack system renders failure detection and remedy very quick. Should any defect occur, the respective rack is simply replaced, the defective part repaired in the workshop and the entire unit measured on a test bench, so the generator can operate without having to be shut down.

IV. ACCELERATOR TUBE AND FOCUSSING SYSTEM

1. DEVELOPMENT AND TESTING OF THE ACCELERATOR TUBE

1.1 Electric strength of the accelerator tube

The upper limit of accelerating voltage attainable with an electrostatic ion accelerator is affected, among others, by two things: the electric strength of the voltage source, which is located in an insulating gas and thus forms a complicated electrostatic system, and the electric strength of the ion accelerating system, consisting of an electrostatic system of series-connected high-voltage vacuum spark gaps. The accelerator tube itself is located at the boundary of the above two electrostatic systems, and thus has to meet the requirements made with both of them. The external electric strength of an accelerator tube maintained in a high-pressure gas atmosphere presents significantly less problems than the internal electric strength, and can be established in close connection with the electrostatic system of the voltage source. The internal electric strength constitutes a more complex problem.

The electric strength of a vacuum spark gap is influenced by many factors. Since of these the material and shape of the solid insulator, as well as the method of its fitting to the electrodes played the most important role, at first we dealt with these aspects in the initial phase of the building of the accelerator tube. Design of the primary and secondary particle flows in the tube was made simultaneously with the above work, and the total, simultaneous effect of all factors was obtained only when the completed ac-

celerator tube was tested.

1.2 Selection of the profile of the insulator and testing of the accelerator tube sections

Comparison tests were performed with profile samples of porcelain and glass insulators and small-scale tube section models, and various section profiles made of the same material. Measuring was made by spark conditioning with a 200 MOhm resistor inserted. In the course of measuring, the number of breakdowns occurring within a given period of time /generally 2 min./ at various voltage levels were established in the successive conditioning runs, distinguishing the initial corona and brush discharges from the actual breakdowns. It is only natural that the vacuum maintained during these tests was not constant because of the discharges, although in all runs it remained throughout of the same order as at the beginning /1-2 x 10^{-6} mm Hg/.

The materials used for testing are given on Table III1.

Table III

Material	ε	ρ [Ωcm]	Manufacturer
A./ Porcelain /high-voltage, industrial finish/	6	10^{15}	Pécs Porcelain Factory of Fine Ceramic Works
B./ Glass /mark C-9, hard vacuum glass/	4.2	1.07×10^{14}	Karcag Glass Works of Glass Industry Works

First of all, the tests relating to the fitting of electrodes and insulators were performed for dia. 12 mm glass rods of 23 mm height, as well as Rogowsky electrodes made of aluminium. Of several measuring arrangements tested, the one shown on Fig. 30 proves, in harmony with the results of other

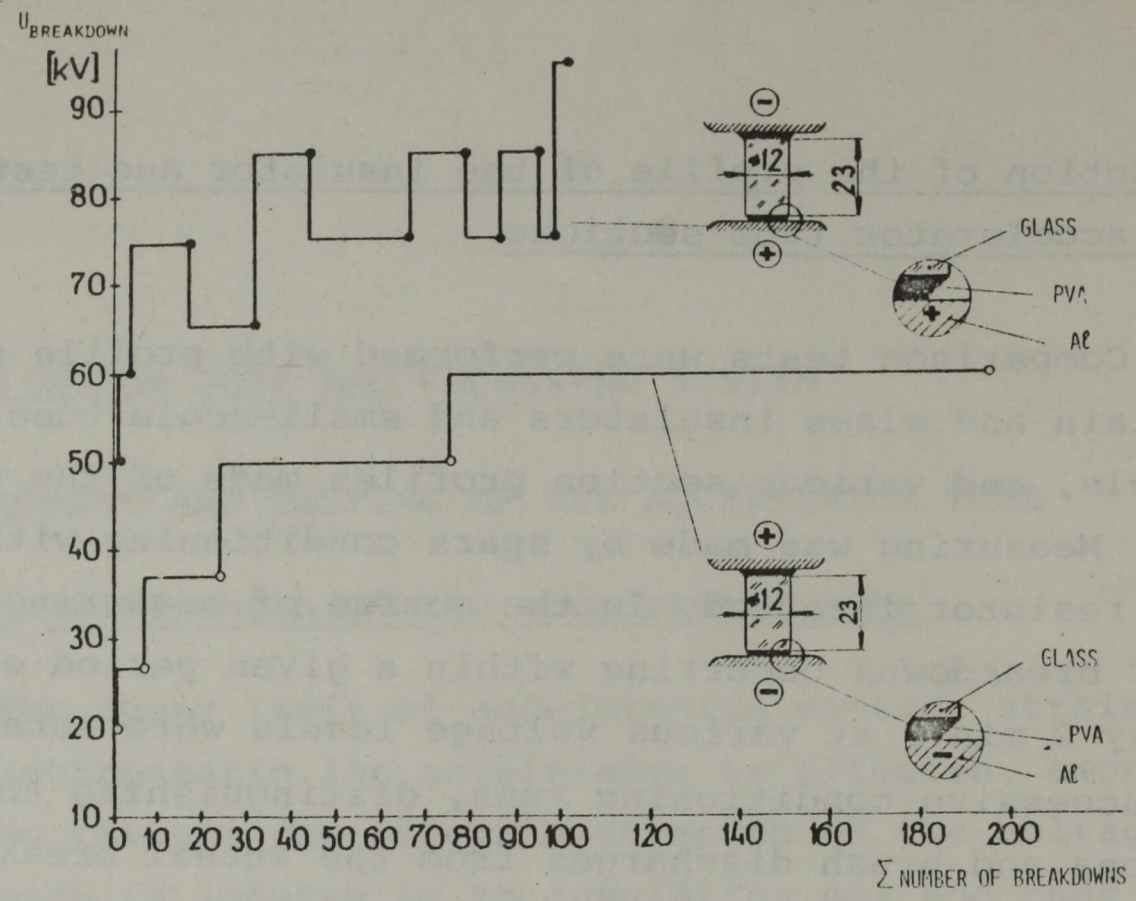

Fig. 30 Effect of dielectric-electrode coupling design on dielectric strength

authors as well [32, 33], that the breakdown voltage of the same spark gap can be more than doubled if the fit is provided without any spalts at the side of the negative electrode, and this can be obtained even if - due to the inferior quality of the insulator surface, as in the present case - the conditioning process has failed to improve electric strength to a significant degree. By scraping off a small piece of cement, it was possible to create a disadvantageous condition with one of the electrodes of the spark gap shown on the Figure. The final design of the fitting of the insulator to the electrode was decided upon with the knowledge of the above test results.

As is well known, positive and negative charge ranges can be established on the surface of a solid dielectric medium in vacuum, depending on the angle included by the electric field and the surface of the insulator [34]. If helped by the conditions, these ranges prevent the pre-discharges from growing further, and provide a useful screen for the point where the cathode contacts the insulator. On Fig. 31,

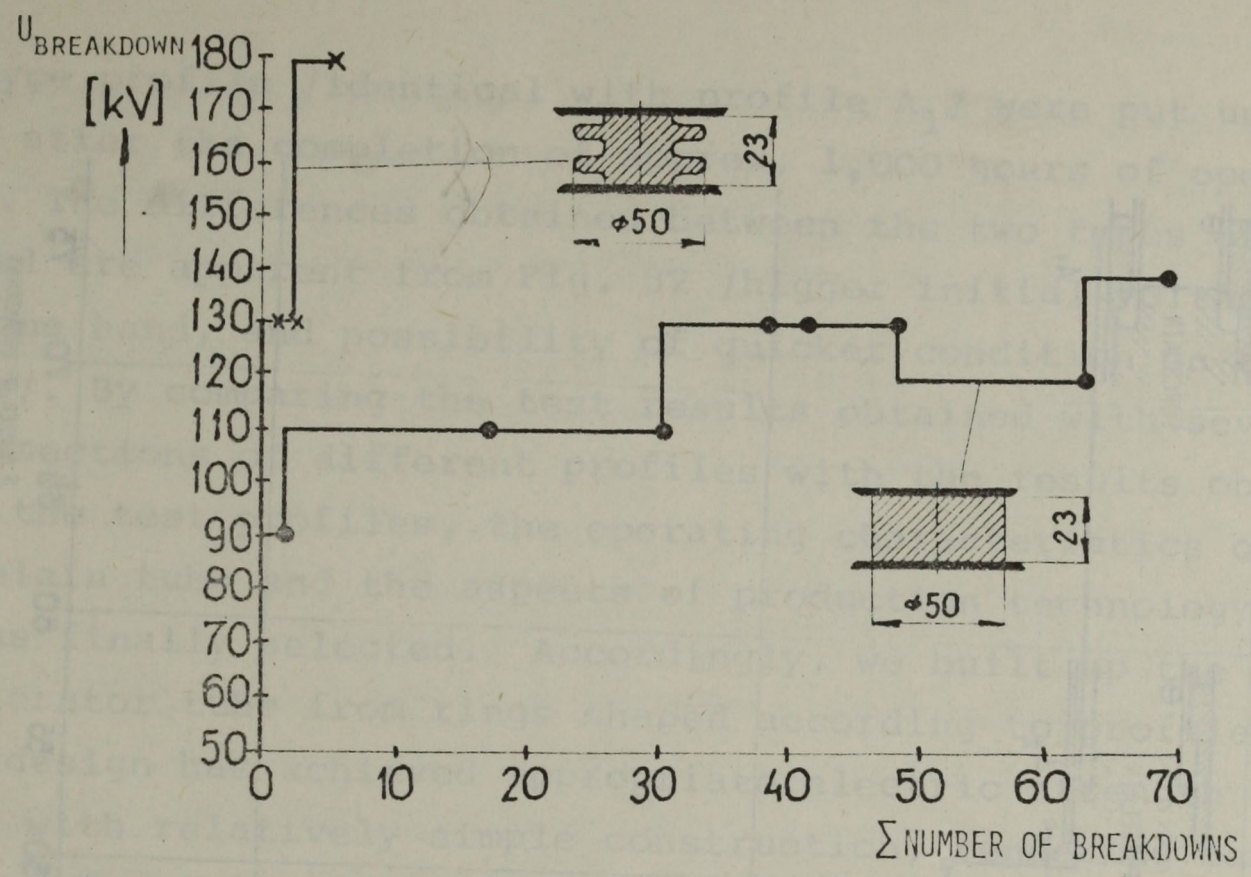

Fig. 31 Effect of shape of the insulator on dielectric strength

two extreme cases obtained in the course of measuring insulating surfaces of various profiles. Although both spark gaps had been fitted without any clearence and provided with appropriate surface finish, both the initial voltages and the possibility of conditioning gave widely different results for the simple cylindrical and the appropriately profiled solid insulators. These test results facilitated the selection of the optimal shape of the insulator.

Preparatory to the design of the first version of the accelerator tube, tests were then performed on small--scale tube sections. Owing to the limited industrial facilities available for the project, this version was made of porcelain /Profile A_o on Fig. 32/. The electrodes were shaped to provide a torus-like screen for the connection between the metal and insulator. Later on, a modified version of this tube section was successfully tested /Profile A_2/.

With the knowledge of the results obtained with the porcelain tube, experimental glass tube sections having a

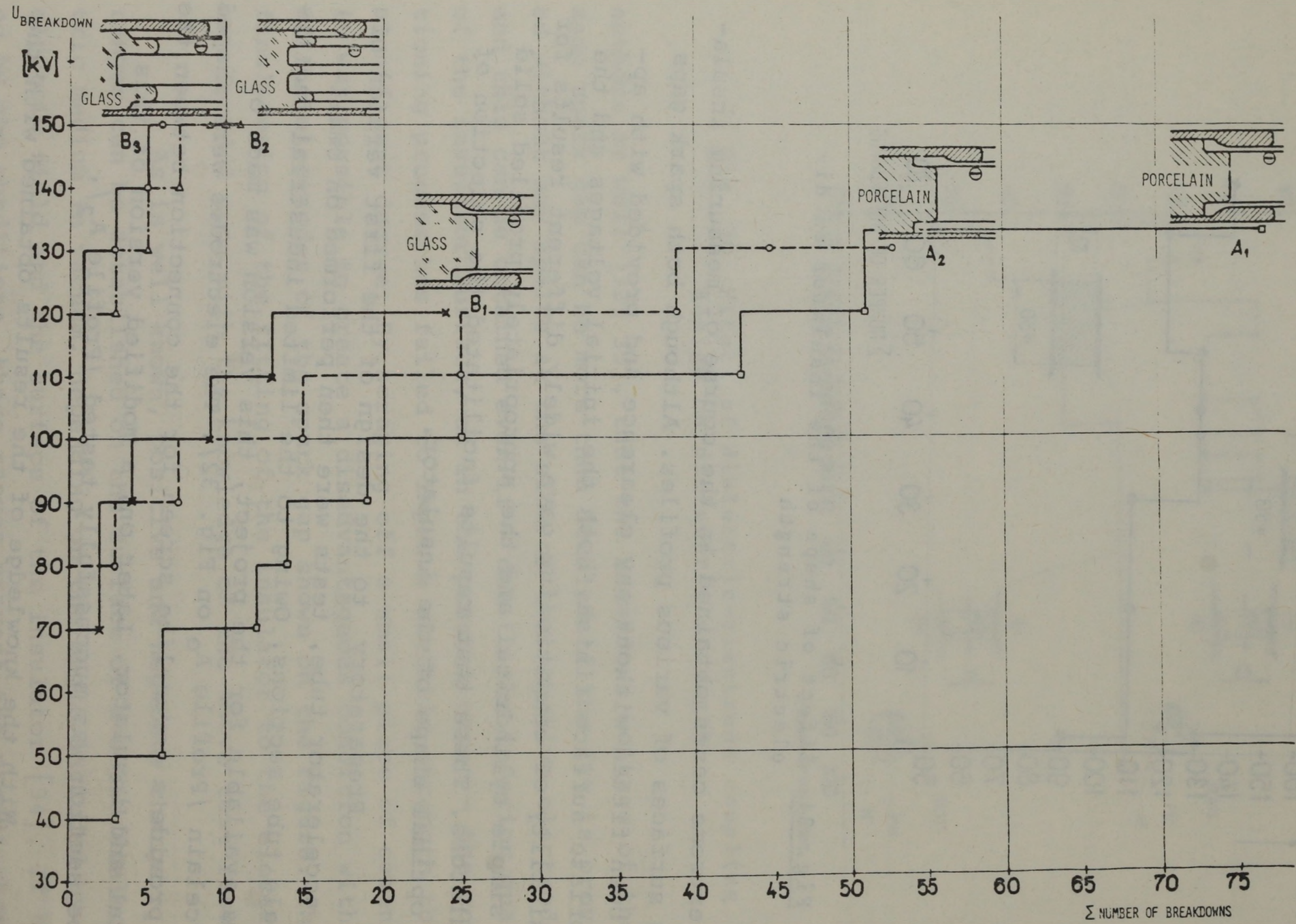

Fig. 32 Dielectric strength of tube sections

B_1-type profile /identical with profile A_1/ were put under test after the completion of approx. 1,000 hours of operation. The differences obtained between the two types of material are apparent from Fig. 32 /higher initial voltage on the one hand, and possibility of quicker condition on the other/. By comparing the test results obtained with several tube sections of different profiles with the results obtained with the test profiles, the operating characteristics of the porcelain tube and the aspects of production technology, Type B_3 was finally selected. Accordingly, we built up the glass accelerator tube from rings shaped according to profile B_3. This design has achieved appropriate electric strength combined with relatively simple construction, rendering manufacture feasible within rather short period of time.

After completing the testing of sections Type B_3 in our Laboratory, we checked the results in the Ion Acceleration Laboratory of the Nuclear Physics Institute of the Czechoslovak Academy of Sciences with help from Dr. F. Nový and Dr. R. Džmuráň. The more effective instruments of that Institute have confirmed the favourable results obtained with our test equipment [62].

1.3 Manufacturing techniques adopted for producing the accelerator tube

1.3.1 Main stages of manufacture

Simultaneously with the laboratory tests aimed at establishing the optimal design of the ion accelerator tube, we have elaborated manufacturing techniques for producing a tube coming close to the laboratory results as much as possible, and not only quickly but relatively economically as well. Owing to the high production costs involved, a long-lasting and high-quality accelerator tube had to be produced.

The main stages of production were as follows:

a/ Preparing the glass insulating rings.

b/ Making the electrode support rings, electrodes, high-tension screening rings, spark gaps and tube end flanges.

c/ Cementing together the tube sections for a third-part of the tube.

d/ Mounting the accelerator tube out of the cemented third--parts, and performing control measurements.

1.3.2 Structural materials and accuracy of manufacture

Apart from the stress-relieving heat treatment adopted for the glass tube, the main stages of producing the porcelain and the glass tube were essentially the same. The rough rings delivered by the Manufacturer were ground to size in our workshop and shaped to the required profile on their inner sides. The final dimensions and the planar surfaces were made parallel to an accuracy of $\pm$ 0.01 mm. The aluminium electrode support rings were produced to a similar high standard /Fig. 6/, special machining methods being used to ensure exact parallelness of the cementing surfaces.

The electrodes were made of a special "VD 50" Fe-Ni-Co alloy produced by the Metal Works of Csepel Iron and Steel Works, Budapest. The electrodes developed in the same plane were cut out of pre-roughed 0.8 mm thick sheet by means of a shearing die. After cleaning and grinding, their final form was given in a stamping die, ensuring clean conditions. All edges were very carefully chamfered. The electrodes manufactured in this manner are sufficiently flexible to lend themselves to be snapped into the grooves of the support rings of the accelerator tube.

The shapes of the end flanges located at the ends of the tube sections were determined by separate tests. The aim of these was to produce a shape ensuring that no deformation exceeding 0.001 mm at right angles to the planes of the flanges, i.e. along the cementing surfaces, could occur under the mechanical power effects usually arising in them.

This requirement could be met only by the loose flange design adopted.

1.3.3 Rooms

Our previous experiences had shown that in order to increase electric strength of the accelerator tube, dust has to be kept outside of it by all means. Accordingly, the stage of manufacture involving the cementing of the sections was sited in two rooms reserved solely for this purpose. The walls, ceilings, floors and all kinds of equipment of the rooms were washable, the doors and windows sealed well, and ventilation was made by fans delivering air through dust filters. The entrances were provided with admission chambers. One of the rooms served for preparations and cleaning, and the other for assembling and cementing.

1.3.4 Cementing process

After the matching surfaces had been carefully cleaned, the actual cementing process started by applying a polyvinyl acetate-toluol solution. Application was made on all surfaces to be treated by means of a rotary-disc feeding machine provided with a charging device /Fig. 33/. During 12 hours allowed for desiccation, and while drying the cement at a temperature of 150 centigrades, the surfaces were carefully protected from contamination. Thereafter, the tube sections were assembled in a sandwich-like manner in a jig. Throughout the following procedures a compressive force of approx. 5 kP/sq.cm. was applied on the sections.

Cementing was performed in an electric furnace especially built for this purpose /Fig. 34/. The assembled tube part was surrounded by three longitudinal heater provided with independent temperature control, whereas a fourth heater was located at the bottom end of the cementing jig. Temperatures

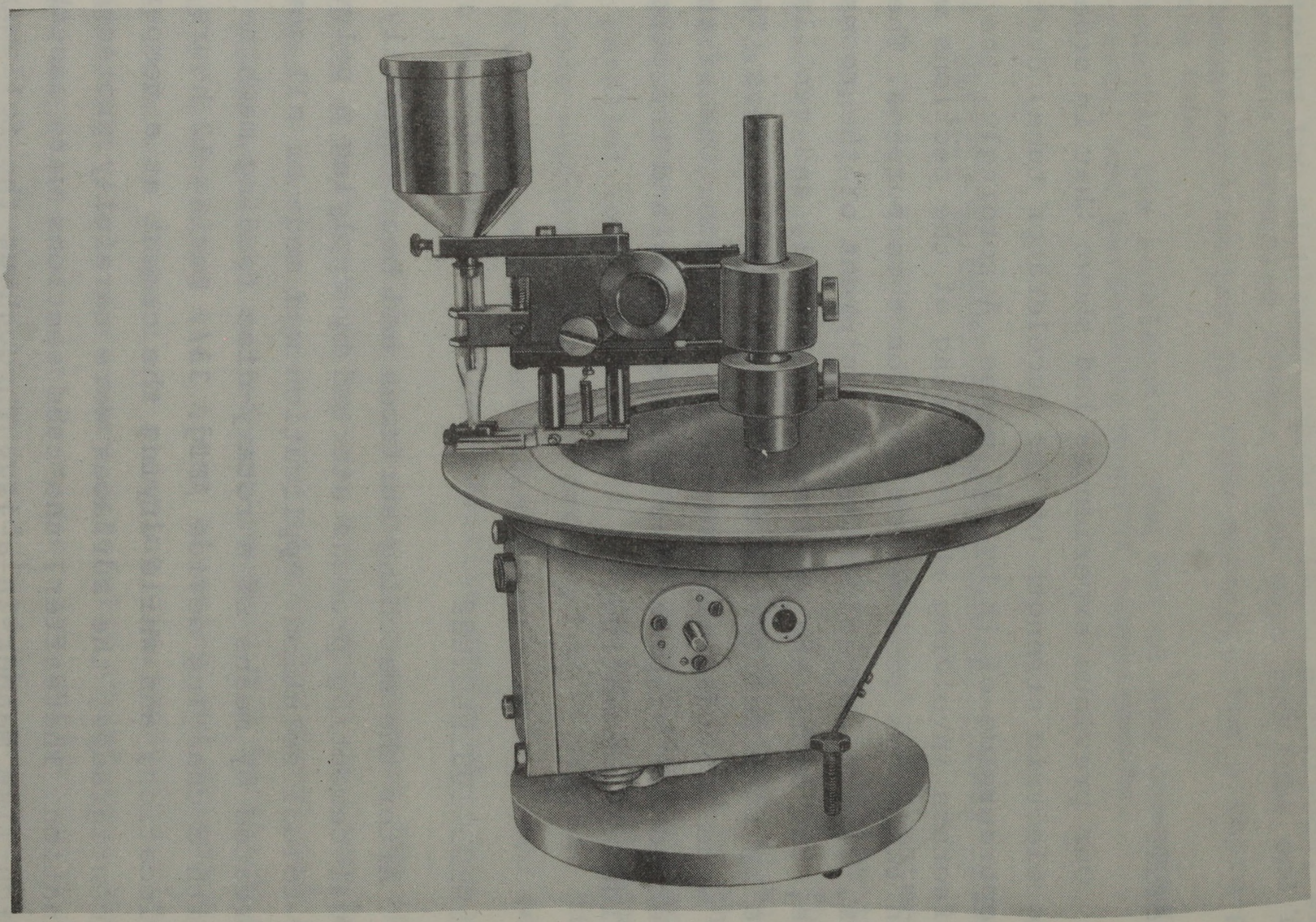

Fig. 33 Mechanism for applying polyvinyl acetate

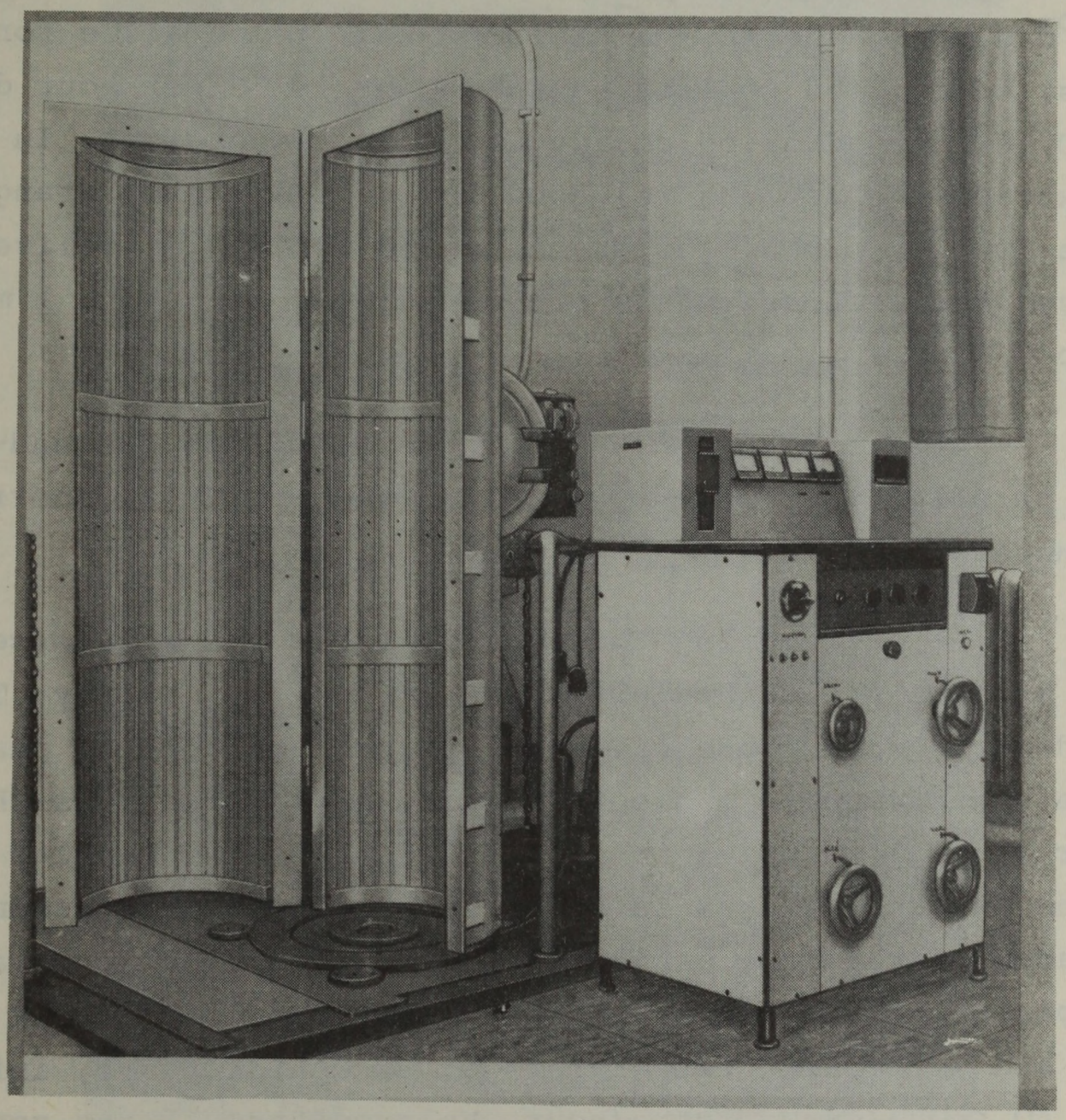

Fig. 34 Accelerator tube cementing furnace in open position

were taken by 5 thermo-couples directly inserted into the sections of the electrode support rings overhanging the glass insulators. Temperature uniformity attained was $\pm$ 1 ^{o}C. Cementing was performed in the following steps: Heating to 180 ^{o}C during 3 hours; maintaining that temperature for 12 hours, controlled cooling at a rate of 15 ^{o}C per hour down to 80 ^{o}C; uncontrolled cooling to room temperature. In order to extract the vapours released in the temperature range above 100 ^{o}C, dry N_2 gas preheated to 180 ^{o}C was delivered through the sections; this process required approx. 1 m^3 of gas per hour.

After cementing, matching surfaces of the end- flanges were parallel to 0.02 - 0.04 mm. In this manner no correction was necessary.

After removing the tube parts from the furnace they were at once sealed and exhausted to 10^{-3} mm mercury. The third-parts were transferred and stored outside the plant only while under vacuum. The optical axis of the tube was checked after it was assembled in its full length. The angular error of the two end-flanges is below 29 seconds. After assembly, the accelerator tube was subjected to a simultaneous vacuum and pressure test. Under an external gas pressure of P = 15 ata. and an ambient temperature of 20 centrigrades, inflow was $\Delta Q < 0.1$ mm Hg litre/hour. Voltage test of the accelerator tube was performed under operating conditions, in the ion accelerator itself.

A section of the glass tube is shown on Fig. 35, and the entire tube under installation on Fig. 36.

2. FOCUSSING OF THE ION BEAM

In order to increase voltage resistance and vacuum conductivity, as well as to adopt a more simple manufacturing process, the original accelerator tube design was modi-

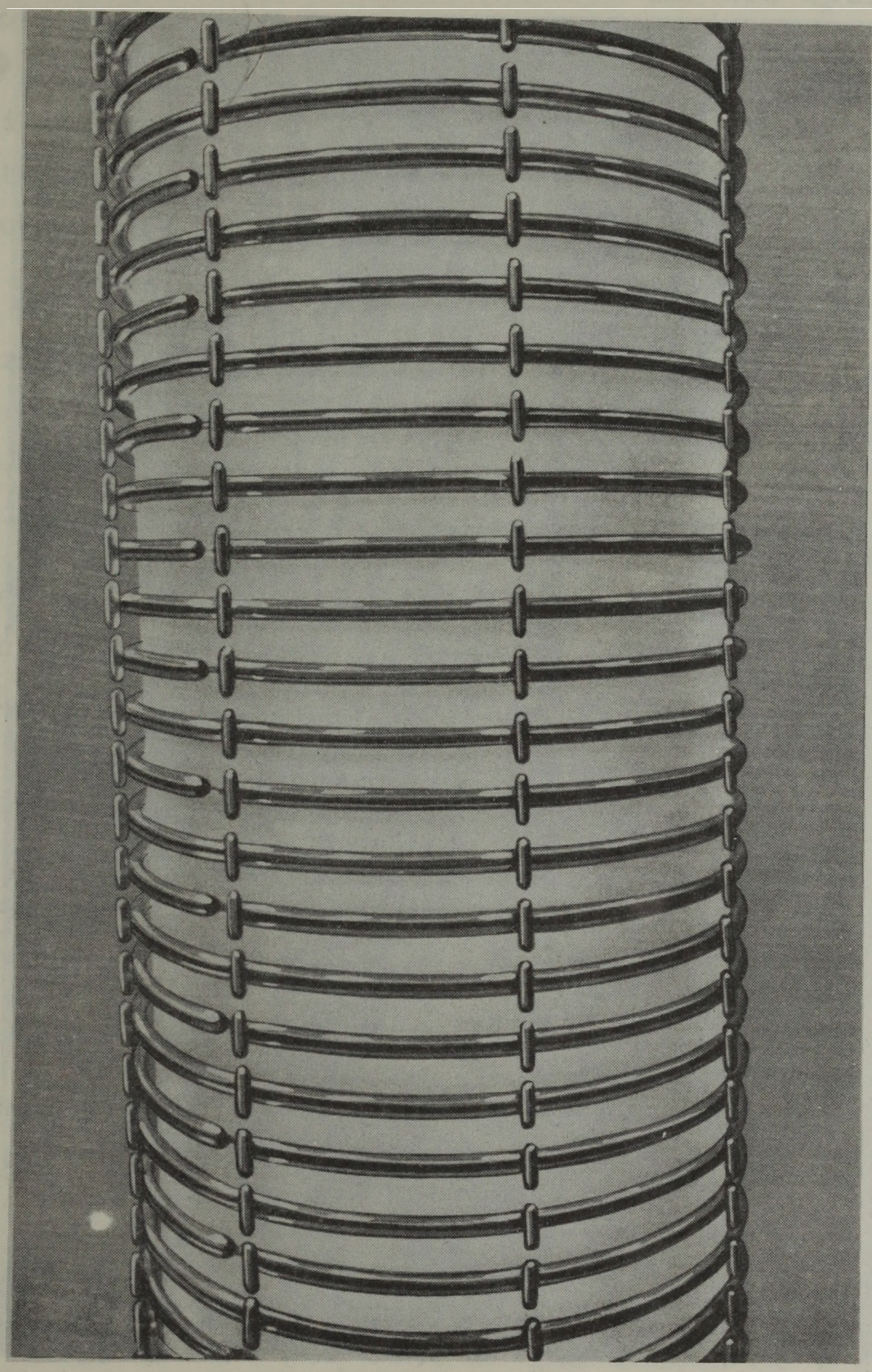

Fig. 35 One third of accelerator glass tube, transilluminated from outside

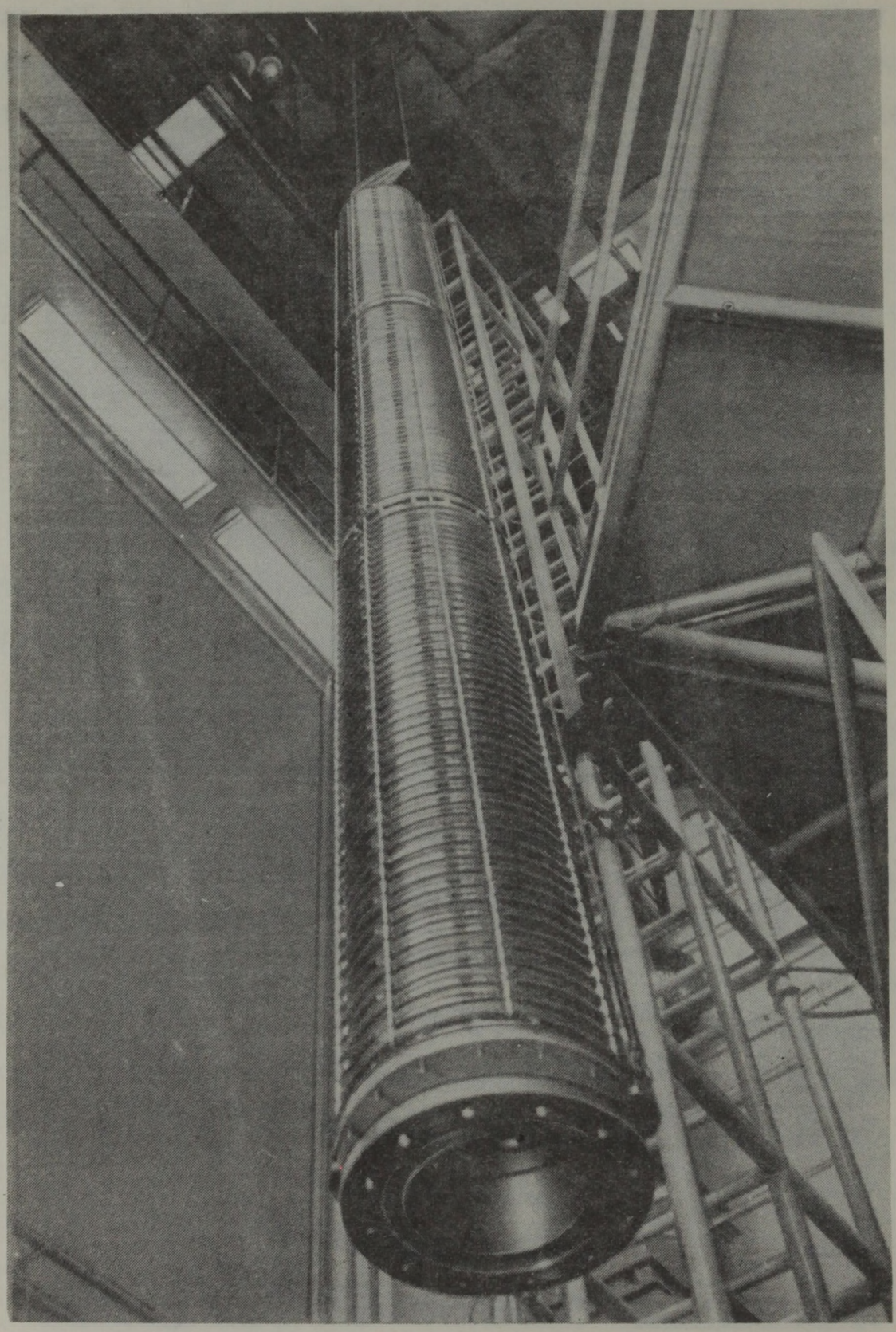

Fig. 36 Installation of whole accelerator tube into the generator

fied in the course of the reconstruction. The ion-optical focussing required the insertion of a pre-focussing lens between the ion source and the tube. This was necessary also for ion-optical compensation of possible alterations in the lens characteristics resulting from changes in the divider or from the shunting effect of dark currents.

In this respect, first the ion-optical behaviour of the ion source - pre-focussing lens - accelerator tube system was established for all conditions that might be encountered during regular operation; this work then led to the design and production of the structural elements required.

The next task that had to be solved was connected with the inclined field electrode arrangement [35] adopted for the second design in order to decrease the load currents and X-radiation encountered in the tube. This required the production of an electrode arrangement which was capable of letting through the ion beam, effectively limiting the trajectories of the secondary particles, and yet not very sensitive to the tolerances of manufacture and assembly.

2.1 Focussing tests performed on a conventional homogenous--field tube

2.1.1 Accelerator tube and pre-focussing lens

Along approx. 90 per cent of the length of the accelerator tube homogeneous electrostatic field is generated by the high-voltag divider. As is well known, the focussing characteristics of a homogeneous - field system depend first of all on the ion-optical effects of the first diaphragm, since the homogeneous field section alone can not form a cross-over. If there are sections of different fields in the system, their focussing effect also interferes with the passage of the beam through the tube [36]. In order to decrease the strength of the first diaphragm and thus that of the op-

tical magnification of the whole tube, the section of homogeneous field with variable gradient was retained over the initial section of the tube [37] in the course of the reconstruction, while the flexibility of the system has been improved by inserting one more ion-optical member. Detailed investigations were extended to the homogeneous electrostatic field on the one hand, and to the ion-optical behaviour of the system on the other.

2.1.11 Field homogeneity

In the course of our investigations it was determined to what extent the set of diaphragms could be regarded as having homogeneous field along the tube sections where voltage distribution was uniform. Namely, if the field is not homogeneous enough, we should calculate the focussing effect of a group of small invidual lenses. The distribution of the field inside the tube was, therefore, calculated by means of a computer [38]. The results obtained indicated that the inhomogeneity arising from the thickness of the electrodes was less than 5 thousandth along two-thirds of the full diaphragm diameter, and less than 4 thousandth along half of the diameter.

2.1.12 Ion-optical characteristics of the conventional accelerator tube

The focussing characteristics of both the input lens and the whole tube were examined, together with the extent of their changes as a result of the changes occurring in the initial elements of the voltage divider. The potential distribution along the whole tube, including that of the last diaphragms at the input and output ends, was available. The calculations made previously yielded the field in points spaced at 0.5 mm grid distances, to an accuracy of the order of 10^{-5}. On the basis of the field data, and by using the equa-

tions of motion, ion trajectories were determined [38]. By determining two independent ion trajectories we obtained the matrix elements of the optical transfer of the accelerator tube [39], [40].

In calculating the optical characteristics of the tube, we proceeded from the requirement of positioning the cross-over at a point located approx. 4.5 m away from the output of the tube. The object plane /L/ associated with this image plane changes immediately with any alternation occuring in the first pieces of the potential dividing chain. This is apparent form Fig. 37, where the voltage ratio U_k/U_o indicates the ratio between the potentials of the input and the output. By changing this ratio, both the point of focus at the

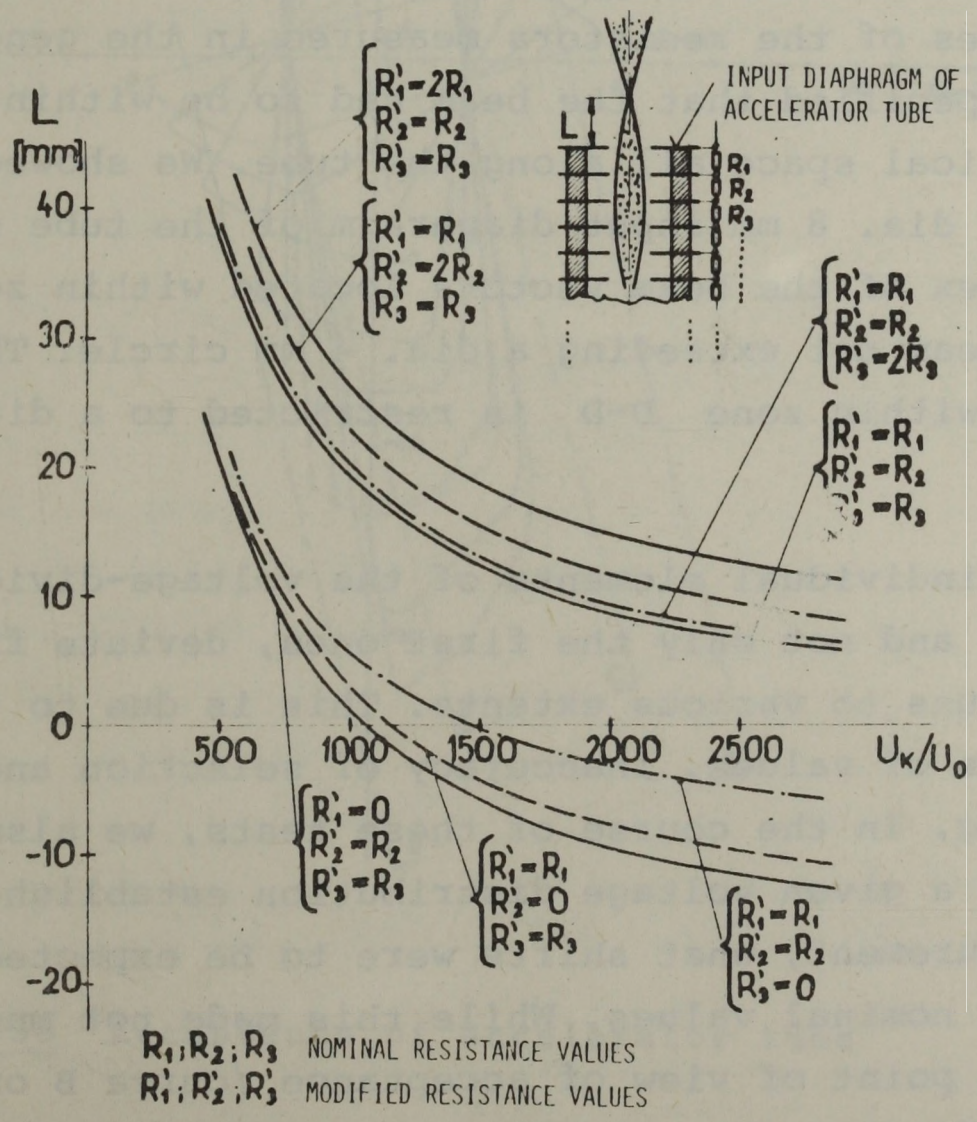

Fig. 37 Variations of object-plane of accelerator tube with variations of the first members of the voltage divider chain

input end of the tube and the focal distance are altered. Provided that the image is appropriate, the usual values of U_k/U_o = 500 to 5,000 mean that the object plane will move over an interval of approx. 65 mm. About 30 mm of this can be attributed to change at the first pieces of the dividing chain.

Since it is necessary that not just the individual trajectories, but the complete beam should pass through the tube, we also determined the acceptance of the accelerator tube under various conditions /40/. In Fig. 38, the acceptances at a distance of L = 29 mm before the input diaphragm of the tube are illustrated. The curves of the diagram were approximated by polygons. In the case illustrated on the Figure, potential distribution along the axis was determined from the values of the resistors measured in the generator. It was also specified that the beam had to be within a dia. 10 mm cylindrical space all along the tube. We showed the effect of the dia. 8 mm input diaphragm of the tube separately. The complex of the beam vectors located within zone C-C indicates a beam not exceeding a dia. 4 mm circle. The section located within zone D-D is restricted to a dia. 8 mm circle.

The individual elements of the voltage-divider resistor chain, and not only the first ones, deviate from the specified values to various extents. This is due to the original deviation of values, inaccuracy of selection and to non-uniform ageing. In the course of these tests, we also investigated, with a given voltage distribution established by resistance measurement, what shifts were to be expected in relation to the nominal values. While this made not much difference from the point of view of acceptance /curve B on Fig. 38/, it exerted definitely more influence on the determination of object plane position than did the variation of diaphragm diameter within wide limits /Fig. 39/.

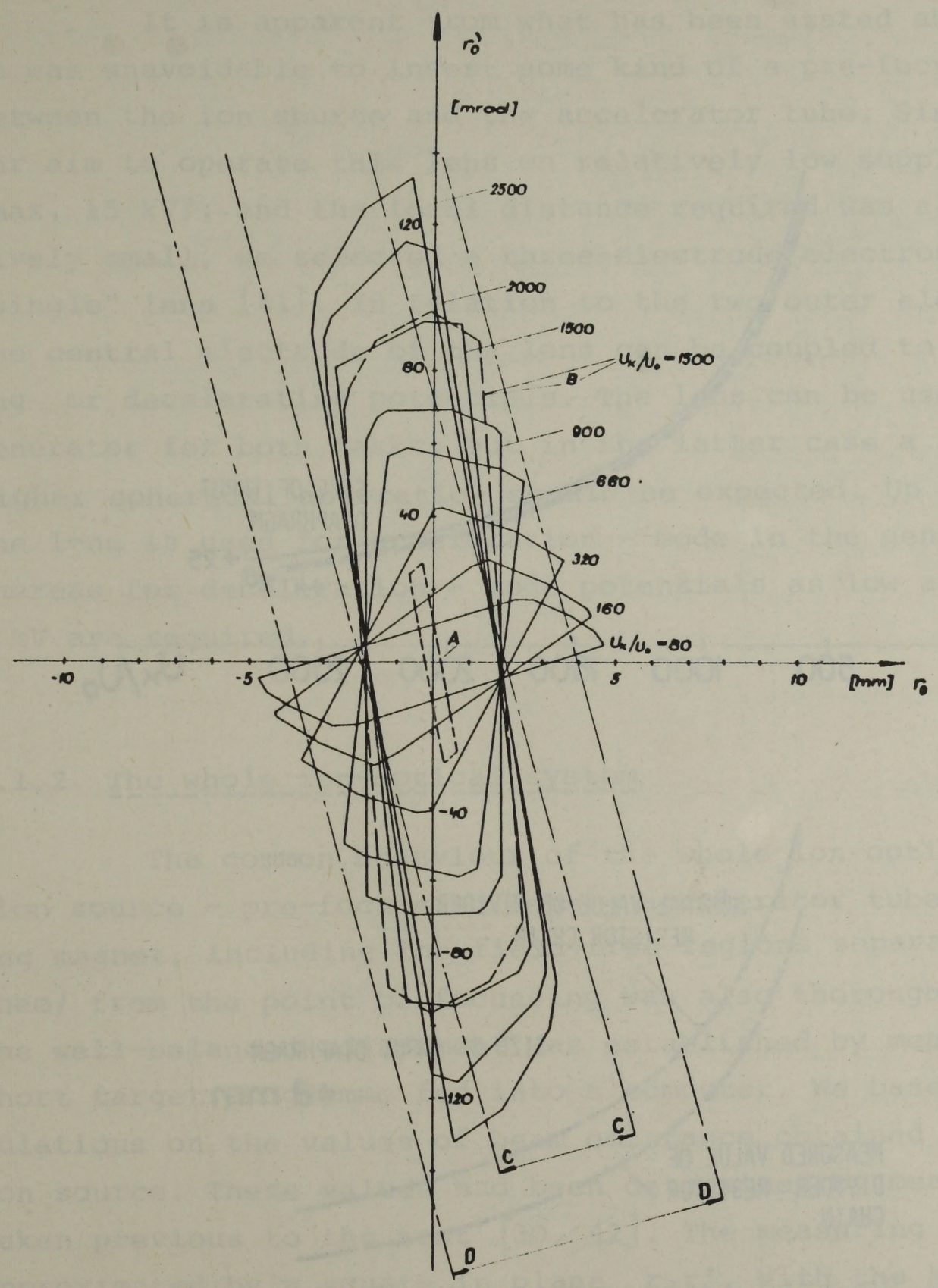

Fig. 38 Acceptance of accelerator tube

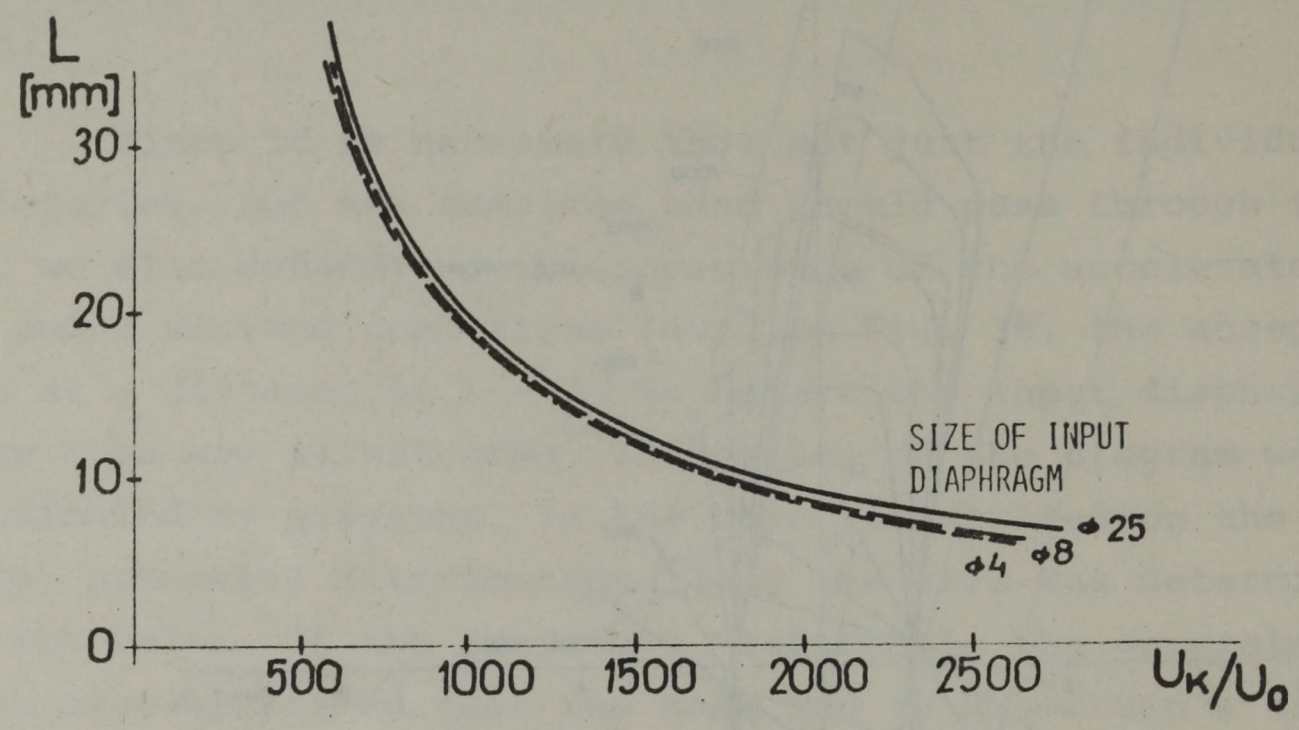

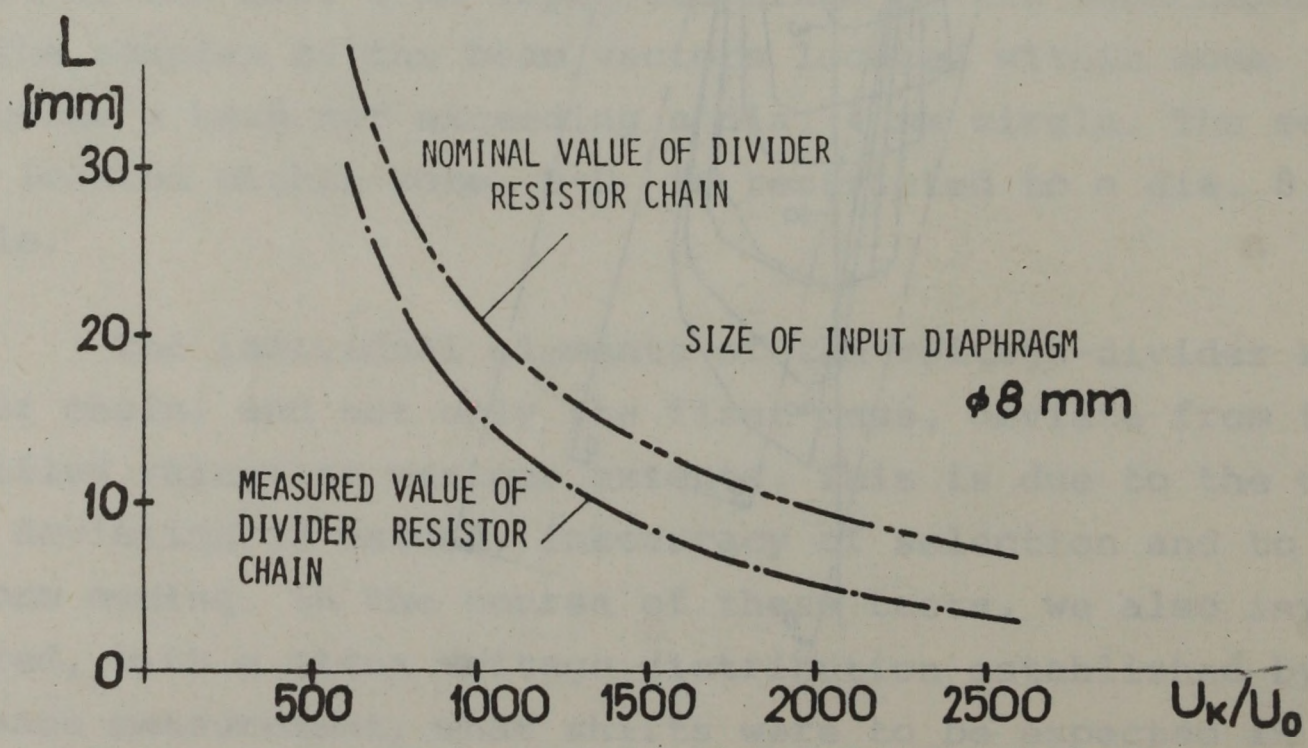

Fig. 39 Effect of input diaphragm size and the deviation of voltage divider chain pieces on the location of object-plane

2.1.13 Pre-focussing lens

It is apparent from what has been stated above that it was unavoidable to insert some kind of a pre-focussing lens between the ion source and the accelerator tube. Since it was our aim to operate this lens on relatively low supply voltages /max. 15 kV/, and the focal distance required was also relatively small, we selected a three-electrode electrostatic "single" lens [41]. In relation to the two outer electrodes, the central electrode of the lens can be coupled to accelerating or decelerating potentials. The lens can be used in the generator for both tasks, but in the latter case a somewhat higher spherical aberration should be expected. Up to 16 kV, the lens is used for acceleration - mode in the generator, whereas for deceleration - mode potentials as low as 0 to 1 kV are required.

2.1.2 The whole ion-optical system

The common behaviour of the whole ion-optical system /ion source - pre-focussing lens - accelerator tube - deflecting magnet, including the field-free regions separating them/ from the point of focussing was also thoroughly tested. The well-balanced adjustment was established by means of a short target programme fed into a computer. We based the calculations on the values of beam emittance obtained from the ion source. These values had been determined by measurements taken previous to the test [30, 42]. The measuring data were approximated by a square in plane r,r'. With the knowledge of the previously obtained matrix elements of the single lens and the accelerator tube as well as the matrix elements of the field-free regions and the analysing magnet [43] and the emittance of the ion source, the configuration meeting our requirements was selected from a number of variations. The lengths of the field-free regions, the voltage ratio U_k/U_o and the potential ratios of the single lens had to be balanced against each other. Since the matrix data of the lenses were available

only for discrete values, evaluation was made by graphical interpolation. The passage of the ion beam through the whole ion-optical system is shown on Fig. 40. In order to facilitate

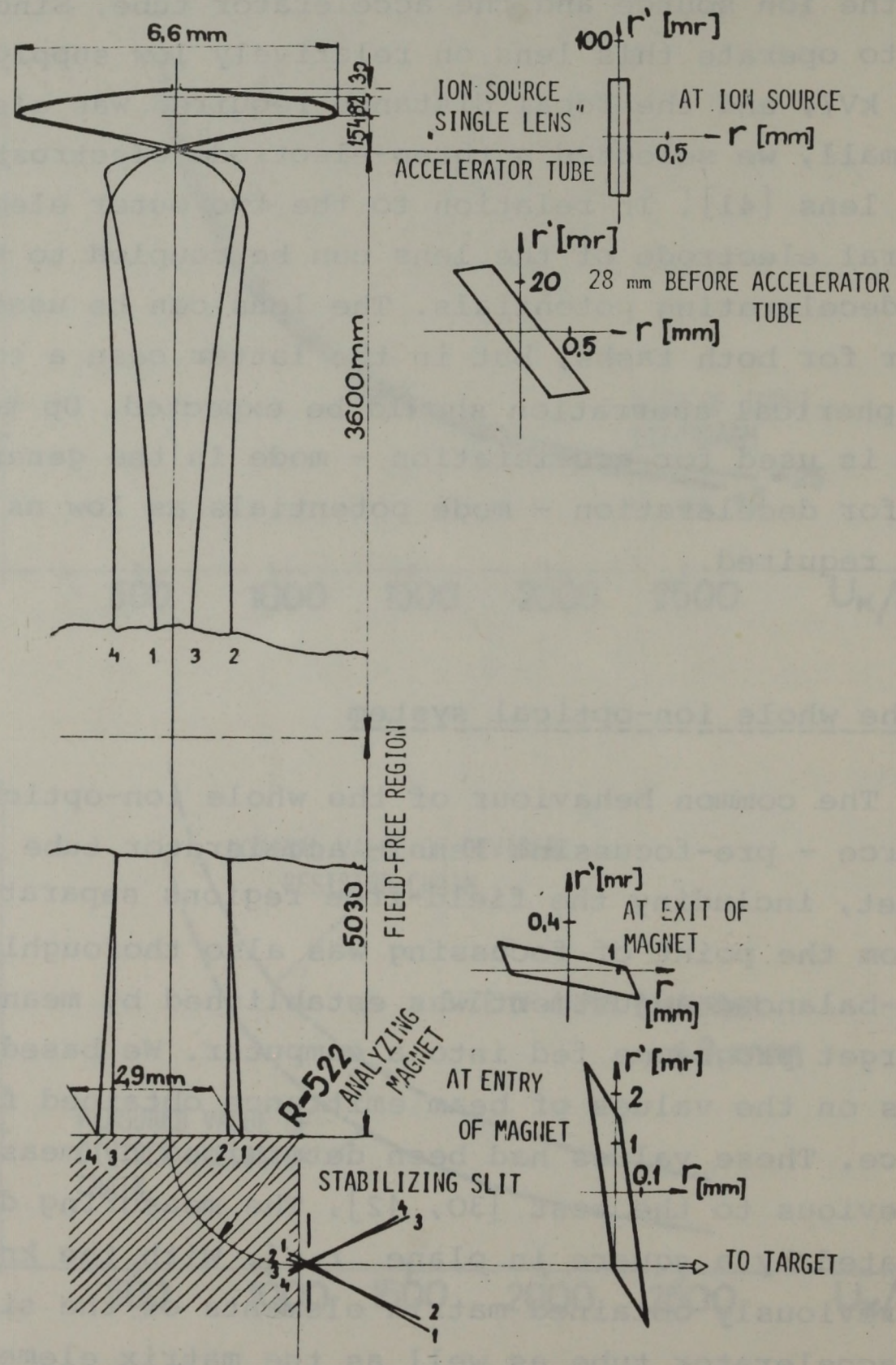

Fig. 40 Passage of ion beam through the whole ion-optical system

the observation of emittance variation, emittance diagrams have been included at several points.The emittance diagram obtained at the tube input is shown also on Fig. 38 /Diagram"A"/.

In the system, as it stands now, a dia. 3 to 8 mm beam can be focussed by means of the pre-focussing lens on to the test quartz plate located above the analysing magnet. Over the range of accelerating voltage U_k = 0.8 to 5 MV, the actual diameter depends mainly on the adjustment of the ion source. According to our measurements, the diameter of the cross-over occurring at the extracting electrode of the ion source alters between 0.2 and 0.5 mm, depending on the ion current intensity /1 to 40 μA/ [30]. Another point to be taken into consideration is that scattering of the beam on the residual gases has not been included in our calculations. The ion beam deflected by means of the analysing magnet can be observed directly after the exit-plane of the magnet. At that point the beam is focussed into a line of the order of 0.5 mm. Widening of the beam, measured by means of another quartz plate located further off, amounts to an average of ± 5-7 mrad.

2.2 Tests performed on the inclined field accelerator tube

By installing an inclined field accelerator tube our aim was mainly to effectively remove the secondary particles occurring in the tube out of the way of the beam after they runed only a short path. This is made by imparting a perpendicular speed component to the tube axis. Since the crossing field component deflects the primary ion beam as well, it is an accepted practice to reverse its direction over regions of the appropriate length; in this manner, the beam travels a wave-shaped trajectory along the axis of the tube.

In the new generator, the length of the accelerator tube, the spacing of the support rings in which the accelerating electrodes are located /25 mm between centre lines/, as well as the 50 mm long short-circuited sections interconnecting the tube parts, were given right from the beginning.

2.2.1 Selection of the inclined field regions

The length of the alternating regions was at first determined by approximation. The tests were started as described in [44], with a configuration consisting of three inclined field regions /Fig. 41.a/. In the following stage, configurations including higher numbers of region were considered [45]. The calculations were then based on regions of different length, joined to each other without any spacing, in which the field is inclined alternately at an angle of $\pm\ \alpha$ to the tube axis /Fig.41.b/. Accordingly, the particles would travel along a

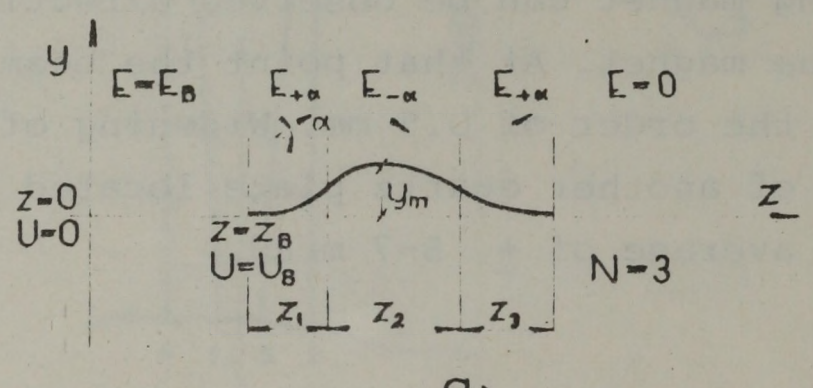

Fig. 41 Electrostatic field models of approximate calculation for inclined field electrode arrangements

wave-shaped trajectory, the amplitude of which is identical throughout the tube. Since several free parameters were not easy to consider, the diagram shown on Fig. 42 was plotted for the theoretical case of a configuration with N = 6 inclined field regions. First in this case the quantity $\xi = y_m \cot g\alpha/p$ should be determined by means of trajectory amplitude y_m; the angle of the electrodes to the tube axis, as well as the

electrode spacing p and thereafter the quantities F_1 and F_2 should be taken in account as the function of ξ from the Fig. 42. F_1 depends on the input energy of the particles /U_B/ and the potential difference existing between two electrodes located next to each other /ΔU/, whereas the parameters of F_2 correspond to the serial numbers of the individual inclined field regions /K_1, K_2 ... K_6/. Length of the whole tube is K_T, whereas the maxima of the trajectory are marked K_{2m}...K_{5m}. The individual lengths can be calculated by the formula

$$Z_n = p.Cn. \left(F_1 + F_2\right) \qquad /2/$$

based on Fig. 42. This Figure greatly facilitated the initial stages of the work. It was clear that the region lengths obtained in this manner could be built indeed, although - quite understandably - the calculations yielded shorter tube sections than needed in practice, since the field strengths envisaged for the joining of the individual inclined field regions were taken somewhat higher than the value employed in practice.

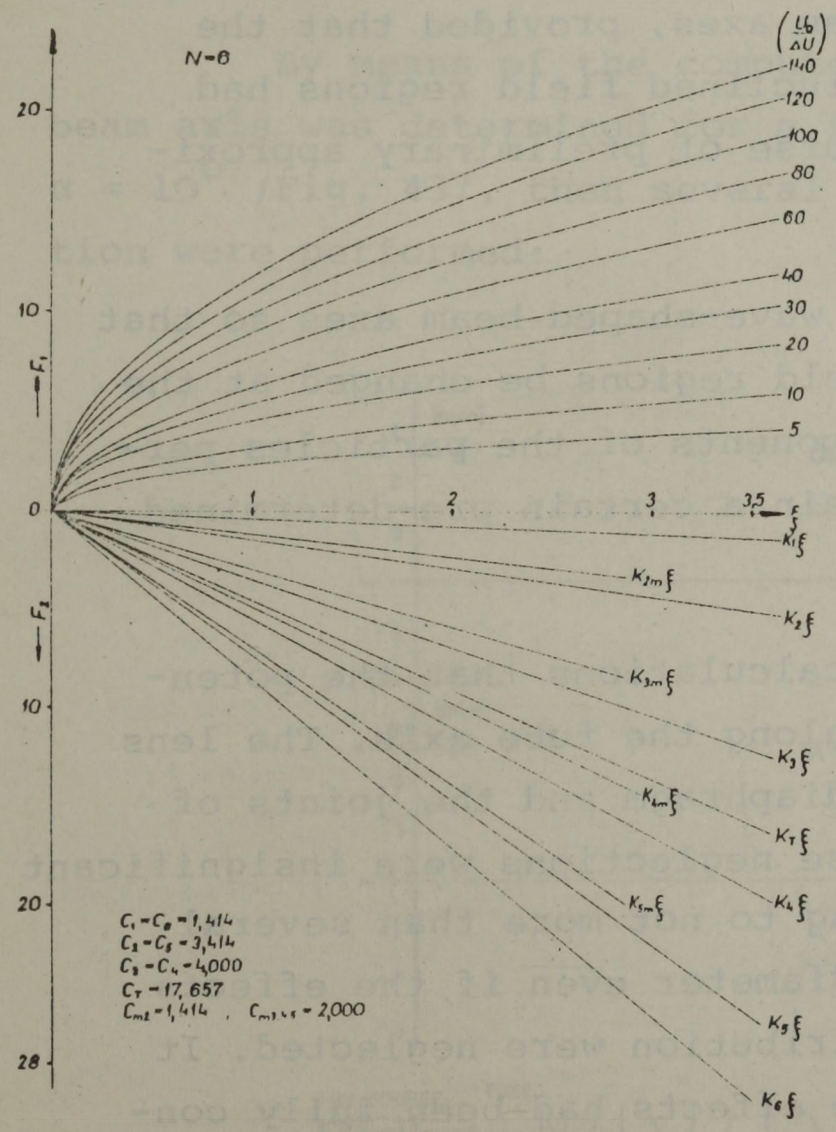

Fig. 42 Diagram for the approximate calculation of region-lengths in the 6-element inclined field accelerator tube

In practice, the inclined field regions cannot be joined without any spacing. It is expedient to select the fields so that they do not differ by more than 10 or 20 per cent from the average.

Since this requirement can be met relatively easily during the manufacturing process, the inclined field regions were joined to each other by wedge-shaped sector spaces overlapping two accelerating intervals. The particle trajectories were thus to be calculated by considering these field sections. In the literature several methods are known for this procedure [46, 47, 48]. For this case, Romanov and Serbinov's method [47] was adopted. In order to obtain highly accurate results, a target program was fed into a computer, which was suitable for

a/ calculating any type of trajectory in sector spaces and inclined and homogeneous sections, with field-free regions between them;

b/ determining wave-shaped beam axes, provided that the lengths of the individual inclined field regions had been established in the course of preliminary approximation tests;

c/ alternatively, determining wave-shaped beam axes so that the individual inclined field regions be changed at the points where the speed components of the particles perpendicular to the axis attain a certain pre-determined values.

We assumed for these calculations that the potential distribution was uniform along the tube axis. The lens effects occurring at the last diaphragm and the joints of tube parts were neglected. These neglections were insignificant for the new equipment, amounting to not more than several tenth of a millimetre in beam diameter even if the effects of the not uniform voltage distribution were neglected. It should be remembered that these effects had been fully considered with the calculations of the conventional accelerator tube.

In the first third of the new accelerator tube, a configuration consisting of three inclined field regions was in-

stalled. There was a good coincidence between the preliminary approximation and the more accurate results obtained by computer. The number of accelerating intervals was at first obtained as $Z_T/p = 21.2$, whereas the computer corrected this to $Z_T/p = 22$; both calculations were based on identical geometrical, voltage and trajectory amplitude data. In the second and third tube parts the configuration consists of six inclined field regions with accelerating intervals of $Z_T/p=90$ and two short-circuited sections. The preliminary approximation yielded in this case $Z_T/p = 91.7$ for the accelerating intervals.

2.2.2 Testing accuracy of the axis

By means of the computer programme, first of all the beam axis was determined for a field having an inclination of $\alpha = 10^{\circ}$ /Fig. 43/, then several types of additional calculation were performed:

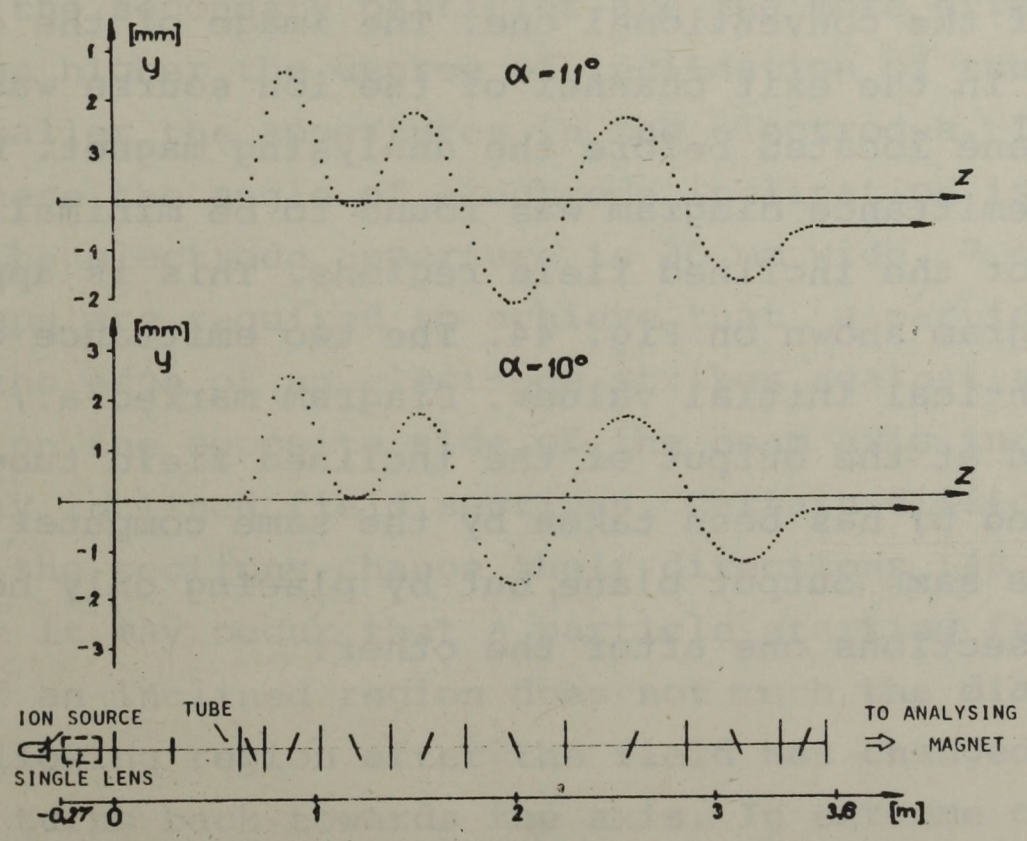

Fig. 43 Beam axis in inclined field accelerator tube, for angles of electrode inclination $\alpha = 10^{\circ}$ and $\alpha = 11^{\circ}$

a/ The axis was checked for α = 11 deg. This value was selected as α = 11 deg. was regarded as the extreme value of tolerances obtained during electrode manufacture. On Fig. 43, the axes established at α = 10 deg. and α = 11 deg. are shown. It is apparent that the two lines hardly differ from each other, and outgoing beam directions are also appropriate in both cases.

b/ Another point examined was the effect of a voltage shift occurring for any reason in the pre-accelerating region on the axis located in a region following that. It was found that if $U_B/\Delta U = 6.6$, the beam passed through the electrode system, but was deflected by 7.7 mm in consequence of the effect at the analysing magnet. This deflection was less than 1 mm over the range of $14 < U_B/\Delta U < 21$, with the angular position of the axis changing by less than 0.1 mrad. If $U_B/\Delta U < 5$, no passage of the beam could be expected.

c/ Owing to the small deflections, the focussing characteristics of the inclined field tube did not differ from those of the conventional one. The image of the cross-over located in the exit channel of the ion source was examined in the plane located before the analysing magnet. Distortion of the emittance diagram was found to be minimal under the effects of the inclined field regions. This is apparent from the diagram shown on Fig. 44. The two emittance diagrams refer to identical initial values. Diagram marked a./ has been obtained at the output of the inclined field tube, and the one marked b./ has been taken by the same computer programme and in the same output plane, but by placing only homogeneous field sections one after the other.

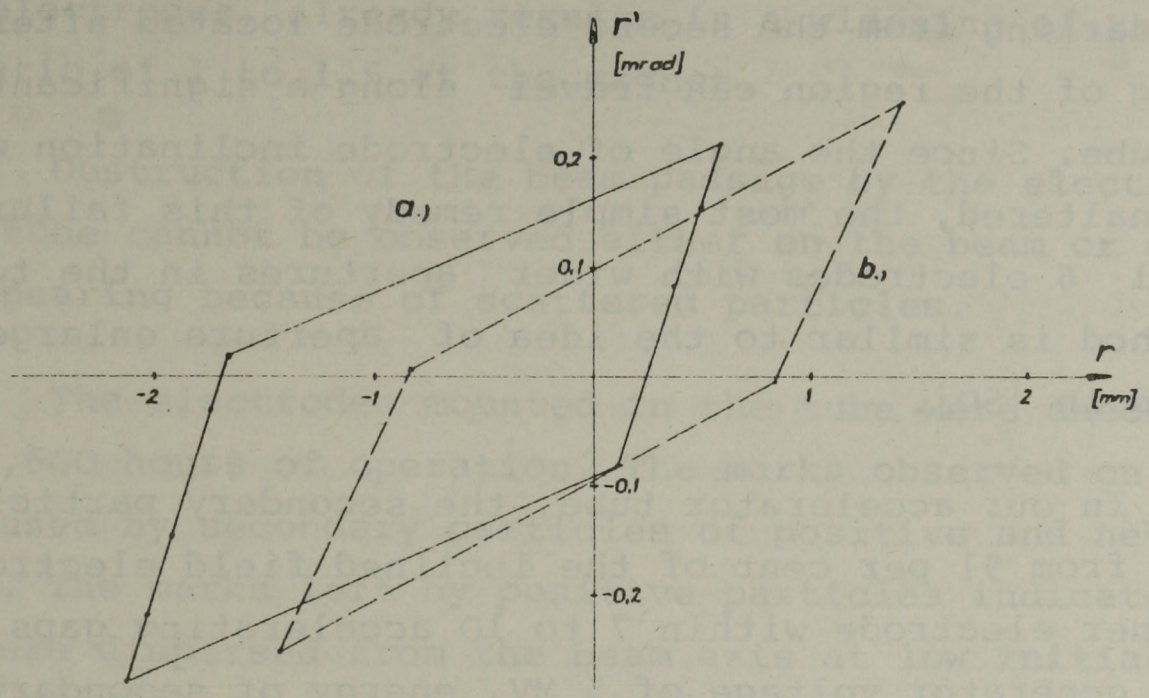

Fig. 44 Emittance diagram at the exit of inclined field (a) and conventional (b) accelerator tubes

2.2.3 Trajectories of the secondary particles

We also examined the possible trajectories of the secondary particles in the accelerator tube. It is only natural that the secondary particles are the more effectively removed the higher the degree of inclination of the electrodes and the smaller the appertures in the electrodes. In our generator, where the angle of electrode inclination is $\alpha = 10$ deg. and the electrode apperture is 30 mm wide, 7 or 8 accelerating gaps are required to achieve that a particle starting from the edge of an electrode strikes against another electrode on the opposite side of the beam axis in region having only inclined field sections. Certain difficulties are met where the sections change their directions [49, 50, 51, 52], since it may occur that a particle starting from the beginning of an inclined region does not touch the diaphragms of the following region after the field has changed direction, but turns back towards the axis. In extreme cases, such a particle may travel along a wave-shaped trajectory all along the tube. The inclined field design envisaged for the accelerator tube was thoroughly analysed also in this respect.

According to our calculations, at changing sections, the particles starting from the second electrode located after the beginning of the region can travel along a significant region of the tube. Since the angle of electrode inclination was to remain unaltered, the most simple remedy of this failure was to instal 6 electrodes with wider apertures in the tube. This method is similar to the idea of aperture enlargement mentioned in [50].

In our accelerator tube, the secondary particles starting from 91 per cent of the inclined field electrodes hit another electrode within 7 to 10 accelerating gaps. At the full generator voltage of 5 MV, energy of secondary particles is less than 380 keV. The particles starting from 10 certain electrodes can travel through 20 to 30 accelerating gaps; most of these electrodes are, however, located in the first inclined field region following the homogeneous - field pre-accelerating - part of the tube. With these, the energy expected is max. 700 keV. In the homogeneous field pre-accelerator region the energy of the secondary particles can be max. 600 keV.

The inclined field tube has met the expectations. The beam appears at the analysing magnet located after the tube in the right direction and being appropriately focussed. Into a spot of only several mm in diameter, the beam can be focussed at values U_L/U_o = 5.2 - 6 of the preceding single lens according to optical magnification. The spot appearing on the quartz plate located at the magnet is an ellipsoid, with its longintudinal axis pointing in the direction of the inclined field component. When operating at lower voltages, the spot becomes more elongated, whereas under 4 MV is close to a regular circle. Widening of the spot was obtained in the calculations based on ideal conditions to a somewhat lower degree /approx. 15 per cent/, since the lens errors and dispersion occurring in the tube were not considered. It is easy to show that only a few tenth of a mrad shift in the direction of the beam, especially near the first inclined

field electrodes, already results in a widening of the spot in a ratio of 1 to 1.5 at the magnet.

Obstruction of the beam passage by the electrodes of the tube cannot be observed either on the beam or on the halo appearing because of scattered particles.

The electrodes mounted in the tube were checked after 1,600 hours of operation. The marks observed on them were caused by secondary particles of positive and negative charges. The marks left by positive particles indicated that these were dispersed from the beam axis at low initial energy, and hit the electrodes from directions corresponding to 10 - 11 degrees. This was concluded from the fact that these marks appeared at the beginning of every inclined field region, at the 3rd or 4th accelerating gap located after the change of the crossing-field components. At the same time, the marks vanished on the opposite side. The marks left by the secondary particles of negative charge appeared on the lower sides of the electrodes. It could be proven that these were the corresponding marks of the positive particle marks. These particles had started from the electrodes and impacted after having travelled through 7 or 8 accelerating gaps. Accordingly, the stronger marks appeared on the 7th or 8th electrodes after changing regions, whereas the marks left by the particles overrunning the previous region were visible on the opposite side of the aperture at a few accelerating gaps following the change. Some weaker marks of course indicated that negative particles, not originating from electrode surfaces, had also been present in the tube. The widths of the marks, as well as the extent of overlapping of the electrodes located above each other, indicated trajectory angles of 10 to 11 degrees in this case too.

The marks have thus shown that the inclined field arrangement is effective in preventing most of the secondary particles from travelling long distances along the tube. In complete agreement with this finding, the level of X-radiation

measurable at identical voltages is by 1 or 2 orders lower than that obtained with conventional homogeneous field accelerator tubes.

3. PUTTING IN WORK

All the above ideas relating to the passage of ion beam and its focussing are valid only if the electrostatic field on which the trajectory calculations have been based is in fact established. This means that the electrode system is to meet not only the requirements of focussing but also all criteria of electric strength in the case of the whole tube too. It follows from this that electric strength is to be established first, since without this the focussing of the beam is illusory.

It is extremely difficult to determine the voltage which can be applied without breakdowns on electrodes located in vacuum. The number of studies devoted to the subject runs into hundreds [53], clearly indicating the lack of a comprehensive theory on which technical dimensioning could be based. The voltage applicable on the electrodes depends on very many parameters, and this fact holds true on the entire tube to an even greater extent than on a single section.

3.1 Dark current and radiation with the conventional homogeneous field tube

With the first accelerator tube our first intention was to establish the rate at which voltage could be safely increased, as well as the degree of vacuum required for this and the intensity of dark current to be expected; these tests were carried out at first without any accelerated ions. The intensity of dark current was important for two reasons: individual electrons may result in producing further ones, leading to an avalanche, and even if an avalanche and the breakdown result-

ing from it can be avoided, the electrons hitting against the high-voltage end of the accelerator tube generate Bremstrahlung there. As a result, the insulating gas of the generator is ionized and the accelerating voltage can be coupled to the tube decreased.

At the beginning, electrodes made of stainless steel were used. Since these showed a very high secondary emission factor, the intensity of dark current flowing through the tube, and thus also the level of X-radiation, were too high. The voltage attained without an ion beam was 5,148 kV. This, however, required the utilization of the so-called "pressure effect" [54], achieved by increasing internal pressure to 6.6×10^{-5} mm Hg. The lack of current, i.e. the difference between the current delivered by the belt and the current flowing through the voltage divider, was even so as high as approx. 30 - 100 μA. Since increasing the pressure results in dispersing the beam and defocussing, acceleration inevitably pays the price for it.

Evaluation of the test results, as well as testing of the materials used, indicated that the stainless steel from which the electrodes had been made was not sufficiently pure, causing extremely high secondary emission. Accordingly, electrodes made of Fe-Ni-Co alloy marked VD-50 to very strict specification were mounted at the most exposed points, i.e. the diaphragms of the smallest diameter. This measure yielded appropriate results, since the voltage could be increased to 5,220 kV at an acceptable pressure of 4×10^{-6} mm Hg. By impairing the vacuum /to 1×10^{-5} mm mercury/, voltage could be increased to 5,500 kV. In spite of these results, the tube was not considered reliable in operation, since the dark current intensity, and thus the level of X-radiation, were still too high. Measured at the wall of the pressure vessel, in front of a plexi-glass window /i.e. actually without any adsorbent at all/ radiation was found to reach approx. 80 mr/hour. The fact that the lack of current was essentially identical with the dark current is apparent from the correlation between the lack of current and the level of radiation /Fig. 45/.

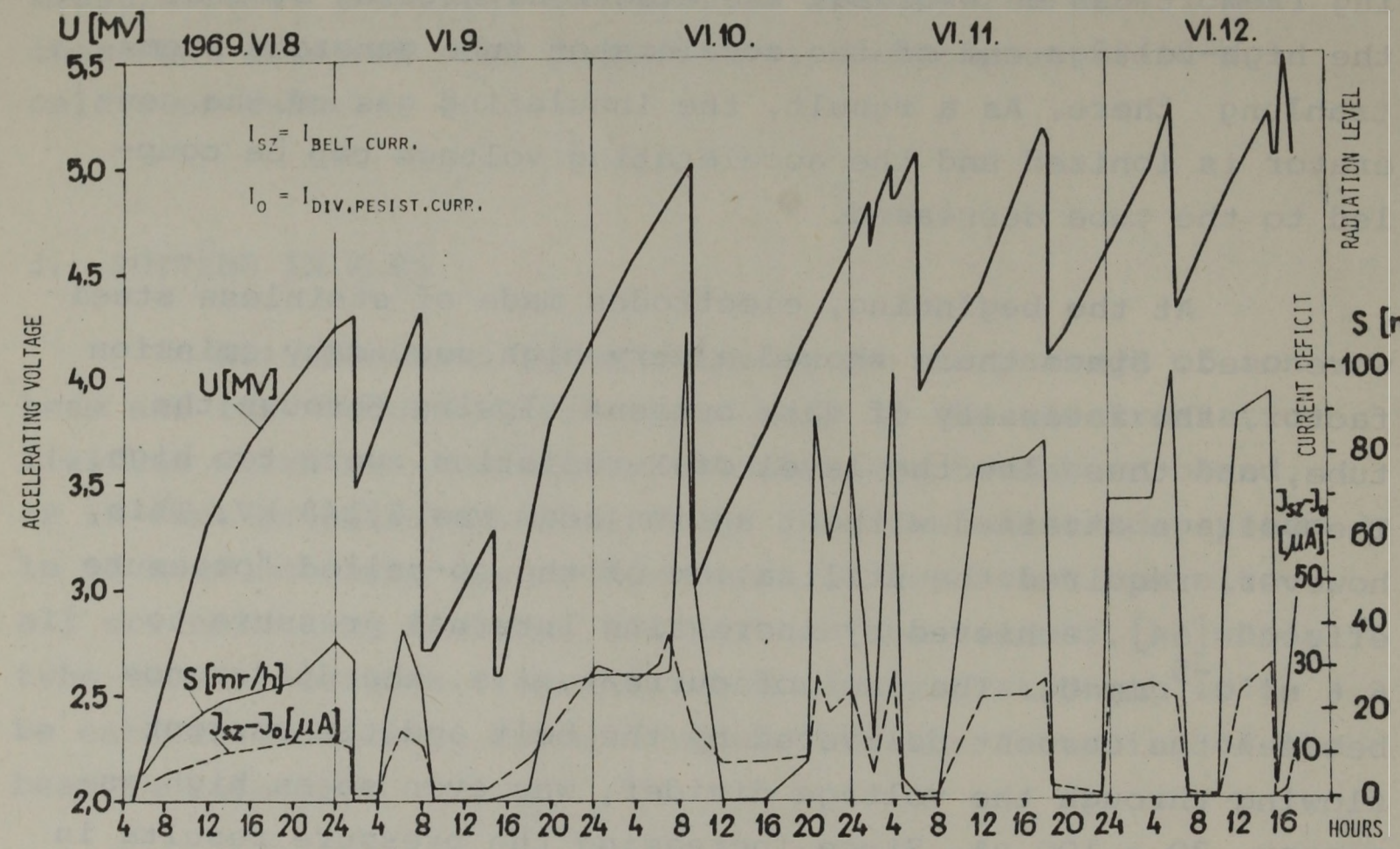

Fig. 45 Correlation of current failure and radiation on conditioning a conventional accelerator tube (I_{ion} = zero; p = 4.10^{-6} mm mercury)

The tube was thereafter tested with ion beam as well, but although an acceleration voltage of 5050 kV was attained, the result was regarded as unsatisfactory, since when the beam was started, the level of radiation increased to approx. 1 r/hour.

It became quite clear that the fundamental task was to prevent the occurrence of secondary particles or, should this be unfeasible, to annihilate such particles in a minimal length of travel.

It is completely hopless to strive after the complete elimination of secondary particles. Even under the best vacuum conditions attainable at present, there will always be dispersed ions triggering off secondary electrons. It was obvious that, with the geometry chosen, the insulating material used and the cementing technology adopted, the tube was meet-

ing the requirements, and the main problem encountered had been caused not by the electric strength but rather by the secondary electrons. The effect of secondary electrons is generally mitigated by the so-called inclined field accelerator tube design, and this is what we too have adopted for solving this problem.

3.2 Effects of the inclined field

With this arrangement, the problem first of all was to calculate the trajectories of primary ions and secondary electrons. This aspect has already been dealt with. Switching of voltage on the tube, and the behaviour of the tube on encountering transients were also problematic. The data furnished by our sources of literature on conditioning [55] were fairly sparse, thus we had no information on e.g. under what degree of vacuum the tube should be conditioned, and whether it was advisable, or not, to use an ion beam for this purpose.

3.3 Micro-discharges and their causes

The results obtained with the inclined field accelerator tube were highly encouraging from the beginning. Although on the very first test some lack of current and radiation were observed /Fig. 46/, later on both of these failures significantly decreased. On the other hand, micro-discharges appeared in the tube. Their effect was clearly observed on the current of both the generating voltmeter and the divider. At the same time, flashes were observed also on the quartz plate located at the output of the accelerator tube.

All tests, measurements and results mentioned so far related to an accelerator tube built with porcelain rings. It was this tube on which micro-cracks and holes were observed after some breakdowns occurring between the high-voltage column and the pressure vessel, mainly if the breakdowns oc-

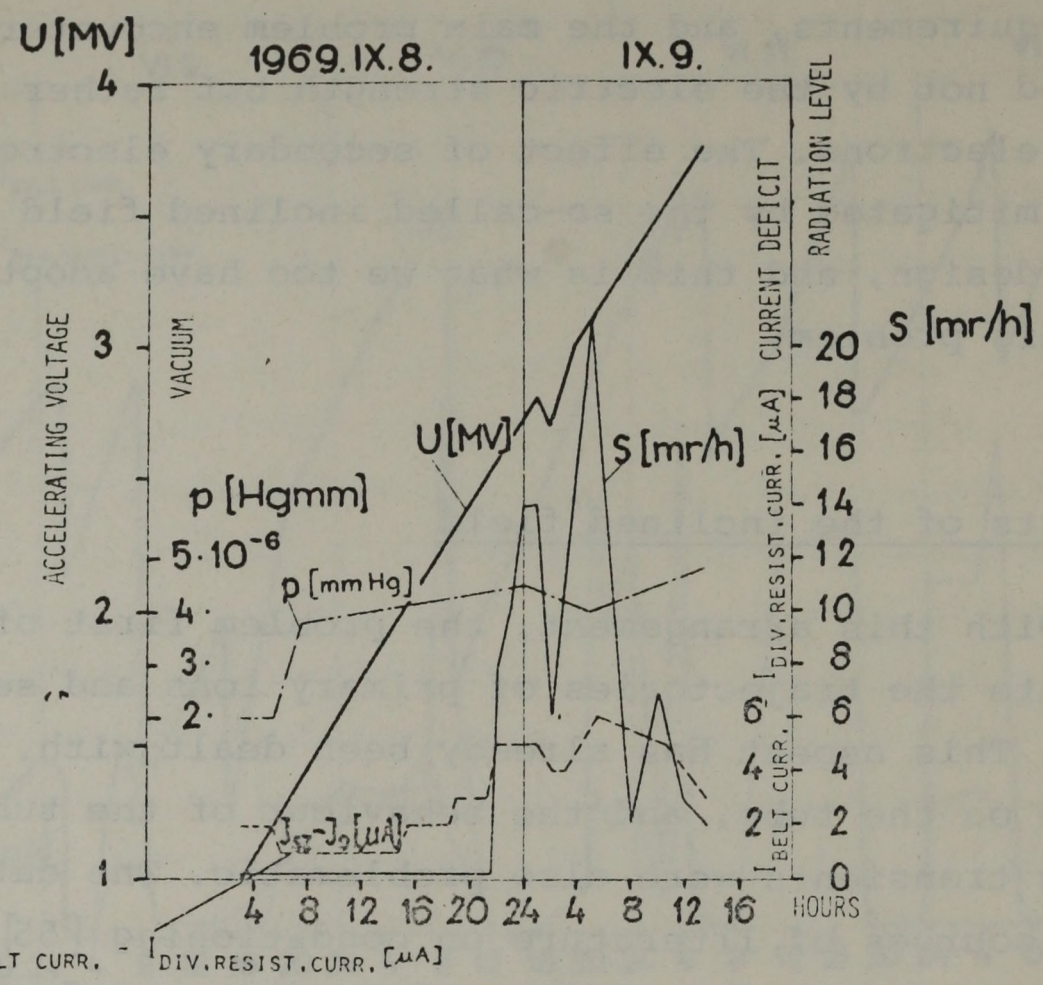

Fig. 46 First voltage test performed on inclined field electrodes mounted in a porcelain accelerator tube

curred at or above 5 MV. The micro-cracks tended to expand on their internal side, facing the vacuum chamber, and resulted in most cases in partly bursting the rings concerned. As a result, there were porcelain fragments of various sizes all over the tube. It was found that the micro-discharges were connected with these contaminations.

Clearing up the reasons of ring bursts was very interesting. After consulting several times with a number of experts of the porcelain industry, the following picture could be obtained: since porcelain is a crystalline material, significant stresses remain in the rings after firing, which cannot be eliminated. Until temperature and load conditions prevailing around the rings are uniform, the above stresses seldom present any difficulty at all. However, as soon as any local load is applied on the rings, as happens in heating-

-up after breakdown in our case, stresses may be equalized at a burst-like speed. This usually occurs at the points of maximal mechanical stress, which in our tube were located on the sides of the steps ground on the inside of the rings.

Since micro-discharges impair the stability of ion beam, we tried to eliminate them, together with the breakdowns causing their occurrence.Thus up to the summer of 1970, the voltage of the generator was limited at 4 MV. A total of approx. 2,000 hours of operation were completed by adhering to this voltage limit.

3.4 Installation of the glass accelerator tube

Originally, our intention was to build a glass accelerator tube, and the porcelain tube had to be built only on account of certain difficulties met in the purchase of glass rings. Since, however, this problem was later on solved, a glass tube could be built. As proven by the section tests described before, the glass tube is significantly more reliable than the porcelain one. Right after the first switching on it was obvious that there was no dark current and, apart from some calibration differences, charge belt current and distributing chain current were identical /Fig. 47/.

Encouraged by these favourable results, the measurements were attempted also with the ion beam /Fig. 48/. Although the beam was not constantly focussed in an optimal manner, radiation remained at a tolerable level. As apparent from the Figure, radiation depends to a great extent on the focussing of the ion beam, and thus it may be assumed that the dark current generating radiation consists of secondary electrons triggered off by ions rather than of electrons leaving the electrodes by cold emission. In the course of the tests, an accelerating voltage of 4.4 MV was attained while we observed not more than one or two breakdowns. The voltage increase tests were then repeated several times. The results show that in the

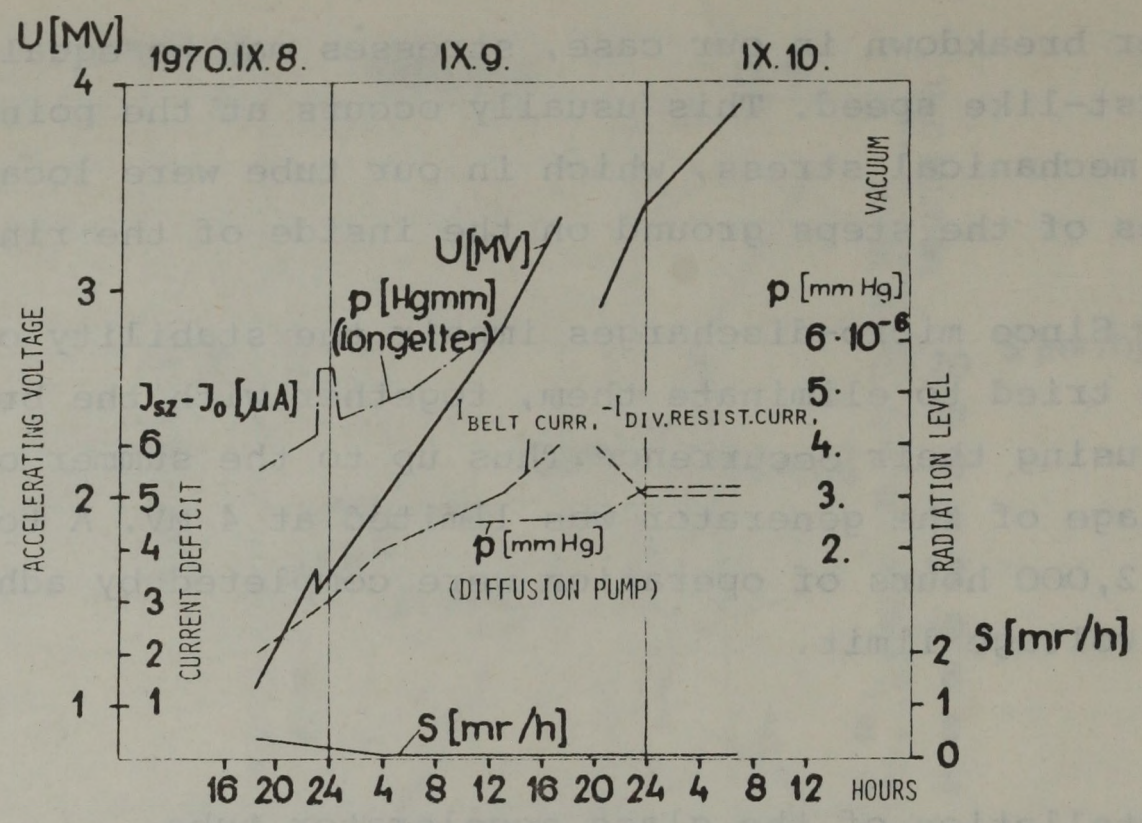

Fig. 47 First voltage test performed on inclined field electrodes mounted in a glass accelerator tube

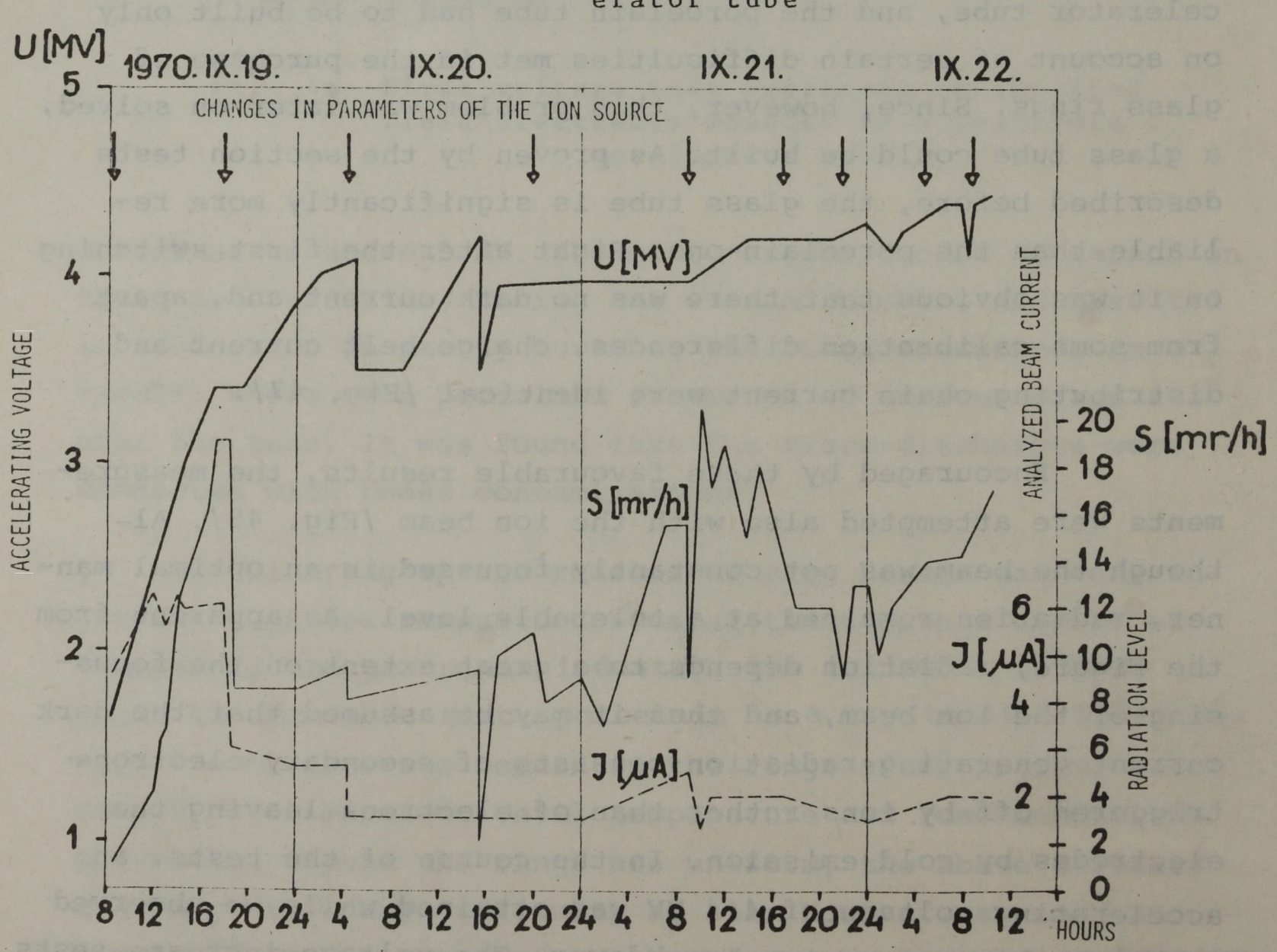

Fig. 48 Voltage test performed with an ion beam on an inclined field glass accelerator tube

conditioned tube there was only a minimal dark current, and if no ion beam was generated, the resulting radiation generally remained below 1 mr/hour, thus being two or three times as high as the background value generally obtained. Other tests were carried out for establishing the energy spectrum of the radiation, and it was found that the maximum in intensity occurred in the vicinity of 300 keV, as predicted by the focussing calculations. Accordingly, the secondary electrons get stuck in the tube after having travelled through a few accelerating gaps. This has been proven by both the experiences gained later on and the marks described under Para. 2.2.3. An accelerating voltage of 5 MV was attained without any difficulty at all, and the voltage in the conditioned tube could be increased within a minute from 1 MV to 5 MV, both with and without an ion beam /Fig. 49/.

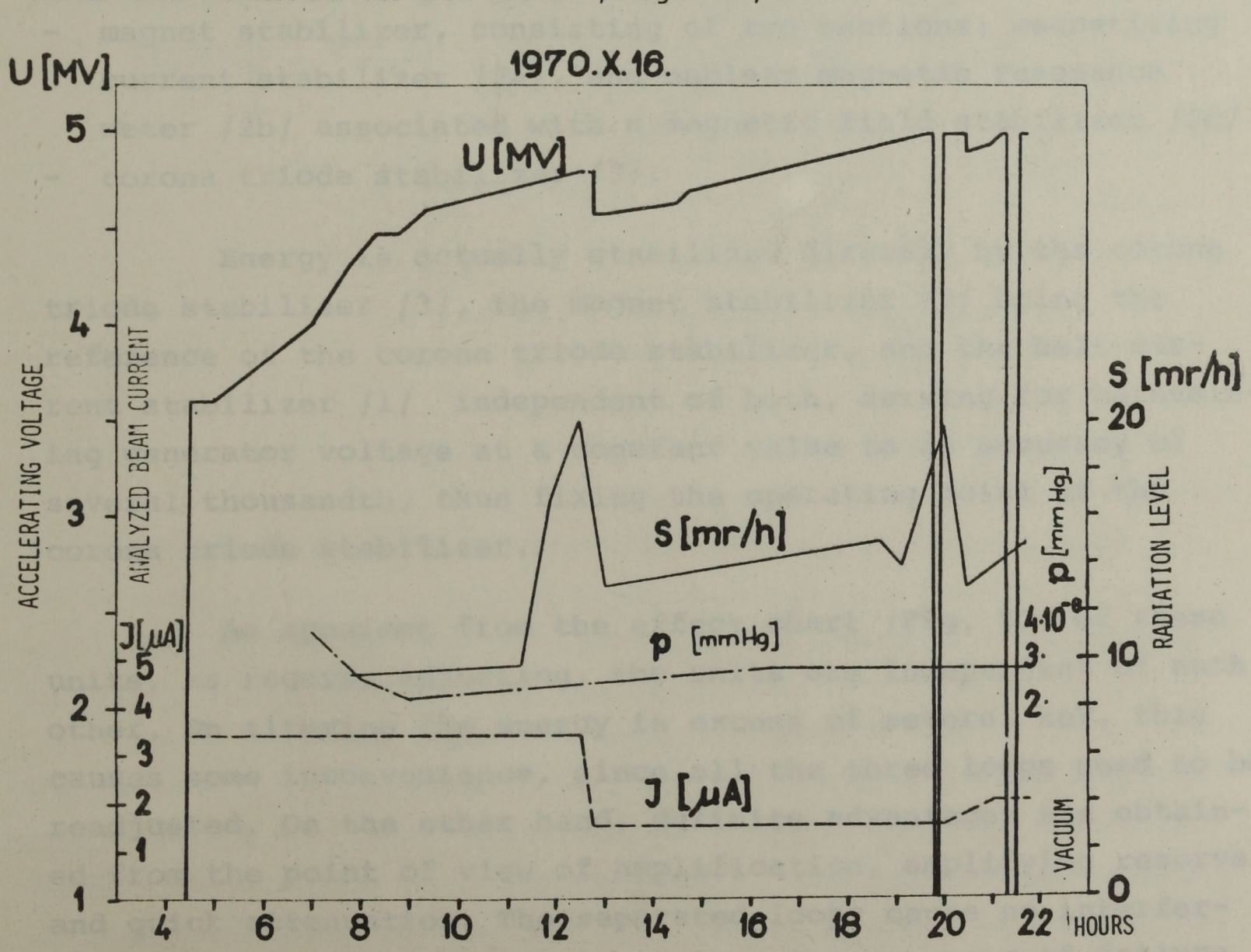

Fig. 49 Voltage test performed with an ion beam on an inclined field glass accelerator tube, up to 5 MV

The assertion that accelerating voltages exceeding 5 MV could be safely attained seems to be well founded. This will, however, require a number of tests which at present can not be performed since the equipment is being used for nuclear measurements. The generator completed 4,453 hours of measurement between 19. September 1970, the date the glass tube was installed, and 19. July 1971. During this period, the accelerator tube presented no problem at all.

V. DEVELOPMENT OF THE ENERGY STABILIZATION SYSTEM

Energy is stabilized /i.e. the acceleration voltage maintained at a constant value/ in our ion accelerator as a result of the balanced functioning of three self-contained units. These are shown on Fig. 50, where they are marked as follows:

- charging belt current stabilizer /1/;
- magnet stabilizer, consisting of two sections: magnetizing current stabilizer /2a/, and nuclear magnetic resonance meter /2b/ associated with a magnetic field stabilizer /2c/
- corona triode stabilizer /3/.

Energy is actually stabilized directly by the corona triode stabilizer /3/, the magnet stabilizer /2/ being the reference of the corona triode stabilizer, and the belt current stabilizer /1/ independent of both, serving for maintaining generator voltage at a constant value to an accuracy of several thousandth, thus fixing the operating point of the corona triode stabilizer.

As apparent from the effect chart /Fig. 50/ of these units, as regards adjusting, the units are independent of each other. On altering the energy in excess of several keV, this causes some inconvenience, since all the three loops need to be readjusted. On the other hand, definite advantages are obtained from the point of view of amplification, amplifying reserve and quick attenuation. The separated loops cause no interference effects on each other, while possible sources of failure can be fairly simply located. The individual units can be controlled and tested by simple means. Attainable energy-

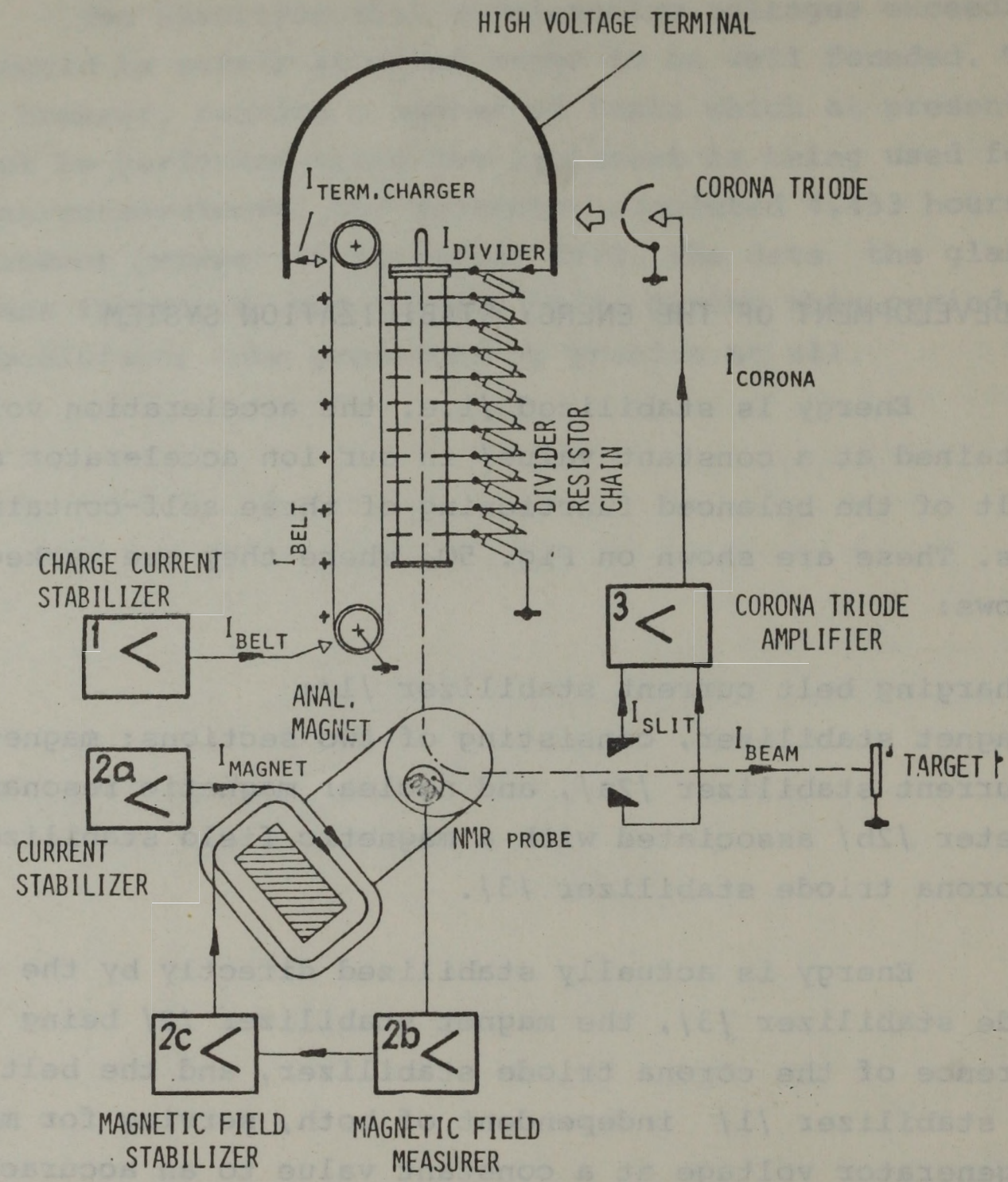

Fig. 50 Block diagram of energy stabilizing system

stability is $\Delta E/E \simeq 1.5 \times 10^{-4}$.

In the following the units are dealt with in some detail, mainly those which were installed as new units in the course of the reconstruction /the NMR meter and magnet stabilizer/. For the sake of completeness the units used before reconstruction /belt current, magnetizing current and corona triode stabilizers/ will be briefly treated as well [2].

1. CHARGING BELT CURRENT STABILIZER

The current required for belt charging is supplied by a current stabilizer. The function of the amplifier of the stabilizer is to stabilize the charging current flowing out of the charging supply unit. This source supplies current for the voltage divider resistor chain, the corona triode and the ion beam. Intensity of the stabilized current is max. 300 μA. Between values of that current from 0 -300 μA, stability is $\Delta J/J = 2 \times 10^{-3}$. Block diagram of the stabilizer is shown on Fig. 51. The current range of zero to 300 μA can be covered

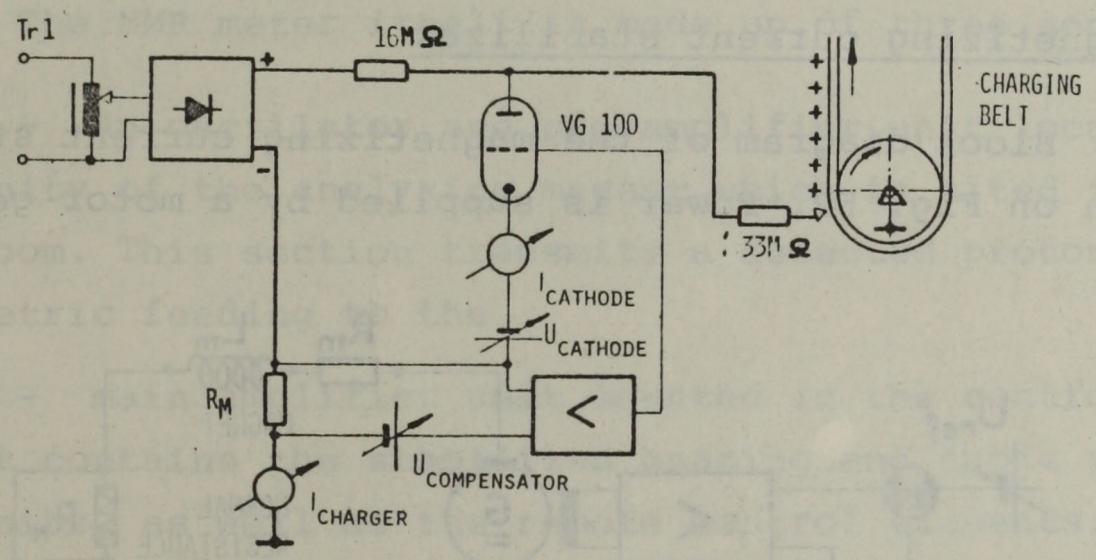

Fig. 51 Block diagram of current stabilizer to belt charger

in one range by a 10-turn helical potentiometer. The final control element is a high-voltage triode Type VG 100 switched in a shunt circuit. Since the function of this stabilizer is to compensate the voltage fluctuations of the lowest frequencies, the feed-back amplifier operates in a direct current circuit. The stabilizer is not effective at fluctuations exceeding 1 c/s because of a powerful filter. The high--voltage supply unit is usually adjusted to 45 kV. Of this output, approx. 30 kV is delivered to the needle assembly. Since this voltage requirement greatly depends on the pressure of insulating gas in the generator, the full circuit can function over a supply voltage range of 2 to 70 kV.

2. STABILIZER OF THE CURRENT OF THE ANALYSING MAGNET

Energy calibration and stabilization of the ion accelerator are based on measuring the magnetic field of a 90-degree analysing magnet. The energy dispersion of the ion beam depends on the stability of this field. Accordingly, we paid an appropriate care to stabilize the field of that magnet. This is done in two steps: first the exciting current of the magnet is stabilized, then the field of the magnet directly.

2.1 Magnetizing current stabilizer

Block diagram of the magnetizing current stabilizer is shown on Fig. 52. Power is supplied by a motor generator

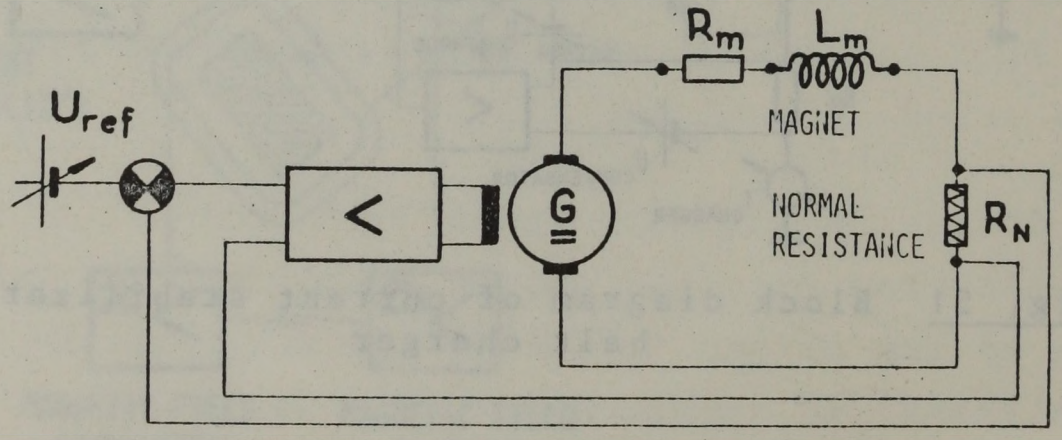

Fig. 52 Block diagram of current stabilizer to magnet supply

unit. With an amplifier inserted, the voltage drop occurring over the normal resistor /R_N/ series-connected with the magnet coil modifies the exciting current of the generator against the changes. Adjustable current intensity range is 7 - 25 A, being adjustable in steps of 1.5 A by means of a ratio switch. The ranges covering the intensities of 1.5 A can be controlled by means of a 10-turn helical potentiometer. The design adopted for the ratio switch permits the following: on reaching "maximal" final position of the helipot, and when further increasing of current intensity by means of the ratio switch is

necessary, no jump of the current is obtained at the moment of switching over. Following that the current intensity can be continuously increased by turning the helipot in the opposite direction. This feature of the design is of importance when the energy is to be altered during acceleration. Stability of excitation current of the magnet is $\Delta I_M/I_M = 10^{-3}$. This stability is sufficient to ensure the reliable operation of the NMR meter and magnetic field stabilizer with it.

2.2 NMR meter

The NMR meter itself is made up of three sections:

- An oscillator and pre-amplifier unit located in the vicinity of the analysing magnet, which is sited in the target room. This section transmits a detected proton signal by asymmetric feeding to the

- main amplifier unit mounted in the control desk; this unit contains the stabilized heating and anode voltage supply units, as well as the remote control elements. After amplification the proton signal and the form of modulating current are transmitted on the

- appropriate input of an oscilloscope, where the resonance signal is obtained.

The material of the sample placed in the magnet field is $H_2O + Fe^{++} NO_2$ /0.1 N/. The frequency range of the marginal oscillator is 4 - 48 Mc/s, and can be changed over 5 bands. Modulation frequency is 250 c/s, with an amplitude of max. 8 Oe. Basic stability of the oscillator is 5×10^{-5}, due to the loose coupling and the stabilization of the oscillation amplitude [56, 57, 58]. The power supplying conditions of the oscillator allow its synchronization by means of a freqency standard /frequency generator Type PDG 3/.

The instrument has been calibrated for signal/noise ratio. The following ratios have been obtained: at 10,000 Oe

20 to 1, and at 1,000 Oe 10 to 1. With the equipment mounted between the poles of the analyzing magnet, we obtained lower signal than the expected one because of the inhomogeneities of the poles. For this reason, the nuclear magnetic resonance stabilizer has such a circuit which cuts the effect of the disturbing impulses to the minimum.

2.3 Stabilizer system of the field of the analyzing magnet

Functioning of the field stabilizer system is based on the information received from the NMR meter. The system is switched on and off by the operating personnel, but switching-on is possible only if there is a proton signal of the appropriate quality /amplitude/. As soon as no proton signal is received, the stabilizer is automatically switched off, this fact being indicated by a pilot lamp. Seventy per cent of the instrument is made up of logical circuit Series EDS 1200 of the Electronic Measuring Instrument Factory [59] , whereas the special circuits making up the rest of the system have been made by ourselves.

The changes occurring in the magnetic field are transformed into impulse width variations by the instrument. By passing these width-modulated impulse series through an auxiliary coil, the change of magnetic field strength is compensated.

By appropriately forming the signals received from the NMR meter an pulse series is obtained, which is the transmitted through a noise-suppression system into a modulating circuit. Width modulation is made possible by the fact that the changes occurring in field strength change the symmetry of NMR impulse distribution in time. Finally, the width--modulated impulse series are transmitted through a gate system into the final amplifier.

The final and output amplifier units are supplied

with signal series marked I and II on Fig. 53. When the stabilizer is in ready state, the final stage is supplied with

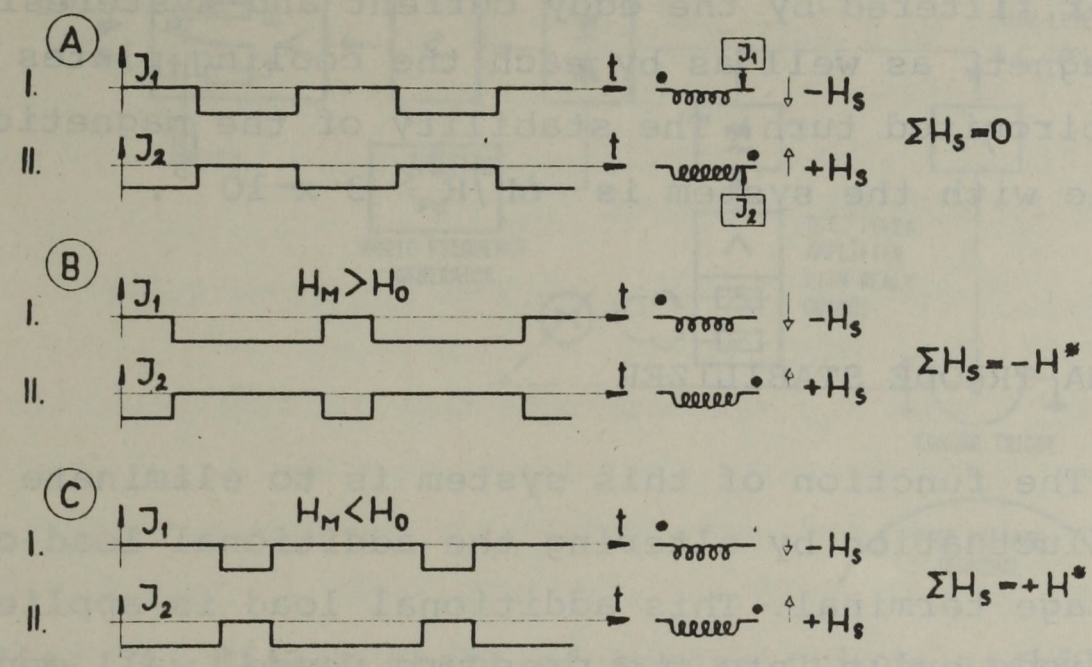

Fig. 53 Pulse series controlling output amplifier of NMR to analysing magnet

the uniform pulses shown on Fig. 53 A, and the same currents flow in all coils at the output coupled in a push-pull circuit. The resultant additional excitation is thus ΣH_s = zero. If, however, the stabilizer is operating as shown on Fig.53 B, where the momentary field strength is indicated by H_M, and the field strength required in accordance with the NMR meter adjustment by H_o, the longer pulses are transmitted to one of the coils in case of $H_M > H_o$, and to the other if $H_M < H_o$, and the magnet is given a positive or negative additional excitation $/H^*/$ in relation to H_M. As a result, provided that the loops are made, the condition of Larmor's precession in the magnet is

$$H_M + H^* = \nu\gamma \equiv H_o, \qquad /3/$$

where ν is the oscillation radian frequency, γ the gyromagnetic coefficient, and H^* serves for compensating lack of excitation $H_o - H_M$ in a push-pull circuit, by means of the stabilizing system.

The currents produced for the auxiliary coils are filtered by a capacitor, another function of which is to simultaneously adjust the feed-back time constant. Field strength is further filtered by the eddy current and hysteresis losses of the magnet, as well as by each the cooling plates forming a short-circuited turn. The stability of the magnetic field obtainable with the system is $\Delta H/H \lesssim 3 \times 10^{-5}$.

3. CORONA TRIODE STABILIZER

The function of this system is to eliminate high-voltage fluctuation by altering the additional load of the high-voltage terminal. This additional load is applied by the corona triode built into the pressure vessel wall opposite to the high-voltage terminal. Functioning of this triode was examined previous to the establishing of this system [60]. Although the geometrical conditions of building-in have been altered in relation to the old generator, this fact has hardly changed the operating parameters. In order to obtain stable functioning of the generator, the system should be adjusted to $I_{kor} \approx 15 - 25$ μA.

The electronic section of the stabilizer comprises two loops, a fast one and a slow one. Sampling is made at a frequency of 452 c/s. The system operates by means of a mechanical chopper forming signals which are proportional to the current difference of the two slit plates located after the analysing magnet. After amplification, the signals are rectified and used for controlling the two loops. Amplification of the fast loop is 105 dB, and of the slow loop 40 dB. The slow loop alters the position of the corona triode /this process can be manually performed as well/, whereas the fast loop serves for controlling the corona needle potential in relation to the earthed grid cap. A schematic effect chart is shown on Fig. 54. During the previous years, this stabilizer system completed more than 10,000 hours of operation in its

present form.

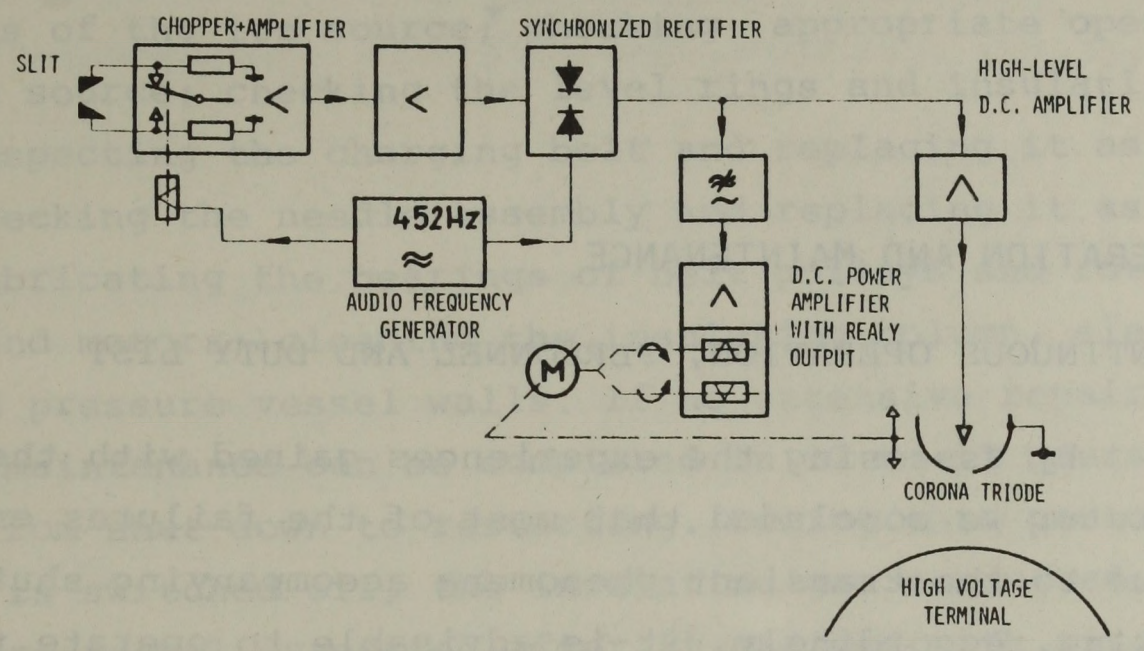

Fig. 54 Effect chart of corona triode stabilizer

VI. OPERATION AND MAINTENANCE

1. CONTINUOUS OPERATION, PERSONNEL AND DUTY LIST

By assessing the experiences gained with the old ion accelerator we concluded that most of the failures encountered were due to the transient phenomena accompanying shut-down and restarting. Accordingly, it is advisable to operate the equipment continuously, which also helps better utilization of time. Continuous operation is now performed by a staff consisting of 8 technicians, who work 12-hour shifts, 7 days a week. As a rule, the day shift /8 to 20 hrs./ consists of two technicians, and the night shift /20 to 8 hrs./ only one technician. One of the duty technicians operates the equipment. The rest of the labour force are required for maintenance, repair and development, as well as in cases of emergency /replacing technicians on holidays, sick leave etc./. Operating parameters are regularly checked in the morning and evening by 2 technicians.

2. MAINTENANCE

The equipment is shut down only when encountering some failure which cannot be remedied during operation, or if the gas bottle of the ion source need be replaced or refilled. Another reason for shutting down the accelerator may be a prolonged interval possibly inserted in the nuclear measuring programme. From time to time, periodical maintenance is performed. On these occasions, the following units are attended: checking and measuring all equipment of the high-voltage terminal; checking the remote control units and control instru-

ments of the high-voltage terminal; measuring and checking the contacts of the high-voltage divider; pressure control in the gas bottles of the ion source; checking appropriate operation of the ion source; checking the level rings and insulating column; inspecting the charging belt and replacing it as necessary; checking the needle assembly and replacing it as necessary; lubricating the bearings of belt pulleys and rotary machines and motors; cleaning the insulating column, electrodes and pressure vessel walls. If no extensive repairs are required, maintenance can be completed in 12 to 17 hours, reckoned from shut-down to restarting. During this period, the equipment is switched off, the insulating gas exhausted, than the pressure vessel evacuated after it charged with air, the manhole opened, all points requiring maintenance and/or repair are attended, an accelerating test is performed in air, the vessel sealed again, then exhausted and maintained under vacuum, insulating gas charged, and finally the equipment started.

Once a year, usually in the summer, general maintenance is undertaken. This includes a through checking of all main assemblies, as well as the repair and replacement of all defective components. If any major development is due, it is also scheduled for this period.

3. PERIODS OF OPERATION COMPLETED

The accelerator came into operation for the purpose of regular nuclear measurements on 12 March, 1970. Between that date and 19 July, 1971, the equipment completed 6,253 hours of operation for that purpose. This was spread over 59 weeks, whereas the rest of the time was utilized for maintenance and development. During 1970, physical measurements were performed in 3,246.5 hours of operation spread over 32 weeks. /This amounts to a weekly average of 101,5 hours./ The same time was in 1971 3,006.5 hours completed in 27 weeks /i.e. a weekly average of 111,0 hours/.

4. EXPERIENCES GAINED WITH LIFETIMES

Regarding the lifetimes of the individual sub-assemblies of the equipment, the following data have been obtained:

Oscillator	1,000 hours
Oscillator supply unit	4,000 hours
Extracting voltage supply unit	4,000 hours
Pre-focussing voltage supply unit	5,500 hours
Ion source	500 - 800 hours
Pd-valve	6,000 hours
Elements of the high-voltage divider	7,000 hours
Plexi-glass high-voltage insulator legs	7,000 hours
Needle assembly	400 hours

VII. ACKNOWLEDGEMENTS

We take the opportunity here to express our gratitude to all those involved in designing, building and calibrating the instrument, first of all the entire staff of the Ion Accelerator Section of the Institute. Our thanks are due to several colleagues from the Engineering Department of the Institute, mainly Mr. József Vályi Nagy /Head of Department/, Mr. László Muzsnay and Mr. László Eszli /Heads of Section/, and Mr. Zoltán Várnai /Chief Engineer/. We are indebted also to many workers of the Nuclear Department of the Institute who encouraged and helped us in our work, first of all to the late Dr. László Nagy /Head of Department/, Dr. János Erő /Head of Department/, and Messrs. István Kovács, Imre Mérey and László Varga, as well as everybody who was ready to offer useful remarks and advices.

Our thanks are offered for co-operation and consultation to the following institutes and companies, as well as their collaborators:

Nuclear Research Institute of the Hungarian Academy of Sciences, Debrecen, mainly Dr. Ede Koltay /Head of Accelerator Section/.

Nuclear Research Institute of the Czechoslovak Academy of Sciences, Rež, Dr. F. Nový /Head of Section/and Dr. R. Džmuráň of the Van de Graaff Laboratory.

Department for High-Voltage Engineering, Polytechnical University, Budapest, Prof. János Eisler /Head of Department/ and Dr. András Csernátony-Hoffer /Associate Professor/.

Aircraft Department, Polytechnical University, Budapest, Dr. Dániel Hadházi /Associate Professor/.

Heavy-current Product Development Institute, Electrical Installations and Appliance Works; Mr. László Billege /Head of Department/ and Messrs. István György and János Patta, development engineers.

United Electric Machine Factory; Mr. László Kanabé /Chief Engineer/.

Telecommunication Research Institute; Dr. János Erdélyi /Head of Department/.

Vacuum Engineering Laboratory, Pestvidék Machine Factory; Mr. Ferenc Kiss /Head of Section/ and Mr. Emil Kiss /Engineer/.

Central Research Institute of the Silicate Industries; Dr. Lidia Kacsanova /Head of Section/.

Pécs Porcelain Factory, Fine Ceramic Works; Mr. László Misángyi /Chief Production Engineer/ and Mr. Lajos Loósz /Head of Section/.

Karcag Glass Works, Glass Industry Works; Mr. Zoltán Suha /Chief Engineer/.

Research Laboratory, Paint Industry Works; Mrs. L. Lukács, chemical engineer, technical adviser.

REANAL Fine Chemicals Factory; Mr. Gábor Klopp, scientific worker.

HUNGARIA Plastics and Rubber Factory; Mr. Dezső Blasek /Chief Engineer/,Mr. Miklós Déri /Head of Section/, and Mr. Jakab Tóbiás /Foreman/.

Metal Plant, Csepel Iron and Steel Works; Mr. Tamás Havas /Engineer/.

Individual Machine Factory, Csepel Iron and Steel Works.

Lenin Metallurgical Works.

Láng Machine Factory

Machine-tool Development Institute

Machine Factory "Április 4"

REFERENCES

[1] J. Erő, E. Klopfer, P. Kostka, I. Kovács, I. Mérey, L. Vályi, L. Varga, *KFKI Közl.*, 13, (1965) 73

[2] J. Erő, E. Klopfer, P. Kostka, I. Kovács, I. Mérey, L. Vályi, L. Varga, *KFKI report (1967)*

[3] E. Pásztor, P. Kostka, E. Klopfer, *1971 Particle Accelerator Conference, Chicago, 1971. March 1-3. IEEE Transaction NS18 June 1971. p. 82*

[4] R.J. Van de Graaff, J.G. Trump, W.W. Buechner, *Reports on Progress in Physics 11, (1948) 1*

[5] Gy. Berecz, *Nukleáris Gépészeti Konferencia, Budapest, (Nuclear Engineering Conference, Budapest, 17 November 1970) B-5. 73*

[6] Gy. Berecz, G. Bürger, B. Horváth, P. Kostka *Nukleáris Gépészeti Konferencia, Budapest, 1970. nov. 17. B-4. 65 (Nuclear Engineering Conference, Budapest)*

[7] S.D. Winter, *Revue d'optique theoretique et instrumentale (1950) 5*

[8] J.W. Boag, *Proc. IEE. 100-IV. (1953) 63*

[9] R.M. Ashby, O. Hanson, *Rev. Sci. Instr., 13, (1942) 128*

[10] L. Vályi, *KFKI Közl., 14, (1966) 401*

[11] L. Királyhidi, P. Kostka, *KFKI Közl., 17, (1969) 129*

[12] E. Pásztor, P. Vidor, *Magyar Építőipar, 4, (1962) 186*

[13] B. Gänger, *Der Elektrische Durchschlag von Gasen, Springer, Berlin, 1953*

[14] J.G. Trump, *Dielectric Material and Application Wiley, N.Y. 1954. p. 147*

[15] J.G. Trump, *Nucl. Instr. and Meth., 28, (1964) 10*

[16] L. Verebély; *Villamos erőátvitel I., (Electric Power Transfer) Tankönyvkiadó, Budapest, 1953*

[17] J. Eisler, *Bevezetés a nagyfeszültségü technikába, (Introduction To High-voltage Engineering) Akadémiai Kiadó, Budapest, 1965*

[18] J.W. Boag, *Proc. IEE 100-IV. (1953) 63*

[19] Вальтер, А.К. и др.: Электростатические ускорители заряженных частиц, Москва, 1963 г.

[20] Kostka P., *Elektrotechnika, 38, (1965) 136, 234*

[21] H. Ritz, *Arch. Elektrotechn., 26, (1932)219*

[22] R.F. Goossens, *CIGRE-report (1948) 117*

[23] Berecz Gy., *KFKI Közl., 17, (1969) 52*

[24] É. Görög, G. Klopp, G. Sipos, *Säurebeständige KLINOSORB Molekulsieb-Adsorbenzien und ihre Anwendungsgebiete, Nagynyomásu Kisérleti Intézet, Budapest (1966)*

[25] Klopp G., *private communication*

[26] Bürger G., Klopfer E., Kostka P., *KFKI Közl., 15, (1967) 357*

[27] H.H. Martinussen, G.R. Bozzoli, *Trans. of the South African Instr., El. Eng., 55, (1964) 133*

[28] S. Frank, *Arch.f. Elektrotechn., 28, (1934) 485*

[29] A.J. Bayly, A.G. Ward, *Can. J. Res., 36, (1948) 69*

[30] P. Gombos, *KFKI Report 71-17*

[31] Bürger G., Gombos P., Klopfer E., Kostka P., *KFKI Közl., 15, (1967) 363*

[32] M.J. Kofoid, *Trans. AIEE 79/III. 999. (1960)*

[33] R. Hawley, *Vacuum, 18, N°7 (1968) 383*

[34] H. Boersch, H. Hamisch, W. Ehrlich, *Z.angew. Physik, 15, (1963) 518*

[35] R.J. Van de Graaff, P.H. Rose, A.B. Wittkower, *Nature 195, (1962) 1293*

[36] M.E. Elkind, *Rev. Sci. Instr., 24, (1953) 129*

[37] L. Varga, *KFKI Report 8/1969*

[38] Kostka P., Dobrosz M., *KFKI Közl., 17, (1969) 59*

[39] U. Timm, *Z. Naturforsch., 10a, (1955) 593*

[40] P.H. Rose, A. Galejs., *Progr in Nucl. Techn., 2, (1967)3*

[41] P. Kostka, *Nucl. Instr. and Meth., 91, (1971) 413*

[42] Királyhidi L., Kostka P., *KFKI Közl., 17,(1969) 129*

[43] S. Penner, *Rev. Sci. Instr., 32, (1961) 150*

[44] А.Н. Сербинов, П.Т.Э. 1967. № 2, 30.

[45] P. Kostka, *Nucl. Instr. and Meth. 1971./Nucl. Inst. and Meth., 97, (1971) 87-90*

[46] E. Koltay, *Physics Letters, 4, (1963) 66*

[47] В.А. Романов, А.Н. Сербинов, П.Т.Э. 1965. № 6, 38.

[48] J.G. Cramer, *Nucl. Instr. and Meth., 62, (1968) 208*

[49] В.С. Кузнецов, Р.П. Фидельская, ЖТФ 35, /1965/ 2004.

[50] B. Gyarmati, E. Koltay, *ATOMKI preprint 1968/5*

[51] А.Н. Сербинов, А.В. Мажулин, П.Т.Э. 1968 № 5 221.

[52] А.Н. Сербинов, А.В. Мажулин, В.П. Якушев, А.И. Лашук, И.П. Саходин, П.Т.Э. 1970 № 3, 58.

[53] R. Hawley, A. Maitland, *Vacuum as an Insulator, Chapman and Hall, London, 1967*

[54] C. Germain, F. Rohrbach, *Proc. of the 6th Int. Conf. on Ionization Phen. in Gases, Paris, 1963. V. 2, p111*

[55] K.H. Purser, A. Galejs, P.H. Rose, R.J. Van de Graaff, A. Wittkower, *Proc. of the Int. Symp. on Insulation of High Voltages in Vacuum, MIT, 1964. Vol. 1, 317*

[56] N.J. Hopkins, *Rev. Sci. Instr., 20, (1949) 401*

[57] Л.В. Василев, Препринт ОИЯИ 2459 (1965).

[58] Kodytek V., Zejda J., *Report UJV. 1033/1964*

[59] *Elektronikus elemek katalógusa VIII., KGM Müszaki Tudományos Tájékoztató Intézet (Catalogue of Electronic Elements, VIII. Technical Scientific Information Institute of the Ministry of Metallurgy and Machine Industry)*

[60] Д. Берец, П. Костка, П.Т.Э. /1969/ № 3. 24.

[61] E. Klopfer, P. Kostka, E. Pásztor, *Nukleáris Gépészeti Konferencia, Budapest, 1970. nov. 17. (Nuclear Engineering Conference, Budapest, 17 November 1970) B-3, 55*

[62] R. Džmuráň, *UJV report 2262-A, 1969*

[63] Gy. Berecz, *KFKI Közl.*, 16, *(1968) 137*

61.906

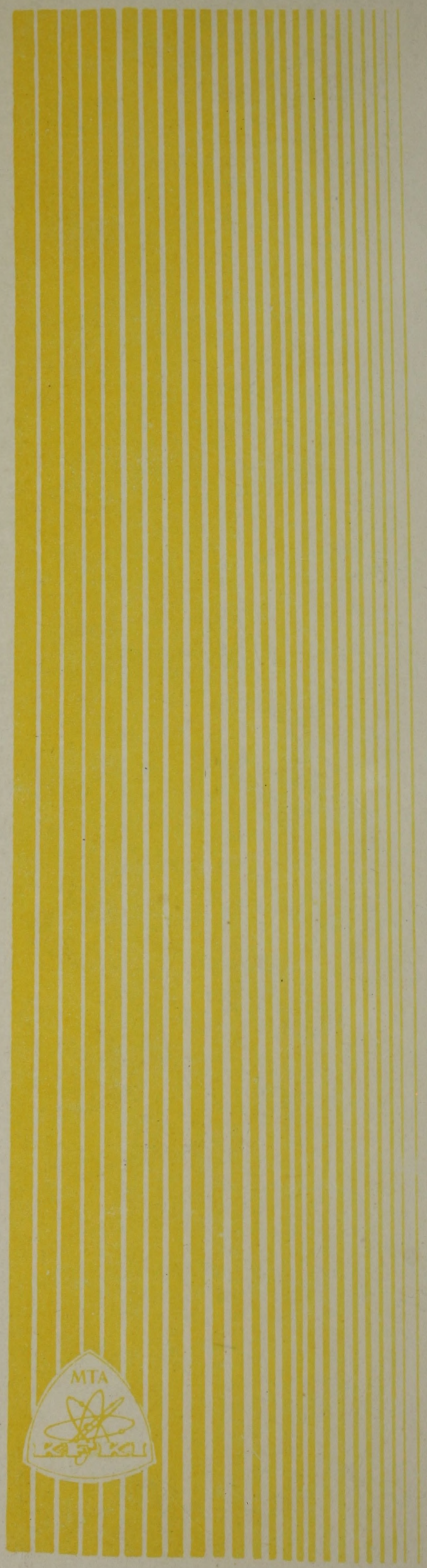

Kiadja a Központi Fizikai Kutató Intézet
Felelős kiadó: Erő János, a KFKI Magfizikai Tudományos Tanácsának elnöke
Szakmai lektor: Szabó Zoltán
Nyelvi lektor: T. Wilkinson
Példányszám: 370 Törzsszám: 71-5928
Készült a KFKI sokszorosító üzemében, Budapest, 1972. február hó